

THE UNIVERSITY OF CHICAGO

THE EPIGENETIC LANDSCAPE OF IL-15 SIGNALING IN TISSUE RESIDENT EFFECTOR CYTOTOXIC  
INTRAEPITHELIAL LYMPHOCYTES

A DISSERTATION SUBMITTED TO  
THE FACULTY OF THE DIVISION OF THE PHYSICAL SCIENCES  
AND  
THE FACULTY OF THE DIVISION OF THE BIOLOGICAL SCIENCES  
AND THE PRITZKER SCHOOL OF MEDICINE  
IN CANDIDACY FOR THE DEGREE OF  
DOCTOR OF PHILOSOPHY

GRADUATE PROGRAM IN BIOPHYSICAL SCIENCES

BY

VU QUOC DINH

CHICAGO, ILLINOIS

AUGUST 2017

Dedicated to mom and dad, I love you with all my heart.

Dedicated to Quynh, for your true love and support.

## TABLE OF CONTENTS

|   |      |
|---|------|
| List of figures.....  | v    |
| List of tables.....   | vii  |
| Acknowledgement .....   | viii |
| Abstract.....   | xi   |
| Chapter 1: Introduction .....   | 1    |
| 1.1    The mucosal immunity and CD8 $\alpha$ β <sup>+</sup> TCRαβ <sup>+</sup> intraepithelial lymphocytes.....                     | 1    |
| 1.2    Introduction to interleukin 15 .....   | 2    |
| 1.3    The roles of IL15 in the context of IELs.....  | 4    |
| 1.4    Known molecular signaling pathways of IL15 in IELs .....   | 8    |
| 1.5    Epigenetics - chromatin accessibility and histone modifications.....   | 10   |
| 1.6    Epigenetics - methylation, demethylation, 5hmC and Tet enzymes.....  | 13   |
| 1.7    Hypothesis and the novelty of our research .....   | 16   |
| 1.8    The broader question: epigenetics and terminally differentiated T cells .....  | 17   |
| 1.9    Scope of thesis.....   | 19   |
| Chapter 2: Methods.....   | 21   |
| 2.1    The isolation of human intraepithelial lymphocytes fraction .....  | 21   |
| 2.2    The sort of CD45 <sup>+</sup> CD3 <sup>+</sup> TCRαβ <sup>+</sup> CD8 $\alpha$ <sup>+</sup> intraepithelial lymphocytes..... | 21   |
| 2.3    The generation of short termed human IEL cell lines .....  | 22   |
| 2.4    Interleukin 15 stimulation .....   | 22   |
| 2.5    RNA isolation and RNA-Seq .....  | 23   |
| 2.6    ATAC-Seq .....   | 23   |
| 2.7    ICE-CHIP for native histone pull down.....   | 24   |
| 2.8    5hmC-Seal IP.....  | 26   |
| 2.9    RT-qPCR and primer tables.....   | 27   |
| 2.10    siRNA against Tet2 and Tet3.....  | 28   |
| 2.11    TCR + IL15 stimulation and FACS staining for cytokines production.....  | 28   |
| 2.12    Edu functional assay .....  | 29   |
| 2.13    Bioinformatics and statistical analysis.....  | 29   |
| Chapter 3: The transcriptomic changes during IL15 signaling.....  | 35   |
| 3.1    Experimental design to study transcriptomic changes under IL15 in IELs .....   | 35   |

|   |  |    |
|---|--|----|
| 3.2   | IL15 triggers major transcriptional changes that exhibit complex temporal behavior – the early responses.....                  | 37 |
| 3.3   | IL15 triggers major transcriptional changes that exhibit complex temporal behavior – the intermediate and late responses. .... | 40 |
| Chapter 4: The epigenetic landscape of IL15 signaling .....                 |  | 47 |
| 4.1   | The chromatin accessibility of IELs is stable throughout IL15 stimulation.....   | 47 |
| 4.2   | The dynamics of histone modifications during IL15 signaling.....   | 53 |
| 4.3   | 5-Hydroxymethylcytosines are abundant and change dynamically.....  | 61 |
| 4.4   | The correlation between DHMRs and DEGs.....  | 66 |
| Chapter 5: The roles of Tet 2 demethylase and 5-hydroxymethylcytosine ..... |  | 70 |
| 5.1   | Tet family in IELs and their expression levels during the signaling cascade.....   | 70 |
| 5.2   | Tet2 knock down (siTet2) and the baseline differential expressed genes .....   | 71 |
| 5.3   | Tet2 knock down (siTet2) and the roles of Tet2 in IL15 signaling .....   | 73 |
| 5.4   | Functional consequences of Tet2 knockdown in IELs .....  | 76 |
| Chapter 6: Discussion and future directions.....                            |  | 78 |
| 6.1   | Overview.....  | 78 |
| 6.2   | The model: preset versus altered epigenetic landscape in IL15 signaling .....  | 79 |
| 6.3   | The roles of 5hmC – demethylation intermediate or stable epigenetic mark? .....  | 83 |
| 6.4   | Tet2 and Tet3 in IL15 signaling cascade .....  | 85 |
| 6.5   | Future directions .....  | 87 |
| 6.6   | Conclusion .....   | 90 |
| References .....  |  | 92 |

## LIST OF FIGURES

|   |    |
|---|----|
| Figure 1: The roles of IL15 in IELs.....  | 4  |
| Figure 2: Autoimmune disorders associated with dysregulation of IL15 .....  | 7  |
| Figure 3: Molecular signaling of IL15 in IELs and target genes .....  | 8  |
| Figure 4: The cycle of Tet mediated active DNA demethylation .....  | 13 |
| Figure 5: Hypothesis on whether IL15 acts on a preset or altered epigenetic landscape.....  | 16 |
| Figure 6: The central question about the roles of epigenetics in terminally differentiated T cells.....   | 18 |
| Figure 7: Experimental schematic to investigate different epigenetic processes during IL15 signaling ....   | 37 |
| Figure 8: Transcriptomic changes in IELs due to IL15 signaling during a period of 24 hours. ....  | 43 |
| Figure 9: Tn5 peaks revealed by ATAC-Seq of IELs during the course of IL15 stimulation.....   | 51 |
| Figure 10: Tn5 Footprinting analysis of different clusters of DEGs .....  | 52 |
| Figure 11: The histone modifications, Tn5 and 5hmC landscape of non-differentially genes expressed at high level in steady state, and not expressed genes. .... | 57 |
| Figure 12: Histone modifications landscape of induced and repressed genes during IL15 stimulation ....  | 58 |
| Figure 13: Early differentiated genes show a higher than average number of activating histone modifications and Tn5 peaks count. ....                           | 59 |
| Figure 14: H3K4me1 is enriched in early and intermediate differentially expressed genes .....   | 60 |
| Figure 15: IL15 induce dynamic 5hmC changes in IELs.....  | 64 |
| Figure 16: Enrichment analysis of 5hmC DHMRs.....   | 68 |
| Figure 17: The overlap between 5hmC dynamic peaks, H3K27Ac and ATAC peaks.....  | 69 |
| Figure 18: Expression of Tet family at base line and during the course of IL15 stimulation in IELs .....  | 71 |
| Figure 19: The baseline effects of siTet2 in IELs .....   | 72 |
| Figure 20: The role of Tet2 in IL15 signaling pathway of IELs .....   | 75 |

|  |    |
|--|----|
| Figure 21: Proliferation rate of siTet2 IELs.....                                | 77 |
| Figure 22: Model - Epigenetic landscape during IL15 signaling in IELs.....       | 80 |
| Figure 23: The overlap between Tet2 controlled genes and dynamic 5hmC genes..... | 85 |

## LIST OF TABLES

|   |    |
|---|----|
| Table 1: Primers list for qPCR analysis .....   | 27 |
| Table 2: KEGG pathways analysis for upregulated DEGs in IL15 signaling pathway.....   | 44 |
| Table 3: KEGG pathways analysis for repressed DEGs in IL15 signaling pathway. ....  | 45 |
| Table 4: Long non-coding RNAs differentially expressed under IL15 signaling .....   | 46 |
| Table 5: Number of total and differentially expressed peaks of Tn5 and various histone marks at 4h post<br>IL15 stimulation ..... | 53 |

## ACKNOWLEDGEMENT

I came to the University of Chicago to pursue graduate studies in biophysical science. I was intrigued with the vision of dual mentorships in which I can have two mentors and do interdisciplinary research at the interface of biological science and physical science. As a recent graduate from Caltech, I jumped at the opportunity with an open mind to explore and an open heart to enjoy science. After years of graduate school, I have learned much and grown beyond what I could initially imagine. Instrumental in my success, my mentor, Bana Jabri deserves tremendous amount of credit and gratitude. Bana has been an exceptional scientist and a role model for me and other graduate students in the lab. She is a self-driven, passionate, brilliant and rigorous scientist. Bana discusses science as if there is nothing else mattered in the whole world. The best gift that you can give Bana is new data. She has been inspirational throughout my graduate years, and she pushes me to be the best graduate student that I can be. I have learned from her so much. I would never forget the long hours discussing science, or the late-night skype calls to analyze new data. Bana, for everything, I thank you.

In addition to Bana, my thesis committee has been extremely helpful with guidance over the years. Chuan He has been inspirational with his passion for science and his willing to explore novel and unexplored areas of science. Albert Bendelac has set the bar very high for scientists with his exceptional vision and brilliant insights. Together, they helped me navigating through data to understand my science and to be a better scientist.

Beside science, my experience at the University of Chicago has been wonderful, thank to my amazing classmates: Sean Gibbons, Peter Dahlberg, Guillermina Ramirez-San Juan, Boleslaw Osinski, Daniel Kerr and Kristen Enright. I feel blessed with their companion and support. We came to the University of Chicago from various different backgrounds. Dan, Peter, Bo and Guillermina did their undergraduates in physics while Sean and Kristen in biology. Somehow, we banded together to become

closest of friends with tremendous support through ups and downs during graduate school. We had pot luck together, went to movies, drank at the university bars, and chatted endlessly about science. The memories were fun, and I would never forget them.

When moving away from California and my parents, I have been missing home a lot. However, I have gained another family for 6 years: the Jabri lab. To my lab mates, you are not only my friends, but also a part of my life – my extended family. I have spent all my twenties with you, and I am so thankful to have known all of you. I will never forget you all: Toufic Mayassi, Sangman Kim, Cezary Ciszewski, Romain Bouziat, Reinhard Hinterleitner, Kelli William, Jordan Earnest, Li Chen, Marlies Meisel, Valentina Discepolo, Zach Earley and Dustin Shaw. Toufic, I am glad to have been your friend since the summer that we rotated in the lab together. I am thankful for your help through the tough times and for your companion through the good times. Cezary, thank you for being my second mentor besides Bana. You have always been so kind and thoughtful, and I have always considered you as an older brother that I did not have.

I would not come to the University of Chicago without the conception and development of the graduate program in biophysical science. I thank Tobin Sosnick and Adam Hammond for being fearless directors of the program. I have never doubted the success of the program when I get to know you and all the talented students that you have recruited. I thank you Michele Wittels and Julie Feder for taking care of us students and for solving many administrative problems with ease. Michele and Julie, you make this program wonderful. You are the true hearts and souls of the biophysics program.

My science and my research would not have gotten far without my amazing collaborators. Thanks to Alain Pacis and Luis Barreiro for their tremendous help on bioinformatics analysis. All of my sequencing data are mapped and analyzed by Alain Pacis. The research without a doubt will not come to fruition without Alain's skills. Thanks to Miao Yu, Boxuan Zhao and Qiancheng You for their help on 5hmC IP,

especially Qiancheng You who tried multiple times to troubleshoot the system. Thanks to Adrian Grzybowski for helping me with the native histone CHIP. Thanks to Cezary Ciszewski and Toufic Mayassi for their help with sorting and isolating the IELs. Thanks to Anne Dumaine for the discussion on ATAC-Seq. Thanks to Aiping Mao for the discussion on Tet CHIP. I am taught in undergraduate that science needs collaboration to advance, and I am thankful to have all your help and contributions to my research.

I want to use this last paragraph to thank mom and dad. My dad is an agricultural engineer. He is passionate to help farmers in Vietnam to improve productivity and crop yield with his complex machinery. My mom is a history teacher who loves to teach and inspire generations of youth to grow and become competent members of the society. Both of them encourage me to follow my dream, and support me unconditionally through thick and thin with their love. I can always talk to mom and dad and let my problems melted away. Mom and dad, thank you for believing in me. You are the best mom and dad in the whole world. I also want to thank my brothers, Khang (Vincent) Dinh and Thai Dinh. You are the best brothers that I can ever hope for. You are kind spirited, supportive, fun and talented. I have always loved to spend my time with both of you. Finally, I want to thank my beautiful wife, Quynh Chu, for her unconditional love and support. Quynh, you may not know (I never told), but I have always been falling head over heels in love with you (since junior high!). Thanks darling for all the sweet memories in our journey together. My accomplishments in graduate school are yours as well.

## ABSTRACT

The epigenetic landscape of interleukin 15 (IL15) signaling in  $TCR\alpha\beta^+CD3^+CD8^+$  intestinal intraepithelial lymphocytes (IELs) has remained unknown despite well characterized molecular pathways downstream of IL15. By using short termed IEL cell lines and various sequencing techniques targeted at the epigenetic landscape (ATAC-Seq, histone CHIP-Seq, and 5hmC Seq), we demonstrated that during IL15 signaling, the chromatin accessibility and histone marks (H3K4me1, H3K4me3, H3K27Ac, H3K27me3) remained stable while the 5hmC landscape changed dynamically in complex temporal patterns. Dynamic 5hmC regions (DHMRs) locate mostly at the enhancer sites, and genes associated with DHMRs are more likely to be differentially expressed. The loss of 5hmC is associated with early induced genes while the gain of 5hmC is associated with repressed genes. By knocking down Tet2, we demonstrated the roles of Tet2 in the generation of these DHMRs and in the transcriptional control of a subset of IL15 regulated genes, mainly cell cycle, defense response and type 1 IFN related gene sets. Altogether, these results suggested that IL15 uses a combination of preset epigenetic landscape and altering epigenetic landscape to promote large transcriptional changes in IELs and carries out its diverse biological functions.

## CHAPTER 1: INTRODUCTION

### 1.1 The mucosal immunity and CD8 $\alpha\beta^+$ TCR $\alpha\beta^+$ intraepithelial lymphocytes

It is estimated that the epithelium of an adult intestine spans an area of 200-400 m<sup>2</sup><sup>1</sup>. With a large surface area, a complex immune system is needed to protect the body from the septic lumen of the small intestine<sup>1</sup>. Such immune system needs to be able to recognize and distinguish between self-antigens, commensal bacteria, foreign antigens and pathogens<sup>2</sup>. The proinflammatory response to pathogens must tightly regulated. Indeed, overactive immune response can lead to excessive damage to the gut environment and barrier, causing severe systemic sepsis<sup>3</sup>. Inability to recognize and tolerate self-antigen can lead to autoimmune disorders such as inflammatory bowel disease (IBD) and Crohn Disease<sup>4,5</sup>. The intraepithelial lymphocytes (IELs) are the main soldiers of this mucosal immune system<sup>6</sup>. Approximately, in between every ten epithelial cells, there is one or two IELs<sup>7</sup>. The IELs are at the frontier of the intestinal barrier. They are in direct contact with the epithelial cells, and in close contact with the lumen and the commensal bacteria, performing vital functions for the front line defense<sup>2,7</sup>. The IEL compartment consists of mostly T cells, and small subset of newly identified ILC1 cells<sup>8</sup>. In human, most IELs are CD8 $\alpha\beta^+$ TCR $\alpha\beta^+$  T cells with smaller populations of CD4 $\alpha\beta^+$ TCR $\alpha\beta^+$  and TCR $\gamma\delta^+$  T cells<sup>7</sup>. In this study, we investigated only the CD8 $\alpha\beta^+$ TCR $\alpha\beta^+$  IELs, and we would call them IELs for short.

CD8 $\alpha\beta^+$ TCR $\alpha\beta^+$  IELs are unique compared to the conventional CD8 $\alpha\beta^+$ TCR $\alpha\beta^+$  T cells in the peripheral blood. They exhibit activation markers CD44 and CD69, and tissue resident marker CD103<sup>9</sup>. CD103 can interact with E-cadherin of the epithelium cells, enabling IELs to remain in the intestinal tissue. These surface markers reflect the differentiated status of IELs: they are terminally differentiated cells, and in the literatures, they are considered as prototypical tissue resident, effector memory T cells<sup>10</sup>. If the naïve T cells in the blood are the newly trained soldiers, the IELs are veterans: activated, differentiated

and ready to carry out robust effector functions. In fact, the IELs are capable of producing high levels of cytotoxic granules (GZMB - granzyme b and PRF1 - perforin), and proinflammatory cytokines (IFNG - interferon gamma, IL2 – interleukin 2) in response to proinflammatory environment without the need of simultaneous T cell receptor (TCR) activation<sup>11</sup>. In addition, IELs have been shown to have stronger, more mature and sustained cytotoxic responses upon infection<sup>12</sup>. In contrast with a contraction phase in peripheral blood T<sub>EM</sub> after pathogen clearance, IELs maintain long term effector phase with sustained release of cytotoxic molecules such as GZMB and IFNG<sup>13</sup>. IELs have different cofactor requirement for activation as well, with the additional requirement of CD40L. Finally, the IELs can express natural killer (NK) receptors (for example NKG2D) to sense stress ligands from epithelial cells independent of TCR recognition<sup>14</sup>. This allows the IELs to detect and kill epithelial cells infected with pathogens that have downregulated MHC molecules.

Even though IELs have the capability to release cytotoxic molecules to mount an immune response, they exist normally in quiescent states<sup>7</sup>. They are capable of killing, but they do not kill automatically. They need to be licensed to exert their cytotoxic functions, and one of the most important cytokines that licenses them to kill is interleukin 15 (IL15).

## 1.2 Introduction to interleukin 15

Interleukin 15 was first discovered in 1994 simultaneously by two different labs<sup>15,16</sup>. In the Waldmann lab, IL15 was characterized as a T cell growth factor in a study of human T cell lymphotropic virus 1 (hTCLV1)<sup>15</sup>. In an hTCLV1-associated adult leukemia T cell line, HuT-102, Waldmann and colleagues discovered that this T cell line was capable of making an unknown cytokine that “stimulated T cell proliferation and cytokine activated killer cell activity”<sup>15</sup>. The functions of the new cytokine were not blocked by antibodies against IL2Ra, but by Mik $\beta$ 1, an antibody against IL2R $\beta$  proving that this new cytokine was distinct from IL2. They named this novel cytokine IL-T, and since its discovery, IL-T has been

shown to be functionally important for the survival and proliferation of T cells. It was subsequently renamed interleukin 15<sup>16</sup>.

The human interleukin 15 is 14-15 kDa long, consists of nine exons and three introns<sup>17</sup>. Via alternative splicing, interleukin 15 has two isoforms, one with long signal peptide (LSP) and one with short signal peptide (SSP)<sup>18</sup>. Due to the different signal peptides, LSP and SSP isoforms have distinct intracellular trafficking, localization, and secretion pathway. The LSP isoform transcript has 316 bp 5' UTR, 486 bp coding sequence and 400 bp 3' UTR. The LSP is encoded by exons 3-5, yielding a 48 amino acid signaling peptide. IL15-LSP isoform is made in the endoplasmic reticulum, transferred to the Golgi apparatus and secreted from the cells as a soluble cytokine<sup>19</sup>. On contrary, the SSP is encoded by exon 4A-5, yielding a signal peptide of 21 amino acid. IL15-SSP is not secreted, and restricted in the cytoplasm and nucleus with potential roles in transcriptional regulation rather than cytokine signaling<sup>20</sup>. In this study, we focused on the secreted long isoform of IL15 as it is the only isoform of IL15 employed by the immune system as an intercellular signal.

IL15 is expressed in a variety of cell types - both hematopoietic and non-hematopoietic cells: monocytes, dendritic cells, lymphocytes, macrophages, bone marrow stroma cells, respiratory system and intestinal system's epithelial cells, fibroblasts and hair follicles<sup>14,21-27</sup>. The expression of IL15 can be changed due to the local environment and the presence of pathogens. IL15 has been shown to be upregulated in epithelial cells during stresses or inflammatory conditions such as in the cases of bacterial and viral infections<sup>28</sup>. IL15 is thought to be controlled via transcriptional factors NFkB and IRF1<sup>29</sup>. Finally, even though both IL2 and IL15 functions as survival and proliferative signals in T cells, they are fundamentally different in the ways they are presented<sup>30</sup>. IL2 is secreted and presented in a soluble form. On the contrary, IL15 is trans-presented: in antigen presenting cells, or epithelial cells, IL15 is made and attached to IL15R $\alpha$ . IL15R $\alpha$  will trans-present IL15 to NK cells or CD8 $^+$  T cells that have IL2/15R $\beta$  and  $\gamma_c$ <sup>31</sup>. Due to close interaction between IL15 with its receptor during trans-presentation, IL15 signal is more

robust, potent and specific than IL2<sup>14</sup>. A low dose of IL15 is equivalent to a very high dose of IL2<sup>32</sup>. Upon the binding of IL15R $\alpha$ /IL15 to IL2/15R $\beta$  and  $\gamma_c$  on targeted cells, IL15 starts its signaling process and carries out its immunological functions.

### 1.3 The roles of IL15 in the context of IELs

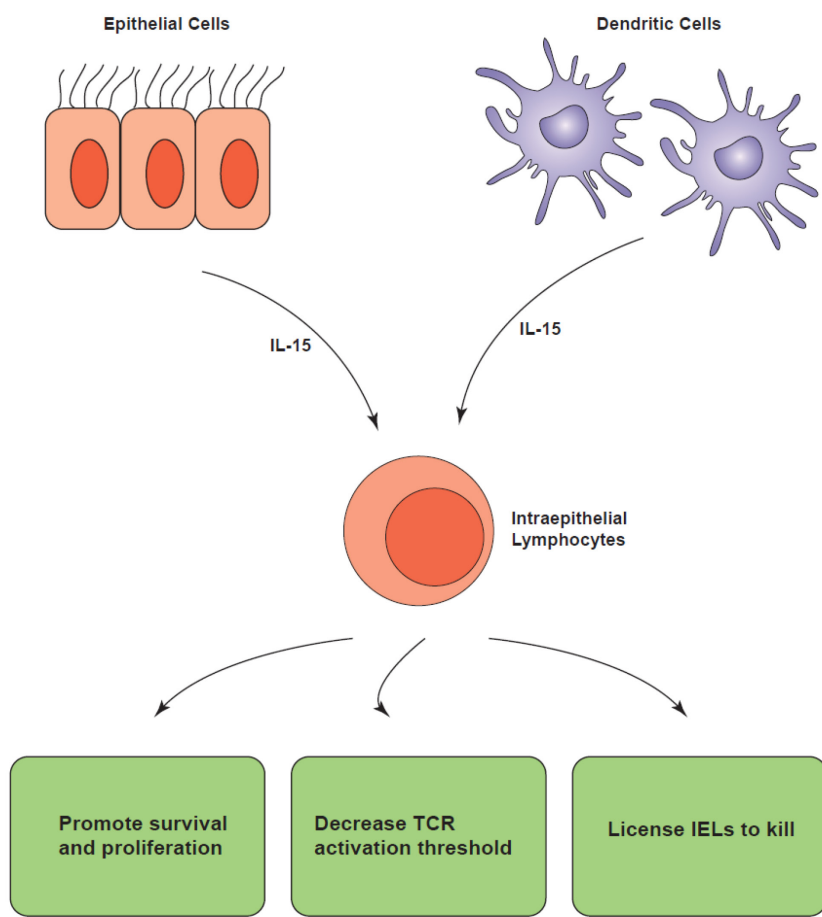


**Figure 1: The roles of IL15 in IELs**

Interleukin 15 are produced and secreted by epithelial cells or dendritic cells to the intestinal environment. Upon encountering IELs, IL15 can promote the survival and proliferation of IELs, decrease the TCR activation threshold and license the IELs to kill.

Due to the scope of this thesis, we will discuss mainly the roles of IL15 in IELs. However, it is important to note that IL15 has many potent functions in other target cells. For example, IL15 plays important roles in the development, maintenance, proliferation, and activation of memory CD8<sup>+</sup> T cells (CD8<sup>+</sup>CD44<sup>hi</sup> T cells), invariant natural killer T cells (iNKT cells), and natural killer cells (NK cells)<sup>33-37</sup>. IL15 can induce ILC1 cells to produce a large amount of IFN $\gamma$  to induce early inflammatory responses in order to protect tissues against pathogens<sup>8</sup>. IL15 promotes dendritic cells (DCs) to express proinflammatory cytokines such as IL-12 and IL-23 to trigger Th1 responses and immunity<sup>38</sup>.

The first role of IL15 in IELs is to promote the survival and proliferation of IELs<sup>21</sup>. Without IL15 (or IL2), IELs will go through the default pathway and die. To counter death, IL15 activates the JAK3/STAT5 pathway to turn on the expression of various anti-apoptotic factors such as BCL-2, BCL-XL and MCL-1. These anti-apoptotic factors can be translocated inside the mitochondria to inhibit pro-apoptotic signaling of BIM, PUMA, BAK and BAX, preventing the release of toxic cytochrome C and enabling the IELs to survive<sup>39</sup>. In addition, IL15 also activates several pro-oncogenes such as C-MYC, C-FOS and C-JUN and acts through MAPK pathways to trigger mitotic division and cell proliferation<sup>18</sup>. Interestingly, in *Jabri et al*, the authors suggested that for *in vivo* IELs, the survival signal may come from IL15 and not IL2<sup>14</sup>. It is due to the fact that IL2 is not produced at high level by antigen presenting cells or epithelial cells, while IL15 is readily made and trans-represented by both of these cell types<sup>40</sup>. In addition, IL2 can be very rapidly consumed by Treg and CTLs in the lamina propria, making it hard to reach the sufficient level to promote the survival of IELs<sup>41</sup>. In contrast, due to the close proximity between epithelial cells and IELs, and the high affinity of the trans-representation (ten folds higher for IL15 than IL2), IELs can be sustained easier by IL15. Therefore, at physiological conditions, the cytokine that promotes the survival of IELs should be IL15 rather than IL2.

The second role of IL15 is to lower the TCR activation threshold, enabling IELs to carry out their cytolytic effector functions<sup>14</sup>. From traditional concept, in order for a naïve or central memory T cells to

be activated, they need two signals: one from the TCR stimulation with cognate antigens, and another one from co-stimulation of co-receptor such as CD28<sup>42</sup>. In the case of effector T cells, such as IELs, it is initially thought that the activation requires one signal from TCR recognition of cognate antigens (without the need of costimulatory molecules)<sup>43</sup>. However, recent studies have debated this notion as only partially true. *In vitro* activation of effector CD8<sup>+</sup> T cells via high dose of anti-TCR stimulation can only result in low level of cytokines production. This observation suggests that a secondary costimulatory signals from the environments is still needed<sup>11</sup>. IL15 has been argued to be such costimulatory signal<sup>14</sup>. Indeed, in the presence of IL15, gluten specific T cells can kill non-specifically and mediate villous atrophy in celiac disease<sup>44</sup>. In this case, IL15 has been shown to act through phosphoinositide 3 kinase (PI3K) and MAPK in a similar fashion as CD28 co-stimulation.

Last but not least, the third role of IL15 is to induce lymphokine-activated killer activity (LAK activity) in IELs, or “license IELs to kill” based on the presence of stress signals rather than the typical cognate antigen<sup>14</sup>. LAK activity is defined as the ability of a cytokine (such as IL15) to induce cytotoxic functions of IELs to kill in a TCR independent manner or in the absence of MHC class I molecules<sup>14</sup>. This function of IL15 is particularly important in the context of mucosal immunity. In various mucosal infections such as mycobacteria, viruses, and listeria, pathogens can downregulate MHC class I to escape TCR recognition by patrolling IELs<sup>1</sup>. In an evolutionary arm race to counter this strategy, the local infected cells (such as stressed epithelial cells) can produce IL15 as a “danger signal” to license IELs to kill. IL15 can induce LAK activity via two mechanisms: promote the expression of various activating NK receptors and act in synergy as a costimulatory signals (similar to the second role discussed above) to facilitate the release of cytotoxic molecules<sup>45,46</sup>. For example, when the pathogens downregulate MHC class I, epithelial cells can respond by producing IL15 in the local environment, and expressing stress markers such as MICA and MICB on their surfaces. In turn, IL15 induces the expression of activating NKG2D receptor and CD94 on IELs<sup>47</sup>. With the help of NKG2D-CD94, IELs can recognize MICA and MICB on infected and stressed

epithelial cells and proceed to kill without the need of the traditional TCR - cognate antigens recognition<sup>48</sup>. IELs now can circumvent the escape strategy of the pathogens to carry on their protective function. In addition, IL15 can act in synergy with the signals through the NKG2D receptors to mediate a stronger and robust cytotoxic response independent of TCR. Indeed, IL15 has been shown to upregulate the PI3K-JNK-ERK pathway to activate cPLA2 molecules to act in synergy with the NKG2D-DAP10 signaling, enabling IELs to make perforin, granzyme B, IFNy in large amount without the need of TCR activation<sup>49</sup>. Altogether, IL15 can license IELs to kill via NK receptors.

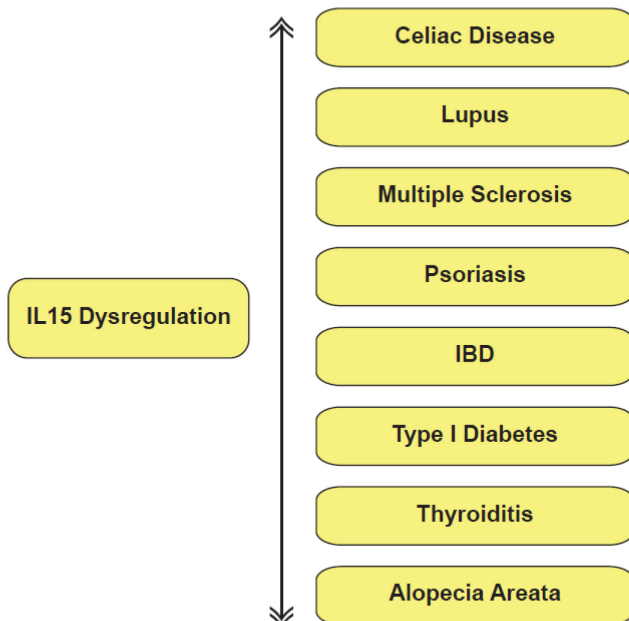


**Figure 2: Autoimmune disorders associated with dysregulation of IL15**

Due to IL15's important functions in IELs, dysregulation of IL15 has been implicated in many autoimmune disorders such as coeliac disease, psoriasis, rheumatoid arthritis, type I diabetes, inflammatory bowel disease (IBD) and lupus<sup>50-55</sup>. Epigenetic dysregulation has also been shown to be strongly associated with autoimmune disorders<sup>56,57</sup>. However, there has been no previous study to look at epigenetic during IL15 signaling. There is no previous attempt to explore the link between IL15

dysregulation, epigenetic dysregulation and autoimmune disorders. Therefore, we started to become interested to explore if IL15 signaling involves epigenetic regulations. Yet, there were other underlining reasons prior to the conception of the research, as explained in the following session.

#### 1.4 Known molecular signaling pathways of IL15 in IELs

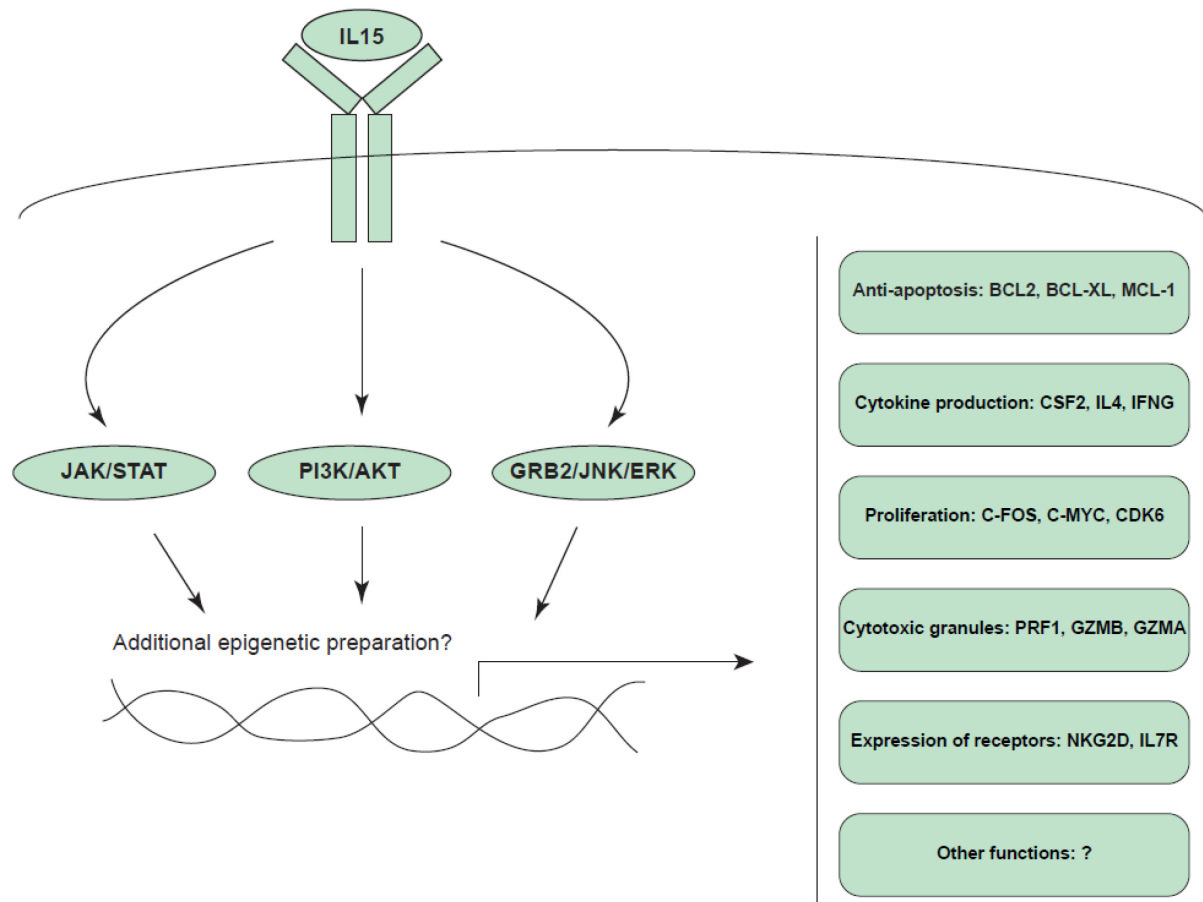


**Figure 3: Molecular signaling of IL15 in IELs and target genes**

IL15 signals through three main molecular pathways: JAK/STAT, PI3K/AKT, and JNK/ERK (MAPK) to control a large set of genes with diverse biological functions from anti-apoptosis, cytokine production, proliferation, cytotoxic granules production and receptors expression.

One of the most striking aspects of IL15 signaling pathways is the diversity of its target genes. In a study to compare and contrast between IL15 and IL2, the Garcia lab has shown that IL15 controls as much as 4776 genes in peripheral blood CD8<sup>+</sup> T cells in mice<sup>31</sup>. The total number of IL15 regulated genes is significant because there are only around 20,000 genes in the human genome, and other cytokines that utilize the  $\gamma_c$  chain do not activate as much targeted genes. For example, IL21 has been shown to activate as low as 300 genes in IELs (unpublished data – Jabri lab). In addition, IL-15 target genes belong to different and non-overlapping gene sets with distinct functions, ranging from proliferation, anti-apoptosis, immune activation, cell cycle to maintenance of genomic stability<sup>21,58</sup>. It is oversimplified to attribute all the transcriptomic program to the regulatory expression of transcriptional factors. It has been known that epigenetic can change the chromatin architecture and accessibility, and alter the available motifs and binding sites of transcriptional factors<sup>59</sup>. However, none has been known about the chromatin landscape or the epigenetic change in IELs under IL15. We hypothesized that there must be additional layers of regulatory mechanism to control such large and diverse transcriptomic program, and epigenetic can play a role in IL15 signaling. Therefore, we set out to characterize the epigenetic landscape underlining IL15 signaling cascade.

Before studying the unknown epigenetic landscape, it is useful to consider what have been known about the molecular cascades under IL15. There are three major IL15 driven pathways in IELs. First, upon the binding of IL15 to the receptor complex IL15R $\beta$ / $\gamma_c$ , the IL15R $\beta$  activates JAK1 and subsequent phosphorylation of STAT3 while the  $\gamma_c$  activates JAK3 and subsequent phosphorylation of STAT5<sup>60,61</sup>. STAT3 and STAT5 can form homodimers or heterodimers, and translocate inside the nucleus to activate transcription of downstream genes<sup>62</sup>. The target genes of the JAK/STAT pathway are anti-apoptotic genes such as BCL2, BCL-XL, MCL-1, cytotoxic genes such as GZMA, GZMB, IFNG, and pro-oncotic genes such as C-MYC, C-JUN, and C-FOS<sup>63</sup>.

Secondly, IL15 can function through phosphoinositide 3-kinase (PI3K) and AKT serine/threonine kinase 1 (AKT) pathway<sup>18</sup>. Upon binding to its receptor, IL15 utilizes an adaptor protein SHC to activate growth factor receptor bound protein 2 (GRB2). Next, GRB2 activates GAB2/VAV, then PI3K and finally AKT via phosphorylation. AKT has been an important master regulator that affects cell growth, cell proliferation, and cell survival<sup>64</sup>. AKT activates the TSC1/TSC2 and mTORC signaling to induce robust cell growth. AKT inhibits FOXO transcriptional factor to shut down pro-apoptotic gene expression such as BID, BIM and BAD. AKT phosphorylates the CDK inhibitors p21 and p27 to induce cell proliferation. Finally, AKT upregulates NF $\kappa$ B pathways to activate proinflammatory responses in IELs<sup>65</sup>.

Third and last, IL15 via SHC can phosphorylate and activate GRB2, which in turn can exchange GDP to GTP and activate the RAS/RAF pathway<sup>66</sup>. RAS/RAF cascade activates mitogen-activated protein kinase (MAPK) pathways. In IELs, IL15 signals through the conventional MAPKs: extracellular signal-regulated kinases (ERKs) and c-Jun N-terminal kinases (JNKs)<sup>14</sup>. The downstream targets of ERK/JNK overlap with the ones of JAK/STAT pathways, which are pro-survival and anti-apoptotic genes, cytotoxic genes, NF $\kappa$ B pathways and proliferative genes<sup>67</sup>.

Altogether, IL15 has acted upon three distinct molecular pathways to carry out its cellular and immune functions: the JAK/STAT pathway, the PI3K/AKT pathway, and the MAPK pathway. However, the epigenetic landscape throughout this signaling processes has not been studied. Due to the implications of IL15 in autoimmune disease, and the fact that many autoimmune disorders have altered epigenetic landscape, it is important to explore if epigenetic involves in normal IL15 signaling (before investigating what has gone wrong with epigenetic in the context of IL15 implicated autoimmune disorders).

## **1.5 Epigenetics - chromatin accessibility and histone modifications**

Epigenetic is the term coined in 1942 by Waddington, in which he defined epigenetic as changes in phenotype without changes in genotype<sup>68,69</sup>. With recent advances in sequencing technologies, and

epigenome mapping techniques, we have a better understanding of such phenomenon<sup>70</sup>. Most cells in our bodies have the same genomic sequence on the DNA level; however, the gene expression patterns are different based on tissues, differentiated states, local environments, molecular signals etc.... Epigenetic is one of the mechanisms in which gene expression pattern can be altered without changing the genotype. There are many notable examples of epigenetic controls: chromatin remodeling, histone variant and exchange, 3D interaction of chromatin structures, histone modification, DNA methylation, long non coding RNA and many more<sup>71-73</sup>. In this dissertation, we explored the three well characterized epigenetic controls: chromatin accessibility, histone modifications and DNA methylation in the context of IL15 and IELs.

DNA of eukaryotes is wrapped around histone octamers (147 bp of DNA wrapped around histones H2A, H2B, H3 and H4) to form a fundamental unit of chromatin: the nucleosome. The complexity of chromatin structure can be used as a regulatory mechanism for gene expression. At the primary structure, the location of nucleosomes, the modifications on histones, the histone variants can affect the compact of DNA packing<sup>74</sup>. Loosely packed DNA and histones can allow transcription of genes, and these chromatin state is called euchromatin. On contrary, tightly packed DNA and histones inhibit gene expression, and the chromatin state is called heterochromatin. On secondary and tertiary structure levels, the 3D structure and interactions of different chromatin domains can add additional regulatory mechanism. In this thesis, we will look at the histone modifications throughout the course of IL15 stimulation. Histone modifications has been shown to carry epigenetic information: a theory called the histone code. It is as followed: the combinational patterns of histone modifications can recruit specific “readers” and “writers” to regulate gene expressions, and influence distinct biological outcomes<sup>74</sup>. The four well studied histone marks are H3K4me3, H3K4me1, H3K27Ac, and H3K27me3; and in this thesis, we monitored them to investigate the dynamic of histone architecture in IELs during IL15 signaling.

H3 Lysine 4 trimethylation (H3K4me3) is associated with the transcriptional start sites (TSS) and promoter regions of genes. H3 Lysine 27 acetylation (H3K27Ac) is associated with actively transcribed genes, and this mark can be found in many genomic regions: on enhancers, promoters and gene bodies. H3 Lysine 4 monomethylation (H3K4me1) is associated with enhancer sites. H3 Lysine 27 trimethylation (H3K27me3) is a repressive mark that correlates with heterochromatin and DNA methylation. The combinations of these histone marks are meaningful to identify epigenetic regulatory elements in specific cell types or tissue<sup>75,76</sup>. In particular, active promoters (defined by the binding of RNA polymerase II in the promoters, and actively transcription of such genes) are enriched for both H3K4me3 and H3K27Ac. Active enhancers are enriched for both H3K4me1 and H3K27Ac. Poised promoters have both H3K4me3 and the repressive mark H3K27me3, the phenomenon called bivalency. During the course of differentiation, or responses to stimulus, the enhancers can lose H3K27me3 and become active. Primed enhancers are not yet active and marked with H3K4me1. The addition of H3K27Ac at a later state will convert these prime enhancers to active enhancers. Finally, latent enhancers are enhancers without any histone marks, and generally are close chromatin. Monitoring these 4 well characterized marks can review new regulatory elements and new open chromatin due to immune responses to cytokine or local environment.

## 1.6 Epigenetics - methylation, demethylation, 5hmC and Tet enzymes

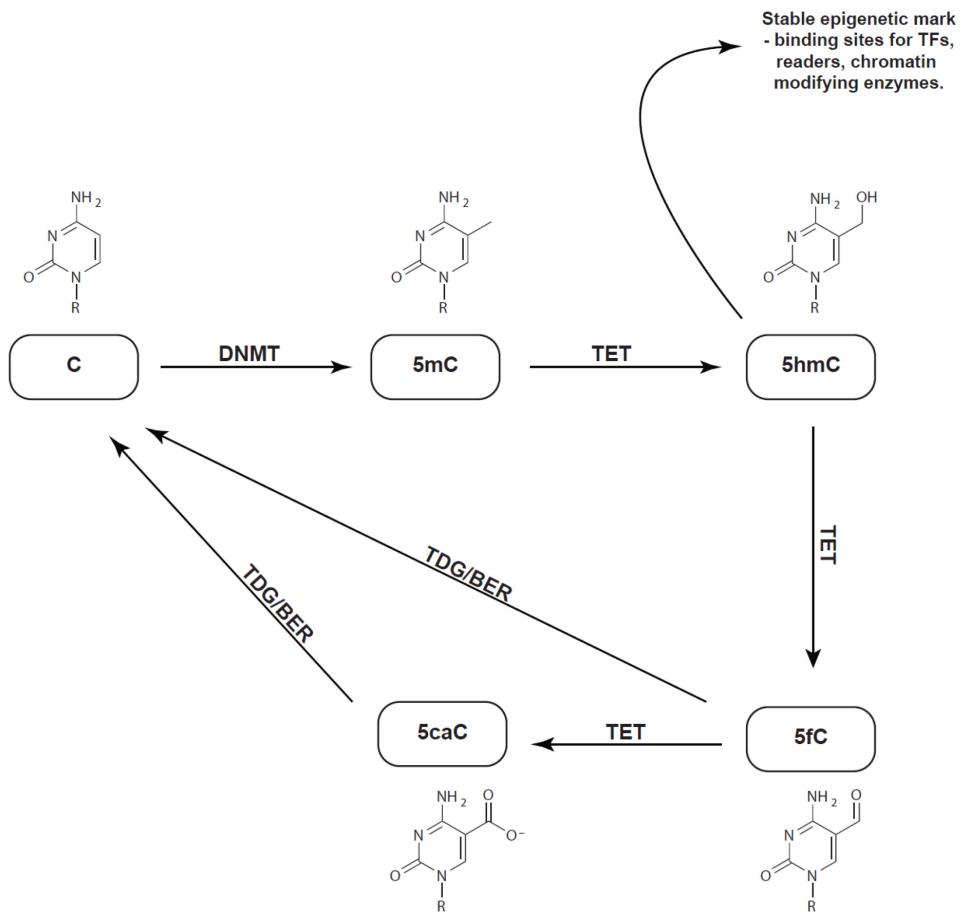


**Figure 4: The cycle of Tet mediated active DNA demethylation**

Cytosine (C) can be methylated to 5-methylcytosine (5mC) by DNA methyltransferases (DNMTs). 5mC can be further oxidized by ten-eleven translocation (TET) enzymes to 5-hydroxymethylcytosine (5hmC), 5-formylcytosine (5fC) and 5-carboxylcytosine (5caC). 5fC and 5caC can be excised out via thymine DNA glycosylase (TDG) followed by base excision repair (BER) to demethylate and restore the unmodified cytosine (C). Alternatively, 5hmC can be a stable epigenetic mark, acting as a binding site for potential transcriptional factors (TFs), 5hmC binding proteins as readers and chromatin modifying enzymes.

5-methylcytosine (5mC) has been called the fifth base in the mammalian genome due to its abundance and relevance in transcriptional regulation. 5mC is particularly abundant on the CpG islands (estimated around 60-80% of CpG islands are methylated), and 5mC constitute around 1% of the total

nucleotides in mammalian genome across different tissue types<sup>77</sup>. 5mC is installed and maintained by the family of DNA methyltransferase (DNMT) proteins. DNMT3A and DNMT3B are *de novo* methyltransferases which can introduce new 5mC marks on DNA in specific scenarios for example: stem cell differentiation. DNMT1 is the maintenance methyltransferase in which during replication, DNMT1 use the hemi-methylated CpG as substrate to reproduce the 5mC patterns on the newly synthesized DNA strand of daughter cells. In general, 5mC is shown to be a repressive mark, in which high level of 5mC on promoter or enhancer can impede the binding of RNA polymerase II, and stop transcription<sup>73</sup>. 5mC has been widely used to regulate gene expression in many biological processes such as genomic imprinting, X chromosome inactivation<sup>78</sup>, stem cell differentiation, developmental processes, cancer and diseases' development<sup>79</sup>. It has long been thought 5mC is very stable, therefore 5mC dynamics has been studied mostly in a long time scale (in term of days): for example in the context of cell fate determination, developmental stages and in cancer<sup>80,81</sup>. For example, genome wide loss of 5mC has been observed during different stages of preimplantation embryos and primordial germ lines between day 1 and day 15<sup>82-84</sup>. However, it remains unknown if 5mC can change in short time frame until the recent discoveries of active demethylation and the ten-eleven translocation (TET) proteins.

In 2011, in a series of publications, 5mC is shown to be oxidized to 5-hydroxymethylcytosine (5hmC)<sup>85,86</sup>. The oxidation can go further to 5-formylcytosine (5fC) and 5-carboxylcytosine (5caC) by the Tet enzymes<sup>87</sup>. At the 5fC or 5caC level, the 5fC-G or 5caC-G pairings can be recognized as a mismatch and excised out by thymine DNA glycosylase (TDG). Through further base excision repair (BER) steps, the unmodified cytosine will be restored<sup>88,89</sup>. It has also been suggested that 5caC can undergo decarboxylation and 5hmC can undergo deamination to convert back to C through BER<sup>90-92</sup>. Altogether, it has been shown that Tet can rapidly demethylase 5mC to restore unmodified cytosine in a process that is called active demethylation<sup>93</sup>. Dynamic *in vitro* studies have indicated the demethylation processes can occurs as quickly as 10 minutes, even though in such studies, the concentration of Tet and DNA template

can be non-physiological. *In vivo* studies of 5hmC in responses to vitamin C, 5hmC has been shown to change in term of hours<sup>94</sup>. Therefore, this oxidation process can have relevant biological functions in the short time scale, suitable to investigate in immune systems (many immune responses can occur quickly in term of minutes after ligand-receptor recognition).

The abundance of 5caC is around .0003% of cytosine, and of 5fC is around .002% cytosine<sup>95,96</sup>. Due to the low abundance of these two marks, they are thought to be transient, and intermediate step during the demethylation processes. 5caC and 5fC are either unstable or are removed quickly by BER; therefore, the appearances of these marks are extremely low. On the contrary, 5hmC can be detected at relatively medium level in both human and mice, for example around 0.1% of cytosine in stem cells, and around 0.03-0.1% in many cancer cell types<sup>97</sup>. 5hmC level is dependent on the cell type and the tissue type, with the most abundance in the brain tissue. Initially, 5hmC is thought to be an intermediate for the demethylation process; however, recent studies has shown that 5hmC can be stable for a long period of time, and 5hmC can function as a new epigenetic mark<sup>98</sup>. 5hmC marks can be binding sites of various transcriptional factors, chromatin remodeling enzymes to exert its biological functions. However, the identification of 5hmC binding partners has been difficult, with only one readers known so far: MBD3, MECP2, and SALL4A<sup>99</sup>.

Tet proteins and 5hmC have played important roles in many biological contexts. After fertilization, active demethylation by Tet3 on both human and mouse zygotes has led to global gain of 5hmC and loss of 5mC<sup>100,101</sup>. Mammalian primordial germ cells (PGC) has undergone Tet1 mediated oxidation of 5mC and active demethylation from stage E9.5 to E13.5<sup>102</sup>. During hematopoietic stem cell differentiation, Tet2 and Tet3 knock down have altered the HSC transcriptomes and skewed the differentiation into myeloid lineages<sup>103</sup>. During the *in vitro* differentiation of Th0 into Th1 and Th2 cells, active demethylation has occurred on lineage specific genes. For example, gain in 5hmC and loss in 5mC has occurred on IFNg locus on Th1, and IL4 locus on Th2 cells<sup>104</sup>. Tet2 mediated demethylation is necessary to activate cytokines

expression in CD4<sup>+</sup> T cells<sup>105</sup>. Double knockdown of Tet2 and Tet3 affect lineage specification and TCR mediated expansion of iNKT cells<sup>106</sup>. Due to the involvement of Tets and 5hmC in various immunological systems, it has been logical to follow up on the roles of 5hmC in our IL15 system.

### 1.7 Hypothesis and the novelty of our research

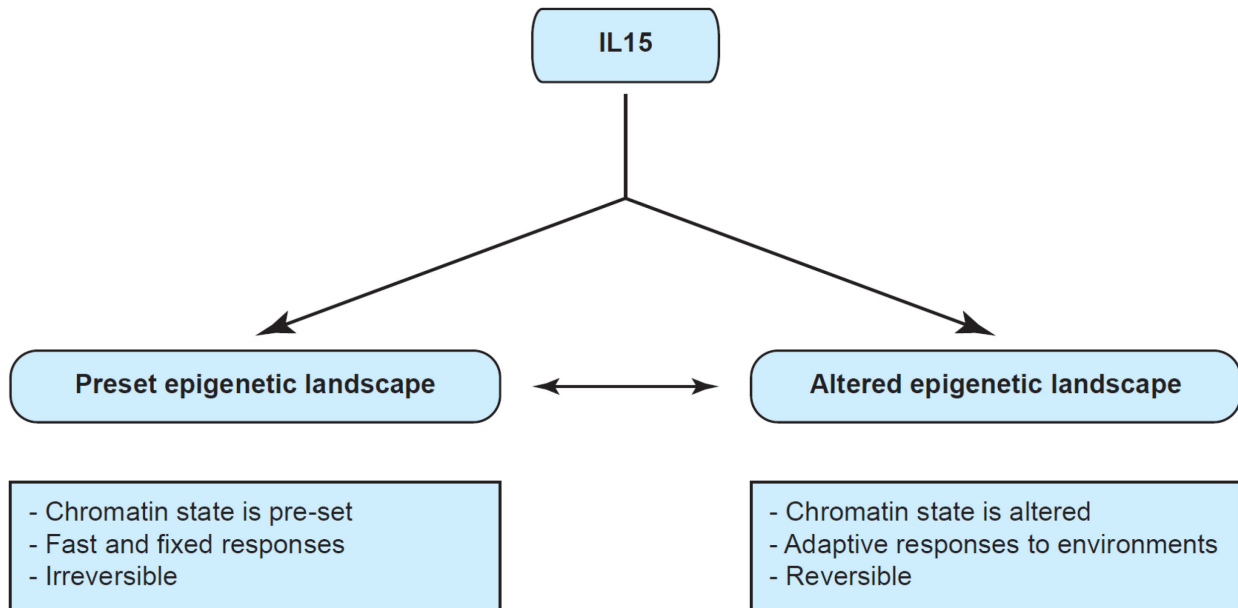


**Figure 5: Hypothesis on whether IL15 acts on a preset or altered epigenetic landscape**

The novelty of the research can be understood from two different angles. First, both IL15 dysregulation and epigenetic dysregulation have been linked extensively to the development of various autoimmune disorders. Specifically, in celiac disease, the non-specific killing of epithelial cells of IELs has been thought to be associated with high level of IL15<sup>44</sup>. Therefore, at the first step, it is important to understand if IL15, IELs and epigenetics can be connected.

Second, there have been extensively studies on how IL15 regulates its large and diverse target genes in human IELs. However, most studies attribute the regulation of such complex molecular network

to phosphorylation events and the expression and translocation to nucleus of three transcriptional factor families (STAT, MAPK and AKT). The explanation is oversimplified, and overlooks what could have occurred to the chromatin within the nucleus. Our study for the first time will map out various epigenetic marks throughout the process of IL15 signaling, and try to investigate if epigenetic preparation on the chromatin is necessary for the transcription of IL15's target genes.

Our hypothesis was that IL15 alters the epigenetic landscape of effector memory CD8+ IEL, and uses these epigenetic changes to promote large transcriptional changes to carry out its diverse biological functions.

### **1.8 The broader question: epigenetics and terminally differentiated T cells**

In a broader sense, this thesis will investigate the connection between epigenetic and terminally expressed T cells. In order to become a terminally differentiated T cells like IELs, T cells must have undergone two types of processes: development and differentiation (Figure 6)<sup>107-109</sup>. During development, the multipotent hematopoietic stem cells (HSC) response to different environmental signals to enter either myeloid or lymphoid lineage. In lymphoid lineage, the common lymphoid progenitors can further develop into either B lymphocytes, T lymphocytes or natural killer cells<sup>110</sup>. Epigenetic has been shown to be crucial for these developmental processes of immune cells. Demethylation occurs on POU2AF1, an important co-activator for mature B cells<sup>111</sup>. *De novo* methylations on myeloid specific genes such as

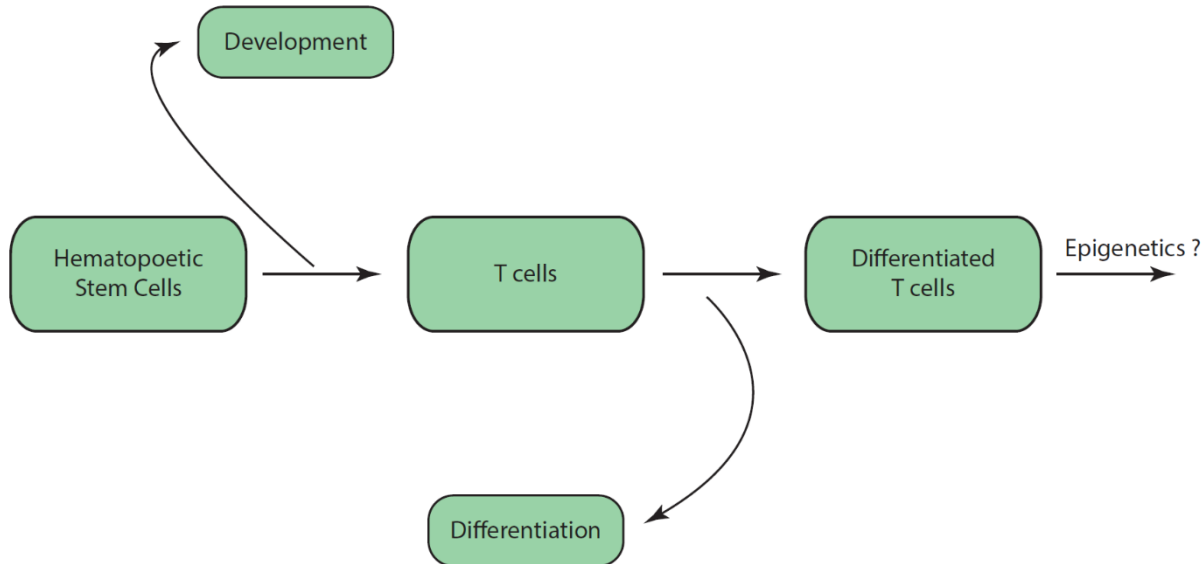


**Figure 6: The central question about the roles of epigenetics in terminally differentiated T cells.**

DACH1 and MEIS1 occur when a cell enters the lymphoid lineage<sup>112,113</sup>. All methylases such as DNMT1, DNMT3A and DNMT3B are important during development. The loss of DNMT1 can lead to hypomethylation and loss of self-renewal capability of HSC<sup>114</sup>. The commitment of HSC to enter either myeloid or lymphoid lineage leads to a global reduction of methylation<sup>115</sup>. The loss of both DNMT3A and DNMT3B results in global hypomethylation and an inability of HSC to exit the multipotent stage to enter lineage specific developmental stages<sup>103,116,117</sup>. On the other hand, TET demethylases play crucial roles as well for the development of HSCs. The loss of TET2 has screwed the development toward the myeloid lineage with the expense of the lymphoid lineage<sup>118</sup>. TET2 loss is further implicated with malignant transformation of the immune cells<sup>118,119</sup>.

After developmental processes, hematopoietic stem cells can commit to become T cells and newly developed naïve T cells continue to grow and differentiate. After leaving the thymus and enter the blood and the spleen, these T cells may encounter cognate antigens and start to differentiate into different subset of T cells: effector T cells, short term memory T cells and long lived memory T cells<sup>107,120</sup>. One again, epigenetic is central and fundamental for T cells' differentiation<sup>108</sup>. During the differentiation of T<sub>h</sub>0 CD4<sup>+</sup>

T cells into  $T_h1$  and  $T_h2$  CD4 $^+$  T cells, 5hmC and 5mC landscape are altered globally. Site specific demethylations occur at important loci such as IFNg for  $T_h1$  cells, and IL4 for  $T_h2$  cells<sup>104</sup>. During the response of a naïve T cells to bacterial infection, the histone landscape and chromatin accessibility of T cells are significantly changed<sup>59</sup>. The distributions of H3K27me3 and H3K27Ac marks are distinct between different stages of differentiation (naïve, effector or memory stages)<sup>121</sup>. During the response of T cells to chronic viral infection, the epigenetic landscape is vastly modified, especially in enhancers of RAR, T-BET and SOX-3 genes<sup>122</sup>. Altogether, the evidences suggest that epigenetic changes are essential to the development and differentiation processes for immune cells, specifically the T cells.

Yet even after the development and the differentiation into terminally differentiated CD8 $^+$  T cells, IELs still have to survey the environment and response to potent environmental signals (such as IL-15) or pathogens. Does epigenetic still play crucial roles for the functions of these terminally differentiated cells? Or are epigenetic changes only required for differentiation and development in which one cell type change to a different cell type and no longer required after these processes? In the literature, there has been very few studies to investigate such question, and none has looked at the roles of epigenetic in IELs' function. There is one recent publication in which long exposure of IELs to IL15 has increase the genome instability and hypermethylation, transforming the IELs to malignant leukemic IELs<sup>123</sup>. Therefore, we were encouraged by the potential link between epigenetic, IELs and IL-15 signaling. We decided to commit to this thesis project. For the first time, with this research, we hope to gain insights into the broader question if epigenetic change is essential for the functions of a terminally differentiated CD8 $^+$  T cells such as IELs' response to the environmental signal of IL-15.

## 1.9 Scope of thesis

My thesis focused on characterizing the epigenetic landscape changes occurred during IL15 signaling in human intraepithelial lymphocytes.

Chapter 1 is the introductory chapter to the concept of intestinal immune system, intraepithelial lymphocytes, interleukin 15, epigenetic, and examples of epigenetic changes in similar immunological context to IL15.

Chapter 2 presents the methods and experimental designs of the study.

Chapter 3 presents the transcriptomic changes induced by IL15 on human intraepithelial lymphocytes. The transcriptional profiles are obtained at 0h, 2h, 4h and 24h post IL15 stimulation. There will also be the information on novel long noncoding RNA involved in the signaling processes.

Chapter 4 presents the study of chromatin accessibility, histone modifications, and 5hmC changes throughout IL15 signaling. The changes in epigenetic are examined in connection with the gene expression in order to understand the relevance of these epigenetic changes.

Chapter 5 presents the roles of Tet2 in the generation and modification of 5hmC peaks and the impact of Tet2 knockdown on IL15 mediated functions of IELs.

Chapter 6 summarizes and discusses the findings in the thesis as well as the future direction of research.

## CHAPTER 2: METHODS

### 2.1 The isolation of human intraepithelial lymphocytes fraction

Duodenal biopsies were collected from consented patients from the University of Chicago. Biopsies were shaken for 20 minutes under 37°C and 250 rpm in a tube with IELs isolation medium (RPMI, 1% dialyzed FCS, 2mM EDTA and 1mM MgCl<sub>2</sub>). Biopsies were then transferred to 7ml of another pre-warmed tube of IELs isolation medium for a second shake of 20 minutes under 37°C and 250 rpm. After the second shake, biopsies were removed. Both tubes were spin at 1600 rpm for 10 minutes to collect the IELs fraction (IELs, intestinal epithelial cells (IECs), stem cells etc...). The IELs fraction was suspended in new RPMI medium + 10% human AB serum (Corning) + GPS. The IELs fraction would then be ready for staining and sorting for pure CD45<sup>+</sup>CD3<sup>+</sup>TCR $\alpha\beta$ <sup>+</sup>CD8a<sup>+</sup> IELs.

### 2.2 The sort of CD45<sup>+</sup>CD3<sup>+</sup>TCR $\alpha\beta$ <sup>+</sup>CD8a<sup>+</sup> intraepithelial lymphocytes

The IELs fraction was stained with the following fluorophore conjugated antibodies (clones in parentheses) – Aqua LIVE/DEAD Fixable stain kit (Thermo Fisher Scientific), CD45 BV711 (HI30) (BD Biosciences), CD3 APC-Cy7 (UCHT1) (Biolegend), TCR $\alpha\beta$  BV421 (IP26) (Biolegend), and CD8a BUV496 (RPA-T8) (BD Biosciences). The IELs fraction was initially stained with Aqua LIVE/DEAD for 10 minutes at 4°C. Then the cells were stained with the mixture of the above antibodies in 100ul Flow Cytometry Staining Buffer (eBioscience) for 30 minutes at 4°C. The cells were wash two times with Flow Cytometry Staining Buffer. Sorting experiments were performed with the Aria Fusion (BD Biosciences). The gating strategy was as follow: gating on live / single cells then CD45<sup>+</sup> and CD3<sup>+</sup>, followed by TCR $\alpha\beta$ <sup>+</sup> and CD8a<sup>+</sup>. Sorted IELs were collected and used to generate short termed IEL lines via the following protocol.

### **2.3 The generation of short termed human IEL cell lines**

Freshly sorted IELs were washed in PBS, collected by centrifugation at 1700 rpm for 10 minutes. IELs were suspended in a small volume of 100ul of medium (RPMI + 10% human AB serum). A minimum of 5 IEL cells is needed to generate a short term IEL cell line. A master mix of human peripheral blood mononuclear cells (PBMCs) from 2 donors and EBV cells (Epstein Barr transformed B cells) was prepared at the ratio 5M PBLs to 0.5M EBVs in 10ml medium (RPMI + 10% human AB serum) for the stimulation of 0.5M of IELs. Adjust the volume of the master mix, the amount of PBMCs and EBVs proportionally depends on the number of sorted IELs to be stimulated. PBMCs can be prepared from buffy coats following by Percoll isolation protocol (GE Health Life Sciences). Prior to stimulation, the PBMCs and EBVs were irradiated with 3,000 RAD for 10 minutes to stop them from proliferating. pPHA-L (EMD Millipore) was added to the master mix to the final concentration of 1ug/ml. Interleukin 2 (IL-2) (Roche) was added to the final concentration of 100u/ml. The master mix was then added to the IELs and the stimulation begins. If the amount of sorted IELs is less than 10,000 IELs, IELs should be stimulated in a 96 well plate. Stimulated IELs were incubated at 37°C and 5% CO<sub>2</sub>. IELs were split as needed, and each time when new medium was added, IL2 was added as well to the new medium to reach final concentration of 100u/ml. IELs were collected and frozen as short term cell lines after 10-15 days based on the status of the IELs. IELs were ready when less than 10% of IELs were blasting (based on the FSC/SSC scatters) and more than 90% IELs were healthy.

### **2.4 Interleukin 15 stimulation**

Short termed IEL cell lines were cultured in RPMI medium + 10% human AB serum +GPS (Corning) with 100u IL2/ml (Roche) for 10-13 days. IELs were ready when they have less than 10% proliferating cells (as seen by FSC/SSC in FACS Canto) and more than 90% healthy. The IELs were starved in fresh RPMI medium + 10% human AB serum (Corning) without IL2 for 48 hours to remove the effect of IL2 and rest

the IELs prior to IL15 stimulation. At the day of IL15 stimulation, IELs were counted and put in new medium at the concentration of 1M IELs/ml and rested for at least 2 hours prior to experimental procedures. IL15 (Biolegend) was added to the medium to stimulate IELs (with the final working concentration of 10 ng/ml). IELs were collected at 0h, 2h, 4h and 24h post IL15 stimulation and subjected to further assays to analyze the transcriptomes or various epigenetic marks.

## **2.5 RNA isolation and RNA-Seq**

RNA from IELs was isolated using all prep DNA/RNA/miRNA universal kit (Qiagen) following the manufacturer's protocol. RNA libraries were made with Ribo-Zero Gold kit and TruSeq RNA Library Prep kit (Illumina) and sequenced using 50-bases single-end reading on a HiSeq 2500 instrument (Illumina). Reads were mapped to the human genome using Tophat2. The bioinformatics analysis was discussed in details in the statistics session.

## **2.6 ATAC-Seq**

ATAC-seq library preparations were performed as described in Buenrostro et al<sup>124</sup>. 50,000 IELs from short term cell lines were stimulated with IL15 and collected at 0h, 2h, 4h and 24h post stimulation. Cells were washed one time with 50 ul cold PBS, collected via centrifugation at 500g at 4°C. IELs were lysed in 50ul cold lysis buffer (10 mM Tris-HCl, pH 7.4, 10 mM NaCl, 3 mM MgCl<sub>2</sub>, 0.1% IGEPAL CA-630), and the nucleus were collected via 500g for 10 minutes at 4°C. The nucleus extracts were labelled with Nextera transposition mix (Illumina) (25ul TD buffer, 2.5ul Nextera Tn5 transposase, 22.5 ul H<sub>2</sub>O) for 30 minutes at 37°C. Reactions were purified immediately after with Qiagen Min Elute kit (Qiagen). PCR amplification were done with 10-13 cycles with pair-ended Nextera barcoded primers (Illumina). The PCR reaction was set up as followed: 10ul of transposed DNA, 10ul of H<sub>2</sub>O, 2.5 ul of Nextera PCR primer 1, 2.5 ul of Nextera PCR primer 2, and 25ul of NEBNext High-Fidelity PCR master mix. A smaller set of this PCR

reaction was run first with SYBR Green I (Invitrogen) to determine the appropriate number of cycles to stop amplification prior to saturation condition (selecting the number of cycles to reach  $\frac{1}{4}$  maximum fluorescent intensity). The thermal cycles were as followed: 1 cycle of 98°C for 30 sec, n cycles of 98°C for 10 sec, 63°C for 30 sec, 72°C for 1 min with n as the necessary number of amplification cycles. Amplified libraries were purified with Qiagen Min Elute columns. ATAC-seq libraries were sequenced using 100-bases pair-end reading on a HiSeq 2500 instrument (Illumina). Reads were mapped to the human genome using Tophat2. Detailed bioinformatics analysis was included in the upcoming statistical session.

## **2.7 ICE-CHIP for native histone pull down**

The ICECHIP protocol followed the native histone CHIP protocol from the Dilworth lab<sup>125</sup> and the ICECHIP protocol from the Ruthenburg lab<sup>126</sup>. The procedure was done with collaboration and help from Adrian Grzybowski in the lab. The detailed protocol bellowed was quoted from Grzybowski et al<sup>126</sup> with specific modification for IELs.  $10^6$  IELs were stimulated with IL15 and collected at 0h, 2h, 4h and 24h post stimulation. Cells were washed twice with 1ml of PBS, twice with 1ml of buffer N (15mM Tris pH 7.5, 15mM NaCl, 60mM KCl, 8.5% sucrose, 5mM MgCl<sub>2</sub>, 1mM CaCl<sub>2</sub>, 1mM DTT, 200uM PMSF, 1x Protease Inhibitor Cocktail). Cells were suspended in 400ul of buffer N and lysed with 400ul of 2x lysis buffer (buffer N + 0.6% NP-40 substitute (Sigma)) for 10 minutes at 4°C. Nuclei were collected by centrifugation – 500g for 5 minutes at 4°C and suspended in 100ul of buffer N. The quantity and quality of nuclei were assessed with hemocytometer. 2ul of nuclei were diluted in 98ul of 2M NaCl in triplicates, and the concentrations of chromatin were measured by Nanodrop (Thermo Scientific), assuming 1 A<sub>260</sub> = 50 ng/ul. Based on the measurement, chromatins were adjusted to 1ug/ul.

The chromatins were subjected to MNase digestion, with 1U of MNase per 4ug of chromatins. Internal standards of various histone marks from the Ruthenburg lab were added to the samples. 100ug of total nuclei were mixed with 66mg of hydroxyapatite (HAP) resin (Biorad) rehydrated with 200ul of HAP

buffer 1 (3.42mM Na<sub>2</sub>HPO<sub>4</sub>, 1.58mM NaH<sub>2</sub>PO<sub>4</sub>, pH 7.2, 600mM NaCl, 1mM EDTA, 200uM PMSF). Nuclei were incubated 10 minutes at 4°C and subsequently applied to filter (Millipore Ultrafree MC-HV 0.45 um). The chromatin-loaded resins were drained and washed four times with 200ul HAP buffer 1, four times with HAP buffered 2 (3.42mM Na<sub>2</sub>HPO<sub>4</sub>, 1.58mM NaH<sub>2</sub>PO<sub>4</sub>, pH 7.2, 100mM NaCl, 1mM EDTA, 200uM PMSF) by centrifugation (600g, 1 minute at 4°C). Nucleosomes were eluted from HAP column with HAP elution buffer (342mM Na<sub>2</sub>HPO<sub>4</sub>, 158mM NaH<sub>2</sub>PO<sub>4</sub>, pH 7.2, 100mM NaCl, and 1mM EDTA, 200uM PMSF). To measure the concentration of purified chromatin fragments, 10ul of eluted samples were diluted in 40ul of 2M NaCl in triplicates, and absorbance was measured by Nanodrop (1 A<sub>260</sub> = 50 ng/ul). Chromatin fragments were diluted to 20 ug/mL with CHIP buffer 1 (25mM Tris pH 7.5, 5mM MgCl<sub>2</sub>, 100mM KCl, 10% (v/v) glycerol, 0.1% NP-40 substitute).

Antibodies used: H3K4me3 (Active Motif AM39139), H3K4me1 (RevMab RM175), H3K27Ac (Thermo Scientific RM172), and H3K27me3 (CST C36B11). The amount of antibodies used per IP were as followed: 3ug of H3K4me3 Ab per 1000ng of chromatin, 1ug of H3K4me1 Ab per 1000ng of chromatin, 1ug of H3K27Ac Ab per 1000ng of chromatin, and 1ug of H3K27Ac Ab per 1000ng of chromatin. 10% of initial chromatin for each IP was set aside as CHIP inputs. Each IP used 12.5ul of protein A Dynabeads (Invitrogen) washed twice with 200ul of CHIP buffer 1. Each antibody was incubated with protein A for 15 minutes on rotator. Beads were washed 3 times with 200ul of CHIP buffer 2 (25mM Tris pH 7.5, 5mM MgCl<sub>2</sub>, 300mM KCl, 10% glycerol, 0.1% NP-40 substitute), then twice with CHIP buffer 3 (10mM Tris pH 7.5, 250mM LiCl, 1mM EDTA, 0.5% Na-Deoxycholate, 0.5% NP-40 substitute). Each wash was 10 minutes on rotator and 1 minute on magnetic rack at 4°C. Beads were rinsed with 200ul of CHIP buffer 1 and 200ul of TE buffer. Beads were eluted with CHIP elution buffer (50mM Tris pH 7.5, 1mM EDTA, 1% SDS) for 5 minutes at 55°C.

Protein digestion was done with 200mM NaCl, 100ng of RNase A, and 20ug of proteinase K (Roche) for 2 hours at 42°C. 10ng of IP DNA was used to construct libraries with NEBNext Ultra II DNA

library prep kit (New England Biolab) and sequenced using 50-bases single-end reading on a HiSeq 2500 (Illumina). Bioinformatics analysis was discussed in details in the statistics session.

## 2.8 5hmC-Seal IP

Selectively 5hmC labeling and IP were done followed the previously described protocol of 5hmC-Seal<sup>127</sup>. IELs from short term cell lines were stimulated with IL15 and collected at 0h, 2h, 4h and 24h post stimulation. DNAs were isolated with Qiagen AllPrep DNA/RNA/miRNA Universal kit (Qiagen). 10ug of IELs DNA was the starting material for 5hmC-seal labeling and IP. DNA was fragmented by Diagenode Bioruptor (Diagenode) with 300 bp targeted size via 6 cycles of 30" on and 90" off. Fragmented DNA was collected and concentrated in 10ul with Qiagen Minelute columns (Qiagen). 5hmC labeling step was done in 100ul mixture of 10ug of IELs DNA, 3mM UDP-6-N3-Glc (Active Motif), 40uM  $\beta$ GT enzyme (homemade - the He Lab), 50mM HEPES pH 7.9, and 25mM MgCl<sub>2</sub>. The labelling mixture was incubated for 1h at 37°C. Labelled DNA was purified with Qiaquick Nucleotide Removal kit (Qiagen). The DNA was subjected to biotinylation reaction with 150uM DBSO-S-S-PEG3-biotin (Glick Chemistry Tool) for 2 hours at 37°C. Biotinylated DNA was purified with Qiaquick Nucleotide Removal kit (Qiagen) and suspended in 100ul of H<sub>2</sub>O. 50 ul of MyOne Streptavidin C1 Dynabeads (Invitrogen) was washed 3 times with 1ml of 1x B&W buffer (5 mM Tris-HCl pH 7.5, 0.5 mM EDTA, 1 M NaCl) and suspended in 100ul of 2x B&W buffer (10 mM Tris-HCl pH 7.5, 1 mM EDTA, 2 M NaCl). 100ul of biotinylated DNA was added to 100ul of prepared MyOne Streptavidin C1 Dynabeads and the mixture was incubated for 15 minutes at room temperature on a rotator. Beads were separated with a magnetic stand, and washed 3 times with 200ul 1x B&W buffer (5 mM Tris-HCl pH 7.5, 0.5 mM EDTA, 1 M NaCl). Finally, DNA was eluted from the beads via overnight incubation in 50mM DTT (Sigma) on a rotator at room temperature. DNA was purified with a Micro Bio-Spin 6 Column (Biorad), following with Qiagen Minelute columns (Qiagen). IP DNA was quantified via Qubit Fluorometer (Thermo Fisher Scientific) and 5ug of IP DNA was made into libraries with NEBNext

Ultra II DNA library prep kit (New England Biolab) and sequenced using 50-bases single-end reading on a HiSeq 2500 (Illumina). Bioinformatics analysis was discussed in details in the statistics session.

## 2.9 RT-qPCR and primer tables

RNA was isolated with RNeasy plus Mini Kit (Qiagen). cDNA was synthesized with Superscript III First Strand Synthesis System (Invitrogen) according to the manufacturer's protocol. 1pg-5ug of RNA, 50 uM oligo dTs and 10 mM dNTP were denatured at 65°C for 5 minutes, then annealed on ice for 5 minutes. 10ul cDNA synthesis mixture was made with 2ul 10x RT buffer, 4ul 25mM MgCl<sub>2</sub>, 2ul 0.1M DTT, 1ul RNaseOUT (40 u/ul), 1ul Superscript III RT (200u/ul). The mixture was added to the RNA, and run for 50 minutes at 50°C. The reaction was terminated at 85°C for 5 minutes. 1ul of RNase H was added to remove remained RNA. Gene expression analysis was performed in duplicate via real time PCR on LightCycler 480 (Roche) using SYBR Green (Clontech). Each 10ul reaction was set up as followed: 5ul of 2x SYBR Green, 2.5 ul of cDNA, 0.25 ul forward primer, 0.25ul reverse primer, and 2ul of H<sub>2</sub>O. Expression levels were normalized to human GAPDH expression. The list of primers were listed in the table below.

| Gene of interest | Forward Primer          | Reverse Primer          |
|------------------|-------------------------|-------------------------|
| TET1             | CAGAACCTAACCCACCCGTG    | TGCTTCGTAGGCCATTGTA     |
| TET2             | GGCTACAAAGCTCCAGAACATGG | AAGAGTGCCACTTGGTGTCTC   |
| TET3             | TCCAGCAACTCCTAGAACTGAG  | AGGCCGCTTGAATACTGACTG   |
| DNMT1            | AGGCGGCTCAAAGATTGGAA    | GCAGAAATTCTGTCAAAGAGATT |
| DNMT3A           | AGTACGACGACGACGGCTA     | CACACTCACGCAAAAGCAC     |
| DNMT3B           | AGGGAAGACTCGATCCTCGTC   | GTGTGTAGCTTAGCAGACTGG   |
| IFNG             | TCGGTAACTGACTTGAATGTCCA | TCGCTTCCCTGTTTAGCTGC    |
| GZMB             | CCCTGGGAAAACACTCACACA   | GCACAACTCAATGGTACTGTCG  |
| BCL-XL           | GAGCTGGTGGTTGACTTTCTC   | TCCATCTCCGATTCAAGTCCCT  |
| BCL2             | GGTGGGGTCATGTGTGTGG     | CGGTTCAGGTACTCAGTCATCC  |
| GAPDH            | ATGGGGAAGGTGAAGGTCG     | GGGGTCATTGATGGCAACAATA  |

**Table 1: Primers list for qPCR analysis**

## **2.10 siRNA against Tet2 and Tet3**

Tet proteins were knock down using Accell siRNA technology (GE Dharmacon) according to the manufacturer's manual. 100,000 IELs were collected and suspended in 100ul delivery medium (GE Dharmacon) with 100u of IL2 in a 96 well plate. Cells would be transfected with 1ul of 100uM siRNA against either scrambled control, Tet2 or Tet3 for 24 hours. The Accell siRNA was pre-coated with lipid particles to allow passive diffusion of siRNA constructs into the cells with minimal cell death. The next day, cells were spun at 1650 rpm and the medium would be exchanged to new, pre-warmed 100ul of delivery medium (GE Dharmacon) with no IL2. Cells would then be transfected with a second dose of 1ul of 100uM siRNA against either scrambled control, Tet2 or Tet3. Cells would be incubated for another 48 hours in 96 well plates at 37°C and 5% CO<sub>2</sub>. At the end of the siRNA knock down period, delivery medium was exchanged back to regular RPMI medium with 10% human AB serum (Corning) prior to subsequent experimental procedures such as IL15 stimulation or functional assays (proliferation quantification or ELISA). 10% of IELs would be collected separately to quantify the level of knock down via qPCR for Tet2 or Tet3 transcripts.

## **2.11 TCR + IL15 stimulation and FACS staining for cytokines production**

96 well plates were pre-coated with in 0.5ug/ml anti-CD3 antibody (eBioscience) in 200ul of sterile PBS overnight at 4°C. At the day of experiments, the plates were washed 2 times with 200ul of sterile PBS. 100,000 IELs (siCtrl, siTet2 or siTet3) were suspended in 100ul of medium with or without 10ng/ml IL15, and added to the pre-coated plates for TCR stimulation. Cells were collected at 3h and 6h post TCR stimulation. Cytokines secretion was blocked throughout the process with 1ul of Golgi Stop and Golgi Plug (BD Bioscience) per 1ml of IELs / medium. Intracellular cytokines staining for IFNg, TNF and GZMB were done with BD Cytofix/Cytoperm (BD Bioscience). Post TCR stimulation, IELs were fixed in 100ul of BD Cytofix/Cytoperm solution for 20 minutes at 4°C. IELs were then spun at 1800 rpm for 5 minutes to remove

the supernatant, and suspend again in 50ul of Perm/Wash buffer and conjugated antibodies – IFNg APC (4SB3) (Biolegend), TNF $\alpha$  PECy7 (Mab11) (Biolegend) and GZMB PE (QA16A02). The mixture was incubated for 30 minutes at 4°C. IELs were washed 2 times in Perm/Wash buffer prior to flow cytometry analysis. Samples were run on a FACS Canto II (BD Bioscience). Data was analyzed using FlowJo (Tree Star).

## **2.12 Edu functional assay**

To monitor the proliferation rate of IELs under siCtrl, siTet2 and siTet3 conditions, we performed the knock down of Tet as previously described in session 2.10. Post siRNA, IELs were stimulated with IL15 (10ng/ml) for a period of 48 hours. The proliferation rates of IELs were measured with the Click-it Plus EdU Imaging Kit (Thermo Fisher Scientific) according to manufacturer's manual. 10uM of edU was added to the medium at the time of IL15 stimulation. Negative staining controls were samples with no addition of edU. 48 hours post IL15 stimulation, the IELs were harvested and fixed with 3.7% formaldehyde in PBS for 15 minutes at room temperature. Next, IELs were washed twice with 3% BSA in PBS, following by permeabilization with 0.5% Triton X-100 in PBS for 20 minutes at room temperature. edU was labelled with Click chemistry in the following reaction mixture for 100,000 IELs: 44ul of 1x Click It reaction buffer, 1ul of copper protectant, 0.12ul of Alexa 647 picolyl azide, 5ul of reaction buffer additive (Thermo Fisher Scientific) for 30 minutes protected from light. Next, IELs were washed twice with 3% BSA in PBS. Samples were suspended in 100ul of PBS + 10% FCS per sample and run on a FACS Canto II (BD Bioscience). Data was analyzed using FlowJo (Tree Star).

## **2.13 Bioinformatics and statistical analysis**

*The following session is written by Alain Pacis, as all the bioinformatics analysis is done by Dr. Luis Barreiro and Alain Pacis from the University of Montreal.*

### **RNA-seq data processing and identification of differently expressed genes between conditions**

A total of n=40 RNA-seq samples were processed in this study (see Table SX). Adaptor sequences and low-quality score bases (Phred score < 20) were first trimmed using Trim Galore ([http://www.bioinformatics.babraham.ac.uk/projects/trim\\_galore/](http://www.bioinformatics.babraham.ac.uk/projects/trim_galore/)). The resulting reads were aligned to the human genome reference sequence (GRCh37/hg19) using the TopHat2 software package <sup>128</sup> with a TopHat transcript index from Ensembl. The number of read fragments overlapping with annotated exons of genes was tabulated using HTSeq <sup>129</sup> using the following parameters: -q -m intersection-nonempty -s no. For all downstream analyses, we excluded non-coding and lowly-expressed genes with an average read count lower than 10 in all of the treatment-genotype combinations, resulting in n=13,009 genes in total.

In order to interrogate the effect of TET2 on the transcriptional response of intraepithelial lymphocytes (IELs) to IL15 over the time-course (2, 4, and 24h), we used a nested linear model with the following design: Expression ~ Individual\*Genotype\*Stimulation. From this model, we extracted: 1) IL15 stimulation effects in WT samples; 2) IL15 stimulation effects in TET2KO samples; and 3) Difference between stimulation effects in WT and TET2KO samples (Stimulation × Genotype interactions). Nominal p-values provided by lmFit were corrected for multiple testing using the R package qvalue (<http://bioconductor.org/packages/release/bioc/html/qvalue.html>). The complete results of these DE analyses are reported in Table SX. We considered a gene as differentially expressed between non-stimulated and stimulated samples if statistically supported at an FDR < 0.01 and a  $|\log_{2}FC| > 0.5$ . An FDR cutoff of 0.1 was used to identify genes for which the response to IL15 stimulation is different across WT and KO samples.

### **Gene Set Enrichment Analysis**

We used ClueGO<sup>130</sup> to test for enrichment of functionally annotated gene sets among differentially expressed genes belonging to each cluster, and genes for which the response to IL15 stimulation is different across WT and KO samples. The following parameters were used when running ClueGO: Min GO Level = 3; Max GO Level = 8; Minimum Number of Genes associated to GO term = 15; Minimum Percentage of Genes associated to GO term = 15. The results for these enrichment analyses are reported in Table SX. Enrichment p-values were based on a hypergeometric test using the set of 13,009 genes as background. Benjamini-Hochberg method was applied for multiple testing correction.

### **ChIP-seq Data Processing and Differential Peak Analysis**

We started by trimming adapter sequences and low-quality score bases using Trim Galore. The resulting reads were mapped to the human reference genome using STAR<sup>131</sup> with the following options: --runThreadN 12 --readFilesCommand zcat --alignIntronMax 1. Only reads that had a unique alignment were retained and PCR duplicates were further removed using Picard tools (<http://broadinstitute.github.io/picard/>).

Peaks were first called on ChIP-seq samples (using respective input IPs as a control) using the MACS2 software suite<sup>132</sup> with the added parameters “-g hs -q 0.05 --keep-dup all”. For comparison between samples, all peaks from each sample were merged to provide one set of combined peaks. For quantification of the combined peaks, we used the bamutils count command from NGSUtils<sup>133</sup> to count the number of overlapping reads for each sample. To assess differences in levels of 5hmC and histone modification (H3K4me3, H3K4me1, H3K27ac, H3K27me3) between IL15 stimulated and non-stimulated samples, we used limma<sup>134</sup>. Peaks with low read counts were filtered from the differential analysis by first calculating the global median read count across all the samples. Peaks with a mean read count across samples in each condition lower than this median value were removed. The same strategy was also applied for ATAC-seq data. Differential peaks were used to determine the extent to which changes in

chromatin at basal state control the signal associated with the transcriptional response to IL15 stimulation.

### ATAC-Seq Data Processing and Footprinting Analysis

ATAC-seq libraries were generated from 100,000 cells, as previously described <sup>124</sup> and sequenced on an Illumina HiSeq 2500 using 100-bp paired-end reads. ATAC-seq reads were trimmed for adapter sequences and low-quality score bases and were mapped to the human reference genome. Mapping was performed using BWA-MEM <sup>135</sup> in paired-end mode at default parameters. Only reads that were properly paired and had a unique alignment (mapping quality > 10) were retained. PCR duplicates were removed using Picard tools.

To detect TF binding footprints in the ATAC-seq data we used the program <sup>136</sup> in two steps. In the first step, we determined which transcription factors were active in human intraepithelial lymphocytes (i.e., had motif instances with footprints) using a subset of high-confidence motif instance (10K) for each TF. Using this reduced set of motifs, we calculated a Z-score corresponding to the PWM effect in the prior probability in Centipede's logistic model. The Z-score corresponds to the  $\beta$  parameter in:

$$\log\left(\frac{\pi_l}{1-\pi_l}\right) = \alpha + \beta \text{ PWMscore}_l$$

where  $\pi_l$  represent the prior probability of binding in Centipede's model in motif location  $l$ . We considered a TF binding site as active if the estimate was supported at Bonferroni-corrected  $P < 0.05$  (a list of active TFs detected is provided in Table SX). We then scanned the entire genome for motif instances matching the original PWM of active TFs, and defined all putative binding sites for these TFs as those showing a footprint supported by a posterior probability  $\geq 0.99$ .

### **Enrichment of TF Binding Sites among classes of differentially expressed genes**

Peaks were first called on ATAC-seq samples using the MACS2 software suite. To assess which peaks of open chromatin harbor which TF binding sites, the putative binding sites (i.e., ATAC-seq footprints) were overlapped to these peaks.

Called peaks were then assigned to a gene with the closest TSS using HOMER annotate Peaks command<sup>137</sup>. Finally, we interrogated about the enrichment of specific TFs binding in the vicinity of genes (<100 kb distance) belonging to our six patterns of differential responses to IL15 throughout the time-course, using logistic regression test. Complete results of this test are reported in Table SX.

### **Visualization of Epigenetic Data**

Genome browser tracks were created with the genomeCoverageBed command in BEDTools <sup>138</sup> and bedGraphToBigWig utility from UCSC. Tracks were normalized so that each value represents the read count per base pair per 10 million reads. WashU Epigenome Browser <sup>139</sup> as implemented for track visualization.

Tag density profiles for chromatin modifications and genome accessibility patterns around regions of interest was accomplished with ngs.plot package <sup>140</sup> using default parameters.

### **Citation for statistical methods**

Anders S, Pyl PT, Huber W. 2015. HTSeq--a Python framework to work with high-throughput sequencing data. *Bioinformatics* 31: 166-169.

Bindea G, Mlecnik B, Hackl H, Charoentong P, Tosolini M, Kirilovsky A, Fridman WH, Pages F, Trajanoski Z, Galon J. 2009. ClueGO: a Cytoscape plug-in to decipher functionally grouped gene ontology and pathway annotation networks. *Bioinformatics* 25: 1091-1093.

Breese MR, Liu Y. 2013. NGSUtils: a software suite for analyzing and manipulating next-generation sequencing datasets. *Bioinformatics* 29: 494-496.

Buenrostro JD, Giresi PG, Zaba LC, Chang HY, Greenleaf WJ. 2013. Transposition of native chromatin for fast and sensitive epigenomic profiling of open chromatin, DNA-binding proteins and nucleosome position. *Nat Methods* 10: 1213-1218.

Dobin A, Davis CA, Schlesinger F, Drenkow J, Zaleski C, Jha S, Batut P, Chaisson M, Gingeras TR. 2013. STAR: ultrafast universal RNA-seq aligner. *Bioinformatics* 29: 15-21.

Heinz S, Benner C, Spann N, Bertolino E, Lin YC, Laslo P, Cheng JX, Murre C, Singh H, Glass CK. 2010. Simple combinations of lineage-determining transcription factors prime cis-regulatory elements required for macrophage and B cell identities. *Mol Cell* 38: 576-589.

Kim D, Pertea G, Trapnell C, Pimentel H, Kelley R, Salzberg SL. 2013. TopHat2: accurate alignment of transcriptomes in the presence of insertions, deletions and gene fusions. *Genome Biol* 14: R36.

Li H, Durbin R. 2009. Fast and accurate short read alignment with Burrows-Wheeler transform. *Bioinformatics* 25: 1754-1760.

Pique-Regi R, Degner JF, Pai AA, Gaffney DJ, Gilad Y, Pritchard JK. 2011. Accurate inference of transcription factor binding from DNA sequence and chromatin accessibility data. *Genome Res* 21: 447-455.

Quinlan AR, Hall IM. 2010. BEDTools: a flexible suite of utilities for comparing genomic features. *Bioinformatics* 26: 841-842.

Ritchie ME, Phipson B, Wu D, Hu Y, Law CW, Shi W, Smyth GK. 2015. limma powers differential expression analyses for RNA-sequencing and microarray studies. *Nucleic Acids Res* 43: e47.

Shen L, Shao N, Liu X, Nestler E. 2014. ngs.plot: Quick mining and visualization of next-generation sequencing data by integrating genomic databases. *BMC Genomics* 15: 284.

Zhang Y, Liu T, Meyer CA, Eeckhoute J, Johnson DS, Bernstein BE, Nusbaum C, Myers RM, Brown M, Li W et al. 2008. Model-based analysis of ChIP-Seq (MACS). *Genome Biol* 9: R137.

Zhou X, Wang T. 2012. Using the Wash U Epigenome Browser to examine genome-wide sequencing data. *Curr Protoc Bioinformatics* Chapter 10: Unit10 10.

*End of session.*

## CHAPTER 3: THE TRANSCRIPTOMIC CHANGES DURING IL15 SIGNALING

### 3.1 Experimental design to study transcriptomic changes under IL15 in IELs

Although there have been many studies of IL15 signaling in CD8<sup>+</sup> T cells, the transcriptomic data were limited to those of CD8<sup>+</sup> cells in the human peripheral blood (PBMC) or in mice<sup>32</sup>. Therefore, before investigating the epigenetic landscape of IL15 signaling, we sought to obtain a full transcriptomic change under IL15 in human IELs. To do so, we generated shorted term IELs from 6 different patients' intestinal biopsies followed previously described protocol. Biopsies were collected from patients due to concerns about the intestinal track or regular colonoscopy checkups. The transcriptomic data were generated from control patients, in which they did not have diagnostics for common intestinal diseases. IELs were isolated from the epithelial fraction of the biopsies, and sorted according to the prototypical markers of IELs – CD45<sup>+</sup>, CD3<sup>+</sup>, TCRαβ<sup>+</sup> and CD8<sup>+</sup>. The sorted IELs were confirmed to be tissue resident T cells by flow cytometry with high expression of CD69<sup>+</sup> CD103<sup>+</sup>.

In order to preserve the epigenetic of the IELs as much as possible, we used 2<sup>nd</sup> generation IELs from biopsies for all experiments. *Ex vivo* IELs, freshly collected from biopsies, were stimulated one time to generate stocks which we called 1<sup>st</sup> generation. The stocks were frozen at -80°C for storage over a long period of time. IELs from 1<sup>st</sup> generation would then be expanded to generate cells for various epigenetic assays, and we called these IELs 2<sup>nd</sup> generation. We have monitored the epigenetic of the cells line, and we have shown that for short termed IEL lines, epigenetic and transcriptome of IL15 were conserved at a high level. For example, more than 70% ATAC peaks were conserved between *ex vivo* and short termed IELs. Only after 6 stimulations (>6<sup>th</sup> generation), IELs lost most the epigenetic and surface receptors such as CD103<sup>+</sup> and CD69<sup>+</sup>.

IELs were stimulated and expanded according to the protocols described in the method session. IL2 was added to the culturing medium because IELs would not survive after 3 days without IL2 as a pro-survival cytokine. However, the presence of IL2 posed a challenge for the study, as IL2 was shown to act on CD8<sup>+</sup> T cells in a similar fashion as IL15<sup>21</sup>. Therefore, to remove the effects of IL2, we starved the IELs of IL2 for a period of 48 hours. We have calibrated the conditions, and under 24 hours starvation, the IELs still retained high level of background activation due to previous IL2 exposure such as high level of anti-apoptotic proteins BCL2 and BCL-XL and high level of steady state secretions of GZMB and IFNg. Upon starving IELs of IL2 for a period of 48h, expressions of BCL2, BCL-XL and GZMB returned to baseline, confirming the elimination of previous IL2 effects on IELs. There was concerns that IL2 exposure may change the epigenetic of short termed IELs. However, *in vivo* IELs has been shown to be constantly exposed to low level of IL15/IL2 similar to the exposure to IL2 in culture medium. Therefore, the culture medium in a way mimic the physiological condition; however, more assays can be done to check if the epigenetic indeed was altered during this short term exposure to IL2 in medium.

IL15 stimulation was carried out with suboptimal concentration of IL15 at 10 ng/ml to not overwhelm the system, and obtain meaningful transcriptomic change due to IL15. At high level of concentration, IL15 may cause nonspecific responses mainly due to nonspecific binding of JAK/STAT complexes. 10 ng/ml of IL15 was chosen due to the dose-response curve of IL15 previously characterized in the lab. As in figure 7, in order to characterize various epigenetic landscape in IELs, we collected DNA, total RNA and protein lysates and performed RNA-Seq, ATAC-Seq, Histone CHIP-Seq, 5hmC-Seq and functional assays. We hoped to obtain the transcriptome from RNA-Seq, the chromatin accessibility state from ATAC-Seq, the histone modifications from Histone CHIP-Seq, the 5hmC landscape from 5hmC-Seq. We analyzed and correlated the gene expression profiles to the epigenetic of the same patients to minimize confounding factors. We monitored IELs at 2h and 4h post IL15 stimulation to map out the intermediate and short responses, and at 24h to monitor the secondary responses.

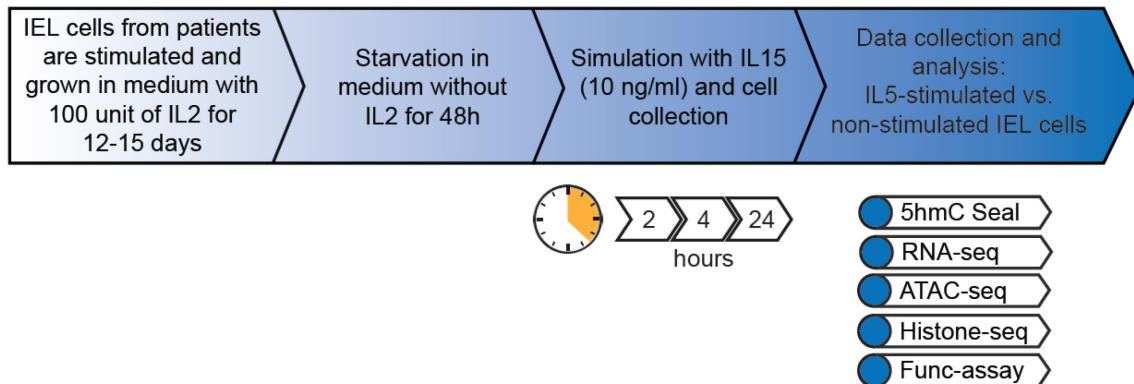


**Figure 7: Experimental schematic to investigate different epigenetic processes during IL15 signaling**

IELs were isolated from intestinal biopsies by shaking and sorting with CD45<sup>+</sup>, TCR $\alpha\beta$ <sup>+</sup>, CD3<sup>+</sup>, and CD8<sup>+</sup>. Short term IEL cell lines were generated according to previously described protocol. These cell lines were in culture from 10 to 13 days to reach resting state in medium with IL2 for survival. 48h before the experiment, IELs were starved to remove the effect of IL2 and to rest the cells prior to IL15 stimulation. IL15 was added to the media at the concentration of 10ng/ml and samples were collected at 0h, 2h, 4h, and 24h post stimulation for further analyses: 5hmC Seal, RNA-Seq, ATAC-Seq, Histone-Seq and functional assays (ELISA, edU analysis and cytokines staining).

### 3.2 IL15 triggers major transcriptional changes that exhibit complex temporal behavior – the early responses.

As mentioned previously, to investigate IL15 signaling in IELs, we performed RNA-Seq at three separated time points: 2 hours, 4 hours and 24 hours post IL15 stimulation. The transcriptomic changes at 2 hours and 4 hours represented the early responses to IL15 while the 24 hours represented the secondary responses to IL15. The time points were chosen due to preliminary data in which prototypical IL15 controlled genes peaked transcriptionally at 2 hours. For the first time, we could obtain IL15 mediated transcriptomic changes throughout the course of 24h with n = 6 biological replicates. In addition, the data set was the first done on human IELs.

We detected 6462 IL15 mediated - differential expressed genes (DEGs) in 24 hours period (with the cut off of  $\text{Log}_2\text{FC} > .5$ ,  $\text{FDR} < .05$  for n = 6 short termed IEL lines). In figure 8A, we had 1743 DEGs at 2h, 2292 DEGs at 4h and 2205 DEGs at 24h. There are unique DEGs at each time point, with 486 unique DEGs

at 2h, 676 unique DEGs at 4h and 1129 unique DEGs at 24h. With first look at the number of DEGs, IL15 has controlled a very large set of target genes which can profoundly impact the functions of IELs. In comparison, IL21 - another cytokine that acts on IELs – controls less than 300 DEGs at 2h post stimulation. Finally, the amount of IL15 controlled genes in human IELs is similar to the amount of IL15 controlled genes in mouse PBLs. Previous studies from the Garcia lab has identified 4776 IL15 controlled genes at 2h and 24h in mouse PBLs.

In order to understand the temporal gene expression patterns of these 6462 DEGs, we performed unbiased supervised hierarchical clustering analysis on these genes. In figure 8B, the DEGs clustered into 6 distinct temporal patterns. In figure 8C, expression profiles of all genes in each cluster were graphed. The solid thick line represented the average z-score of the cluster. In general, we had three clusters that were upregulated, and three clusters that were downregulated by IL15 at various time points. The data was not surprising because IL15 controlled diverse aspects of IELs' functions from survival, proliferation to immune responses. Therefore, IL15 controlled genes should be regulated tightly both in term of magnitude and temporal expression. Among 6 clusters, there were early response genes (cluster 4 and 6), intermediate response genes (cluster 1 and 5) and late response genes (cluster 2 and 3).

Having identified all the DEGs under the signaling of IL15, we asked what the DEGs were. In figure 8D, we performed gene ontology analysis (GO term) and KEGG pathway analysis for the different clusters. The early induced genes at 2h are immune related genes and anti-apoptotic genes. Specifically, G.O. terms are: response to cytokine, defense response, JAK-STAT cascade, inflammatory response and leukocyte differentiation. IL15 is a proinflammatory cytokine, secreted by various cells (epithelial cells, antigen presenting cells etc....) under stressed conditions. First, IL15 induces proinflammatory genes in IELs such as interferon gamma (IFNg), tumor necrotic factor (TNF), granzyme B (GZMB), perforin (PRF1) ... to mount an immune response. Of note, IELs are terminated effector T cells, which have been primed before with a cognate antigen. Therefore, IELs do not require another TCR stimulation to be activated. Evidently in

this case, IL15 alone can induce the expression of relevant cytotoxic genes (IFNG, GZMB and PRF1). A detailed KEGG pathway analysis revealed top molecular pathways in early response: JAK/STAT, MAPK, RAS, and PI3K pathways. IL15 has been known to use the same pathways in peripheral blood CD8<sup>+</sup> T cells, and NK cells.

At 2h, IL15 represses certain signal transducers, transcriptional factor activity, serine threonine kinases and cell surface receptor linked signaling pathway (figure 8D). KEGG analysis reveals repressed molecular pathways: FOXO signaling pathway, PI3K-AKT pathway, autophagy pathway, TGF $\beta$  pathway, cancer related pathway and calcium and phosphatidylinositol pathway (table 2). DEGs associated with PI3K-Akt pathway are ones that need to be shut down for the other genes in the same pathway to function normally (PIK3R1, PIK3R2). Calcium and phosphatidylinositol pathways and serine threonine kinases are usually involved in IL15/IL2R $\beta$  signaling. After 2h post stimulation, IL15 negatively regulates these molecules to turn off excessive signaling from the receptor ligand complex. It is a negative feedback loop to make sure IL15 does not over-activate IELs. TGF $\beta$  pathway has long been known to counteract the effect of IL15 in the intestinal track<sup>141</sup>. To IELs, TGF $\beta$  has been shown to down regulate BCL2 and turn on transcriptional factor SMAD3 to induce apoptosis<sup>142</sup>. IL15 promotes survival, anti-apoptosis and upregulation of BCL2. Hence, IL15 has to shut down its contrary pathway - the TGF $\beta$  pathway. Next, FOXO pathway is functionally important in the NK cells<sup>143</sup>. FOXO1 is required for autophagy, necessary for NK cell development and immune functions. FOXO1 null mutant has impaired development and viral clearance<sup>143</sup>. FOXO3, another important transcriptional factor in the FOXO family, degrades BIM (a pro-apoptotic factor) to maintain the expression of MCL1 (an anti-apoptotic factor). As a result, IL15 secures the survival of natural killer cells<sup>144</sup>. In IELs, IL15 may repress the FOXO family to enhance survival of IELs in similar manner in which IL15 acts on NK cells.

Altogether, the signature of early response to IL15 is the activation of various immune functions, the enhance survivability and the repression of death signals.

### **3.3 IL15 triggers major transcriptional changes that exhibit complex temporal behavior – the intermediate and late responses.**

At the intermediate time point, 4h post stimulation, IL15 upregulates genes involved with ncRNA processing, ribosome biogenesis, RNP complex biogenesis, rRNA processing and tRNA metabolic processing. In addition, KEGG analysis narrows down on pathways associated with metabolic processes, proteins export and spliceosome. At this state, IL15 prepares the machinery for processing and translating the transcripts made at 2h: in particular the spliceosome and protein export complexes. Interestingly, IL15 turns on genes that process various RNA species: from rRNA, tRNA (possibly for ribosomal machinery) and long ncRNA. There have been no study that links lncRNA to IL15's functions. In this research, we reported for the first time the list of IL15 controlled, differentially expressed lncRNAs in Table 4. Further research is needed to understand the functions of these lncRNA and why they are made secondary to the first wave of transcription at 2h. Last but not least, IL15 is capable of changing the metabolic processes in memory T cells and NK cells<sup>145-147</sup>. Specifically, IL15 turns on TFAM (mitochondrial transcriptional factor A) in memory T cells to promote mitochondrial biogenesis and fatty acid catabolism; as a result, IL15 enhances the capacity of mitochondria to generate enough energy for the demand of pathogens clearing and T cell expansion<sup>145</sup>. In our system, IL15 changes the metabolic processes in IELs as well. TFAM is upregulated to a high level, signifying the activation mitochondria biogenesis. In addition, effector IELs undergo a switch from predominantly oxidative phosphorylation to aerobic glycolysis for growth and function. Important master regulators of glycolysis metabolism are upregulated: HIF1a, AMPK, and MTOR. Functional enzymes of glycolysis have also been upregulated: hexokinase, pyruvate kinase, lactate dehydrogenase, and phosphofructose kinase 1. In addition, in order to obtain more materials for the catabolic processes, IL15 turns on the expression of important glucose and amino acid transporters such as GLUT3, GLUT1, TFRC and CD98. Altogether, the transcriptional data at 4h suggests a strong switch in metabolism, an activation

of machineries that process rRNA, tRNA and long noncoding RNA. The function these differentially expressed long noncoding RNA is not known.

At 4h, IL15 represses these gene ontologies: extracellular region, membrane, plasma membrane, chloride channel complex and calcium ion binding. IL15 represses KEGG pathways: TGF $\beta$  pathway, FOXO pathway, calcium signaling pathway, HIF-1 pathway. As stated previously, TGF $\beta$  and FOXO pathways have opposite effects to IL15 (pro-apoptotic or anti-inflammatory), and IL15 maintains the constant repression of these pathways. In addition, IL15 has repressed additional pathways at 4h: the WNT pathway, RAP1 pathway, endocytosis, pathway with miRNA, and the p53 pathway. Again, of great interest, IL15 downregulates of a set of micro RNAs not characterized before. The extensive usage and regulation of miRNA and lncRNA of IL15 can be an exciting topic for future research. Last but not least, endocytosis pathway is suppressed because IELs are actively making cytotoxic molecules, and need to activate the opposite pathway, the exocytosis pathway to release the molecule rather than endocytosis. The suppression of p53 pathway may serve to promote robust and strong cell division at later time point.

At 24h post IL15 stimulation, DEGs ontologies are mitotic cell cycle, cell division, chromosome organization, cell cycle phase transition, DNA replication. The KEGG analysis shows pathways in DNA replication, cell cycle, mismatch repair, base excision repair, and metabolic pathways. At early time points, IL15 activates anti-apoptotic genes to ensure the survival of T cells. At 24h, IL15 primarily sends a strong proliferative signal to promote active cells division. Additional pathways of mismatch repair, base excision repair are upregulated to correct mistakes during cell replication. All the immune related genes or RNA processing genes do not show up at this point, suggesting they are primarily early responses and not late responses. Expression of many relevant cytotoxic genes such as IFNg, GZMB and PRF1 return to baseline levels.

At 24h, IL15 keeps on repressing these ontologies: receptor activity, transmembrane receptor activity, extracellular region, system process and signal transducer activity. In term of KEGG analysis, IL15 represses the FOXO pathway, metabolic pathway, autophagy, endocytosis, P53 pathway, regulation of actin pathway, chemokines and cytokine receptor interaction pathway. The repression of some particular pathways (Foxo, autophagy, p53) remains long lasting over the period of 24h. There are additional repressed pathways at 24h such as ones of actin filaments and chemokine / receptors. At this time point, IELs enter cell division; therefore, their cytoskeleton needs to be controlled to facilitate the transition to various phases of cell division. Actin filament regulation is expected.

Altogether, for the first time, we mapped out IL15 regulated genes in IELs during a period of 24h. From the data, IL15 regulates a large and diverse set of genes, with precise temporal patterns. One can envision different layers of regulation needed to ensure proper transcription of such large gene set. The potential role of epigenetic as a mechanism in IL15 signaling has never been explored before. Due to the importance of IL15 in IELs' immune functions, and IL15 dysregulation in many autoimmune disorders, it is important to explore the epigenetic landscape throughout IL15 signaling process.

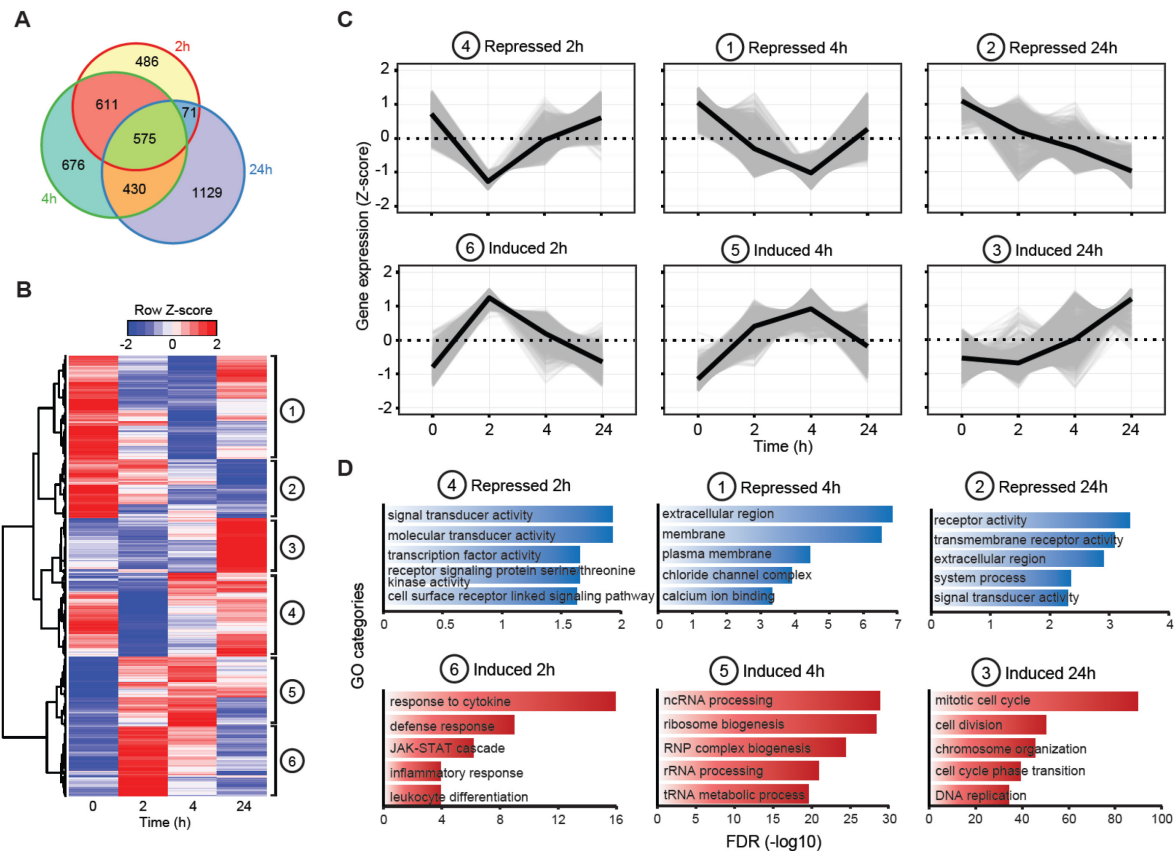


**Figure 8: Transcriptomic changes in IELs due to IL15 signaling during a period of 24 hours.**

**A**, Venn diagram representing the number of differentially expressed genes (DEGs) at 2h, 4h and 24h post IL15 stimulation in IELs ( $\text{Log}_2\text{FC} > .5$ ,  $\text{FDR} < .05$ ). **B**, Supervised hierarchical clustering analysis of 6462 DEGs based on temporal patterns of the gene expression. Shade of red and blue are used to represent the z-score from -2 to +2 to illustrate whether the expression value of a particular gene above (red) or below (blue) the mean expression value. **C**, SOTA clustering analysis for each cluster. The solid thick line represents the average z-score of the group. Each small thin line represents the z-score pattern of an individual gene from the cluster. **D**, Enriched GO term analysis for genes in each cluster ( $p < 0.01$ ).

| <i>KEGG pathways</i>                          | <i>Genes associated with pathways</i>  |
|---|--|
| <b><i>Early induced genes (2h)</i></b>        |  |
| <i>JAK-STAT signaling pathway</i>             | IL4R IL12RB2 CISH STAT1 CCND2 IL6ST IL2RA PIM1 STAT4 SPRY1 CSF2 STAT3 BCL2L1 SOCS4 SPRED2 IRF9   |
| <i>MAPK signaling pathway</i>                 | TAB2 MAP2K4 RELB TGFBR1 MAPK8 NFKB1 SRF MAPKAPK3 ELK1 ATF4 JUND RRAS2 PTPN7 RASA2 CASP3 PRKX DAXX CHUK TNF   |
| <i>RAS signaling pathway</i>                  | ABL2 ARF6 BCL2L1 ELK1 GAB2 GNG10 GNG2 NFKB1 RAB5A RASA2 RRAS2  |
| <i>RIG-I-like receptor signaling pathway</i>  | MAPK8 NFKB1 IFIH1 IRF7 ISG15 CHUK DDX3X TNF  |
| <i>Toll-like receptor signaling pathway</i>   | TAB2 MAP2K4 MAPK8 NFKB1 STAT1 CD80 MYD88 IRF7 CHUK TNF   |
| <i>Cytokine-cytokine receptor interaction</i> | CCR2 CSF2 FLT3LG IL12RB2 IL1RAP IL2RA IL4R IL6ST TGFBR1 TNFRSF1B TNFRSF4   |
| <i>PI3K-Akt signaling pathway</i>             | ATF4 BCL2 BCL2L1 CCND2 GNG10 GNG2 IL2RA IL4R IRS1 LPAR6 NFKB1  |
| <i>TNF signaling pathway</i>                  | ATF4 BCL3 CASP3 CSF2 ICAM1 MAP2K4 NFKB1 TNFRSF1B   |
| <i>Anti-apoptosis</i>                         | BCL2 BCL2L1 CASP3 IL1RAP MYD88 NFKB1   |
| <b><i>Intermediate induced genes (4h)</i></b> |  |
| <i>Aminoacyl-tRNA biosynthesis</i>            | SARS AARS EARS2 CARS DARS WARS2 LARS YARS EPRS NARS2 FARSA IARS CYP51A1 AK2 NDUFAB1 POLR3B GCLM CHPF2 ALDH18A1 OAT HYAL2 POLR1A CAD CRLS1 MTAP DHODH EARS2 PYCRL SQLE CHKA POLR3G UMPs GLSMECR SRM ATP6V0B RPN2 DNMT3A ALG5 AMD1 CHPF ITPA PPAT DCTD ASS1 ACLY ACACA STT3A PSAT1 SUCLA2 EPRS FPGS ATIC COX17 AGPAT9 ETNK1 ND-UFA9 PGD UCK2 DEGS1 PSPH PTGES2 RPIA DGKE ALG8 CBS STT3B MTHFD2L POLR2H RPN1 NANP DPAGT1 SHMT2 NDUFA4L2 UAP1L1 GFPT1 PNP ALG3 POLR3B POLR1A CAD DHODH POLR3G UMPs ITPA DCTD UCK2 POLR2H PNP RPN2 ALG5 STT3A ALG8 STT3B RPN1 DPAGT1 ALG3 |
| <i>Metabolic pathways</i>                     | PSMD8 PSMB3 PSMB2 PSMB6 PSMC3 PSMD1 HSPA5 SEC61A1 SRP54 SEC61B SPCS3 SEC61G BUD31 NCBP2 SRSF7 SRSF6 SNRPB2 PPI1 SF3B4 U2AF1 MAGOH PUF60  |
| <b><i>Late induced genes (24h)</i></b>        |  |
| <i>DNA replication</i>                        | POLA2 RFC2 POLD1 POLD3 MCM5 POLA1 RNASEH2A LIG1 RPA3 RFC5 MCM3 POLE4 RPA1 PCNA DNA2 PRIM2 RFC4 MCM7 RNASEH2C POLE PRIM1  |
| <i>Cell cycle</i>                             | DBF4 E2F2 SMC1A RBL1 CDC7 MCM5 RBX1 CCNE1 SMC3 MCM3 CCND3 CDKN2C CDK2 YWHAH PCNA CCNB1 ANAPC11 SKP2 CDKN2A RAD21 WEE1 MCM7 PLK1 CHEK2 TFDP1 PRKDC  |
| <i>Mismatch repair</i>                        | RFC2 POLD1 MLH1 POLD3 MSH2 LIG1 RPA3 RFC5 RPA1 PCNA RFC4   |
| <i>Nucleotide excision repair</i>             | RFC2 POLD1 POLD3 RBX1 LIG1 RPA3 RFC5 POLE4 RPA1 PCNA CETN2 RFC4  |
| <i>Base excision repair</i>                   | POLE   |
| <i>Metabolic pathways</i>                     | LIG1 NEIL3 PCNA POLD1 POLD3 POLE4 XRCC1 UQCRC1 POLA2 MDH1 PI4K2B CS POLD1 PFKP ACAT1 POLD3 PAFAH1B3 PGM1   |

**Table 2: KEGG pathways analysis for upregulated DEGs in IL15 signaling pathway.**

Information on the molecular pathways that are upregulated by IL15 at early, intermediate and late time points. For each pathway, a list of DEGs associated with the pathway are listed. The pathways are ranked based on the p values of the molecular pathway in KEGG analysis.

| <b>KEGG pathways</b>                            | <b>Genes associated with pathways</b>  |
|---|--|
| <b>Repressed Genes – all time points</b>        |  |
| <i>Metabolic pathways</i>                       | AANAT ABAT ACACB B3GALT4 B3GNT1 B4GALT1 BTD CECR1 CPOX CYP11B1 CYP2R1 CYP2U1 DCK EHHADH EPHX2 EXTL2 FUT7 GAA GALC GBA GLB1 GNS HSD17B6 HSD17B7 IDH1 MGAT3 MGAT5 MGLL PIPOX PLCG2 POLD4 POLG2 PPOX PTGS1 RDH16 SARDH SGSH TM7SF2 WBP1 |
| <i>Pathways in cancer</i>                       | ADCY4 ADCY9 ARNT CDKN1B F2R FGFR2 GLI1 IGF1 IGF1R LAMB3 LEF1 PLCG2 PRKCA PTCH1 RASGRP3 RASGRP4 RUNX1 SLC2A1 SUFU TGFBR2 WNT1   |
| <i>MicroRNAs in cancer</i>                      | ABCB1 ABCC1 ATM BMPR2 CCNG1 CD44 CDC25B CDC25C CDCA5 CDKN1B DDIT4 ERBB3 ITGA5 PLCG2 PRKCA TP63 TPM1  |
| <i>Cytokine-cytokine receptor interaction</i>   | ACVR1 ACVR2A ACVR2B BMPR2 CCL5 CCR8 CXCL16 CXCR3 CXCR6 EDA2R IL15 IL9R TGFBR2 TNFRSF25 TNFSF13B  |
| <i>Transcriptional mis-regulation in cancer</i> | ATM BAIAP3 BCL2A1 BCL6 CDKN1B FLI1 IGF1 IGF1R ITGAM LYL1 MEN1 REL RUNX1 SUPT3H TGFBR2  |
| <i>TGF-beta signaling pathway</i>               | ACVR1 ACVR2A ACVR2B BMPR2 NBL1 SMAD9 TGFBR2 TGIF1  |
| <i>HIF-1 signaling pathway</i>                  | ARNT CDKN1B IGF1 IGF1R PLCG2 PRKCA SLC2A1  |
| <i>Rap1 signaling pathway</i>                   | ADCY4 ADCY9 ADORA2A F2R FGFR2 FYB IGF1 IGF1R ITGAM MAP2K3 PRKCA RASGRP3 RGS14 SIPA1 SIPA1L3  |
| <i>Foxo signaling pathway</i>                   | ATM BCL6 BNIP3 CDKN1B FOXO3 FOXO4 IGF1 IGF1R PLK2 PLK4 RAG1 RBL2 S1PR4 SGK1 TGFBR2   |

**Table 3: KEGG pathways analysis for repressed DEGs in IL15 signaling pathway.**

Information on the molecular pathways that are down-regulated post IL15 stimulation. For each pathway, a list of DEGs associated with the pathway are listed. The pathways are ranked based on the p values of the molecular pathway in KEGG analysis.

**LIST OF LNCRNA CONTROLLED BY IL15**

|   |  |
|---|--|
| <b>Differential expressed IncRNA at 2h</b>  | RP11-932O9.9 RP6-99M1.2 MIR22HG AC084082.3 RP11-316P17.2 MIR155HG RP11-469M7.1 PRKCQ-AS1   |
|   | AC009299.3 MIR29A SNORD3A SNHG15 AC017002.1 AC092580.4 RP11-498C9.15 RP11-497H16.9 RP5-1085F17.3   |
| <b>Differential expressed IncRNA at 4h</b>  | RP11-58E21.3 CTB-58E17.1 RP5-935K16.1 SNHG8 TTTY15 MIR24-2 CTC-503J8.6 RP11-284N8.3 CTC-228N24.3   |
|   | CTC-444N24.11 RP11-611L7.1 RP11-861A13.4 RP11-4F5.2 LINC00667 CTA-217C2.1 CTA-445C9.15 CTC-297N7.8   |
| <b>Differential expressed IncRNA at 24h</b> | CTD-2196E14.9 LINC00116 CTD-2521M24.9 CTD-3195I5.1 RP11-350F4.2 LINC00493 LINC00863 RP11-94L15.2   |
|   | LINC00484 RP11-383J24.6 RP11-220I1.1 RP11-706O15.3 RP11-212P7.2 RNU12 ILF3-AS1 RAB30-AS1 GS1-124K5.11  |
| <b>Differential expressed IncRNA at 4h</b>  | LINC00657 LINC00938 LINC00341 NCBP2-AS2 RMRP CTD-2037K23.2 AC104820.2 TSIX CASC7 AC006129.2 RNU11  |
|   | RP11-343N15.5 MIR4435-1HG CTC-459F4.3 SCARNA2 AC004951.6 JPX LINC00909 EPB41L4A-AS1 RP11-158H5.7   |
| <b>Differential expressed IncRNA at 24h</b> | RP11-95D17.1 RP1-178F10.3 MIR4453 TAPSAR1 7SK TERC RP11-325F22.2 AC159540.1 LINC00969 SNORD116-20  |
|   | RP11-448A19.1 LINC00152 HCG11 RP11-480A16.1 FTX MAPKAP5-AS1 RP11-485G4.2 GMDS-AS1 RP11-488L18.10   |
| <b>Differential expressed IncRNA at 4h</b>  | RP11-946L20.4 XIST CROCCP2 RP11-47L3.1 RP11-346D14.1 ZNF718 LINC00504 MALAT1 RP1-90J20.12 LINC00910  |
|   | EIF3J-AS1 AC092669.3 RP11-252A24.7 MIAT RP11-427H3.3 SNX29P2 RP11-703G6.1 U82695.10 RP11-159D12.2  |
| <b>Differential expressed IncRNA at 24h</b> | LINC00339 LINC00957 RP11-291B21.2 NEAT1 LINC00861 LINC00426 AC084018.1 LINC00324 LINC00847   |
|   | AP001258.4 C11orf95 AC093323.3 RP11-539L10.2 LINC00599 MIR146A   |
| <b>Differential expressed IncRNA at 4h</b>  | RP5-1024G6.8 MIR22HG SNHG15 RP11-61A14.3 AC017002.1 RP11-498C9.15 MIR155HG RP11-497H16.9 RP11-469M7.1 AC092580.4 CTC-503J8.6 PRKCQ-AS1 LINC00341 SNHG8 MIR29A MIR24-2 RP5-935K16.1 RP11-58E21.3  |
|   | CTC-228N24.3 CTA-217C2.1 RP11-284N8.3 LINC00116 CTC-444N24.11 AC009299.3 RP11-4F5.2 LINC00484 CTC-297N7.8 RP11-611L7.1 RP11-220I1.1 CASC7 RP11-350F4.2 RP11-706O15.3 AC104820.2 CTD-3195I5.1 RP11-94L15.2 CTD-2521M24.9 LINC00657 MIR4435-1HG CTC-459F4.3 CTA-445C9.15 RP11-53O19.3 CTD-2196E14.9  |
| <b>Differential expressed IncRNA at 24h</b> | AC006129.2 RP11-383J24.6 NCBP2-AS2 GS1-124K5.11 RP11-485G4.2 LINC00493 JPX LINC00667 RP1-90J20.12  |
|   | MIR4453 ZNF718 SCARNA2 TSIX XIST LINC00957 RNU12 TERC RP1-178F10.3 RNU11 EPB41L4A-AS1 RP11-212P7.2 LINC00969 RP11-95D17.1 ILF3-AS1 C11orf95 HCG11 LINC00909 RP11-448A19.1 AC093323.3 SNORD116-20 7SK RAB30-AS1 RP11-861A13.4 AC159540.1 CTD-2037K23.2 RP11-488L18.10 LINC00152 LINC00504 FTX TAPSAR1 U82695.10 RMRP SNX29P2 SNORD3A AC092669.3 MALAT1 RP11-346D14.1 MAPKAP5-AS1 RP11-343N15.5 CROCCP2 RP11-703G6.1 RP11-946L20.4 GMDS-AS1 RP11-252A24.7 LINC00599 RP11-159D12.2 LINC00938 MIAT RP11-427H3.3 AP001258.4 RP11-325F22.2 EIF3J-AS1 NEAT1 LINC00861 AC084018.1 RP11-291B21.2 LINC00847 RP11-47L3.1 LINC00324 LINC00339 RP11-539L10.2 MIR146A LINC00426  |
| <b>Differential expressed IncRNA at 24h</b> | RP5-1024G6.8 RP11-498C9.15 SNORD3A LINC00341 MIR4435-1HG AC084082.3 RP11-215G15.5 CTC-503J8.6  |
|   | RP11-316P17.2 MIR210HG RP5-935K16.1 RP11-620J15.3 LINC00484 RP11-343N15.5 ZNF718 MIR155HG LINC00116 CTD-3195I5.1 SNHG15 AC092171.4 AP001258.4 RP11-58E21.3 CTC-228N24.3 PRKCQ-AS1 TAPSAR1 AC092580.4 RP11-485G4.2 RP11-469M7.1 LINC00152 LINC00176 RP11-309G3.3 RP11-350F4.2 MIR24-2 RNU12 CASC7 RP11-108P20.1 AC006129.2 LINC00969 RP11-383J24.6 NCBP2-AS2 CTC-459F4.3 RP11-706O15.3 SNHG8 AC104820.2 CTA-217C2.1 AC093323.3 ILF3-AS1 RP11-427H3.3 RNU11 RP11-95D17.1 MIR4453 RP11-611L7.1 LINC00957 RP11-212P7.2 CTD-2196E14.9 CTC-297N7.8 RP11-284N8.3 RMRP AC004951.6 RP11-305L7.1 RAB30-AS1 TSIX MIR29A AC017002.1 CTA-445C9.15 PAXIP1-AS1 JPX RP1-90J20.12 LINC00657 RP11-252A24.7 AC159540.1 CTC-444N24.11 LINC00909 RP11-4F5.2 RP11-220I1.1 LINC00339 SCARNA2 CROCCP2 RP11-94L15.2 LINC00493 RP1-178F10.3 LINC00504 LINC00863 TERC LINC00667 7SK RP11-158H5.7 MAPKAP5-AS1 LINC00938 HCG11 RP11-488L18.10 C11orf95 RP11-448A19.1 RP11-291B21.2 RP11-53O19.3 RP11-159D12.2 EIF3J-AS1 RP11-946L20.4 U82695.10 RP11-346D14.1 RP11-480A16.1 AC092669.3 XIST CTD-2037K23.2 XXbac-BPGBPG55C20.2 CTD-2521M24.9 RP11-703G6.1 LINC00910 SNX29P2 LINC00847 FTX SNORD116-20 MIR22HG LINC00599 AC084018.1 LINC00324 GMDS-AS1 MALAT1 NEAT1 RP11-325F22.2 RP11-539L10.2 RP11-861A13.4 RP13-977J11.2 LINC00861 EPB41L4A-AS1 RP11-690G19.3 LINC00426 MIR146A MIAT RP11-47L3.1 |

**Table 4: Long non-coding RNAs differentially expressed under IL15 signaling**

Informational list of all the differential expressed long noncoding RNA identified during IL15 signaling in IELs.

## CHAPTER 4: THE EPIGENETIC LANDSCAPE OF IL15 SIGNALING

### 4.1 The chromatin accessibility of IELs is stable throughout IL15 stimulation

Having obtained the transcriptomic responses in IELs to IL15, we investigated how IL15 can control a broad yet diverse set of genes. The key question is whether epigenetic changes during IL15 signaling. The logic had been explained in the introductory session. First, we looked at the chromatin accessibility landscape of IELs. ATAC-seq has become the most relevant technology that can replace DNase sensitivity assay to profile the chromatin accessibility with efficiency, reliability and sensitivity<sup>124</sup>. It has been shown before for CD4<sup>+</sup> T cells in the peripheral blood, during the development and differentiation processes, the chromatin accessibility has been changed profoundly<sup>148</sup>. It has also been shown for CD8<sup>+</sup> T cells' response to a bacterial infection, the chromatin becomes more open with clear signatures of key transcriptional factors binding to newly opened enhancers<sup>59,149</sup>. In another paper that studies dendritic cells' responses to viral infection, the chromatin accessibility is altered, allowing the binding of specific transcriptional factors to mount a proper immune response<sup>150</sup>. It has become obvious that during a major differentiation or an immune response to viral or bacterial infections, one may expect the chromatin accessibility to change. However, what would happen to terminal differentiated cells like the IELs? The differentiation has been long finished. Yet, IELs sometime encounter very potent immune signal like TCR recognition of cognate antigen or a potent cytokine like IL15. In such case, would the chromatin accessibility change? In order to directly answer the question, we performed ATAC-Seq for 6 biological replicates (6 IEL short termed cell lines) and investigated the chromatin accessibility at 2h, 4h, and 24h post IL15 stimulation. The time points were selected to match the RNA-Seq data. We had known IL15 was capable of upregulating more than 6462 DEGs during the course of 24h. It became interesting to investigate whether chromatin accessibility altered during IL15 signaling at any time. If so, when would it started to change and what could be the consequences of such change?

As in figure 9A, there are around 35,000 to 50,000 ATAC peaks across the genome of the IELs at the baseline prior to IL15 stimulation. The data are reproducible between the IEL replicates, and the sequencing depth is sufficient to reach a saturating condition for peak calling. Considering that we have around 20,000-25,000 genes throughout the genome, on average, there were around two ATAC peaks per gene. In figure 9C, ATAC peaks distribute mostly at the intergenic region (47%), followed by the intron and promoter regions (27 and 21% respectively) and only 5% in all the 3'UTR, 5'UTR and exon regions. Next, we asked to see if there were differential ATAC peaks during the course of IL15 signaling in IELs. To our surprise, in figure 9B, there are no differential ATAC peaks detected at 2h and 4h post IL15 stimulation. As stated in the previous session, at the early time points, IL15 exerts a very robust and potent response, with the number of DEGs in the 4,000 genes. However, we saw no difference in chromatin accessibility at 2h and 4h – no peaks detected in our current cut off criteria. The data suggest the possibility that most of the DEGs are primed at the baseline with open chromatin landscape. There may be no need to open up additional loci. The chromatin landscape is readily accessible, allowing fast binding of relevant transcriptional factors to key sites, enabling IELs to turn on transcription rapidly without having to utilize the chromatin remodeling machinery. As the result, IELs can mount immune response effectively and quickly. This may be a unique characteristic of terminally differentiated effector cells such as IELs, evolved from the need to carry out fast response to communicate efficiently with other immune cells, and protect the body effectively against pathogens at the front line. To test this hypothesis, we investigated the baseline ATAC peaks, and asked whether the DEGs under IL15 were more accessible than the non-DEGs. We assigned all the ATAC peaks +/- 100kb from the gene body to that particular gene. Indeed, in figure 9D, the average total number of ATAC peaks associated with DEGs is significantly higher than the non-DEGs. This supports the idea that in IELs, as an effector T cells, the chromatin landscape is primed and readily open for the binding of transcriptional factors.

At 24h, we detected a large amount of differential ATAC peaks – around 7893 peaks. At this state, IL15 has fully induced the IELs to enter mitotic division. At the S phases, and the G1-M phases, the chromosomes need to condense and then separate into the daughter cells. Therefore, due to dramatic cell-cycle-mediated change in chromosome structure, we could detect large amount of altered chromatin structures and accessibility (7893 DE peaks). Yet, cell division complicates the analysis, as we do not know among the 7893 DE peaks, how many DE peaks are due to cell division, how many are due to a late response to IL15 at 24h. Upon the analysis of G.O. terms, the DE ATAC peaks do not belong to any particular immunological pathways or processes. There is no enrichment for any other pathways. Therefore, it can be concluded that the whole chromatin landscape became more accessible nonspecifically. What we detected was the consequence of IELs entering mitotic division.

Overall, from the ATAC data, we can conclude that the chromatin accessibility of IELs is stable, and does not change during the early time points of IL15 signaling. There are more than 4035 DEGs at 2h and 4h; yet there is 0 differential ATAC peak. Therefore, it is likely that most of the relevant loci are readily accessible for transcriptional factors binding in IELs, supporting the preset landscape model.

In addition, we performed Tn5 footprinting analysis for the ATAC data to understand better the binding of various transcriptional factors (TFs) post IL15 stimulation. When a TF binds to a gene locus and occupies the physical space, Tn5 transposase cannot access the binding site, and there will be a drop in sequencing signal at the location as a result. From the sequences of these occupied sites, we could perform motifs search and identify class of TFs that may bind to these locations. In figure 10A, the IL15 DEGs can be classified into 6 different clusters based on the temporal patterns in transcriptomic analysis. In figure 10B, due to motifs search and footprinting analysis of the promoter regions, we identified various transcriptional factors associated uniquely to each cluster. Interestingly, we have identified novel TFs associated with IL15 regulated genes. In particular, upregulated DEGs at 2h were associated with the following TFs: STAT, ETS, TBS1, RUNX1 and IRF1. Upregulated DEGs at 4h were associated with TFs: CBT,

MYC and EDS1. Upregulated DEGs at 24h were associated with TFs: RDR1, CREB and E2L. On the contrary, the repressed DEGs were associated with distinct set of other TFs: YRR1, E2F1 and CEP3. In figure 10C, we could observe the binding persisted from 0h to 4h post IL15 stimulation for 3 representative TFs: STAT1, IRF1 and RUNX1 for the upregulated DEGs at 2h. It seemed that the TFs were pre-bound in the system, and the binding persisted as long as 4h post stimulation. It remained to be explored what have activate these pre-bound TFs to allow initiation of transcription post IL15 stimulation.

Taken together, previous knowledge that IL15 acted only through JAK/STAT, MAPK and PI3K was not sufficient. From the footprinting analysis, clearly IL15 has employed many more TFs to control its transcriptomic program. We have identified novel TFs associated w IL15 such as IRF1, TBS1, ETS and RUNX1. The results were sound. It was hard to imagine IL15 could control 6462 genes via only 3 families of TFs. In fact, our data advocated for a complex TFs network employed by IL15 to exert its biological functions.

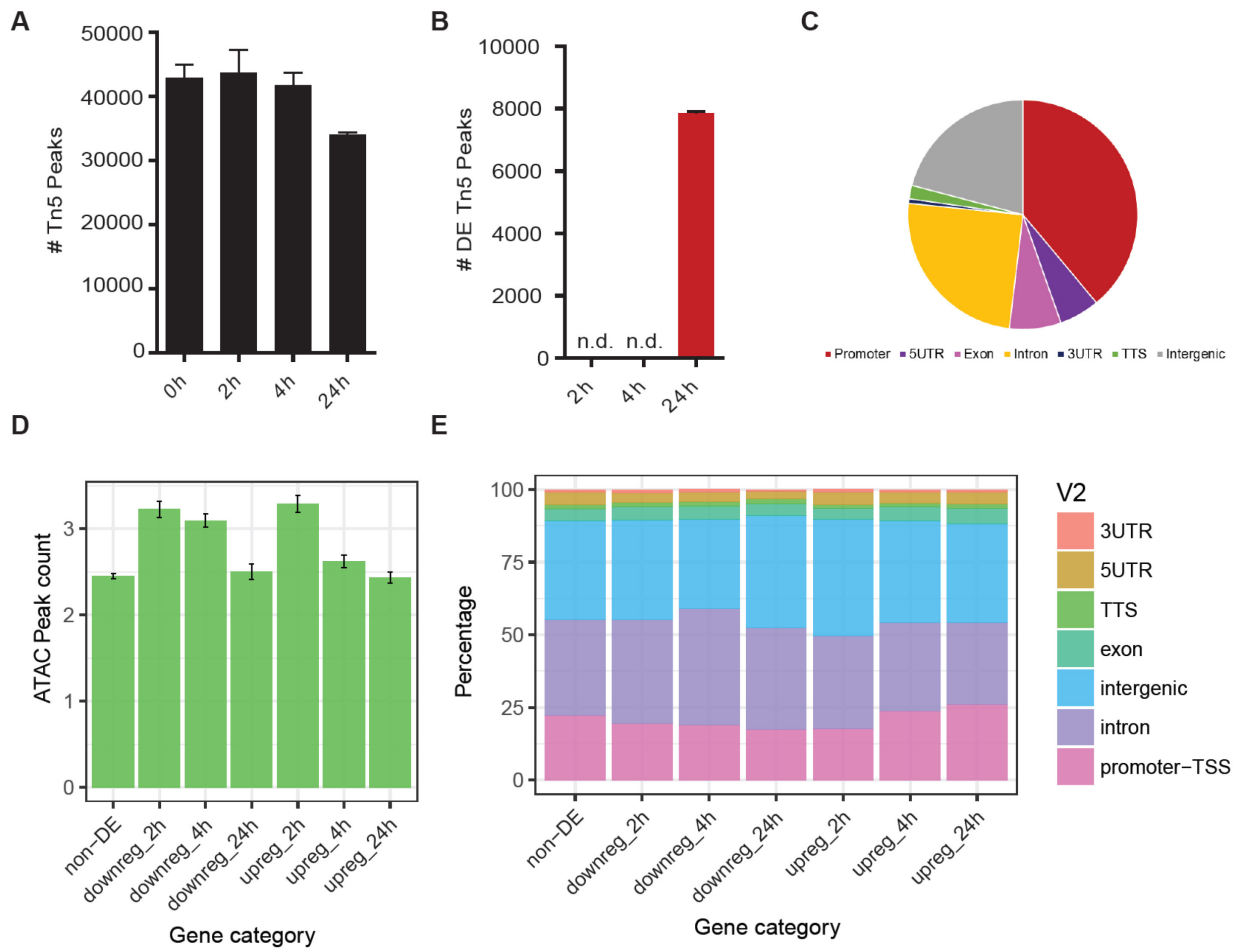


**Figure 9: Tn5 peaks revealed by ATAC-Seq of IELs during the course of IL15 stimulation**

**A**, The average number of Tn5 peaks at 0h, 2h, 4h and 24h post IL15 stimulation. n = 4 biological replicates.

**B**, The number of differential expressed Tn5 peaks at 2h, 4h and 24h post IL15 stimulation. D.E. are called based on the difference with the 0h, FDR < 0.05. **C**, Genomic distribution of total Tn5 peaks at the steady state (0h time point). **D**, The average number of Tn5 peaks in each category of genes based on the response to IL15. The Tn5 peaks are associated with a gene if the peaks are within +/- 5kb from the TSS to TES of the correspondent gene. **E**, The genomic distribution of the Tn5 peaks on D for each category of genes.

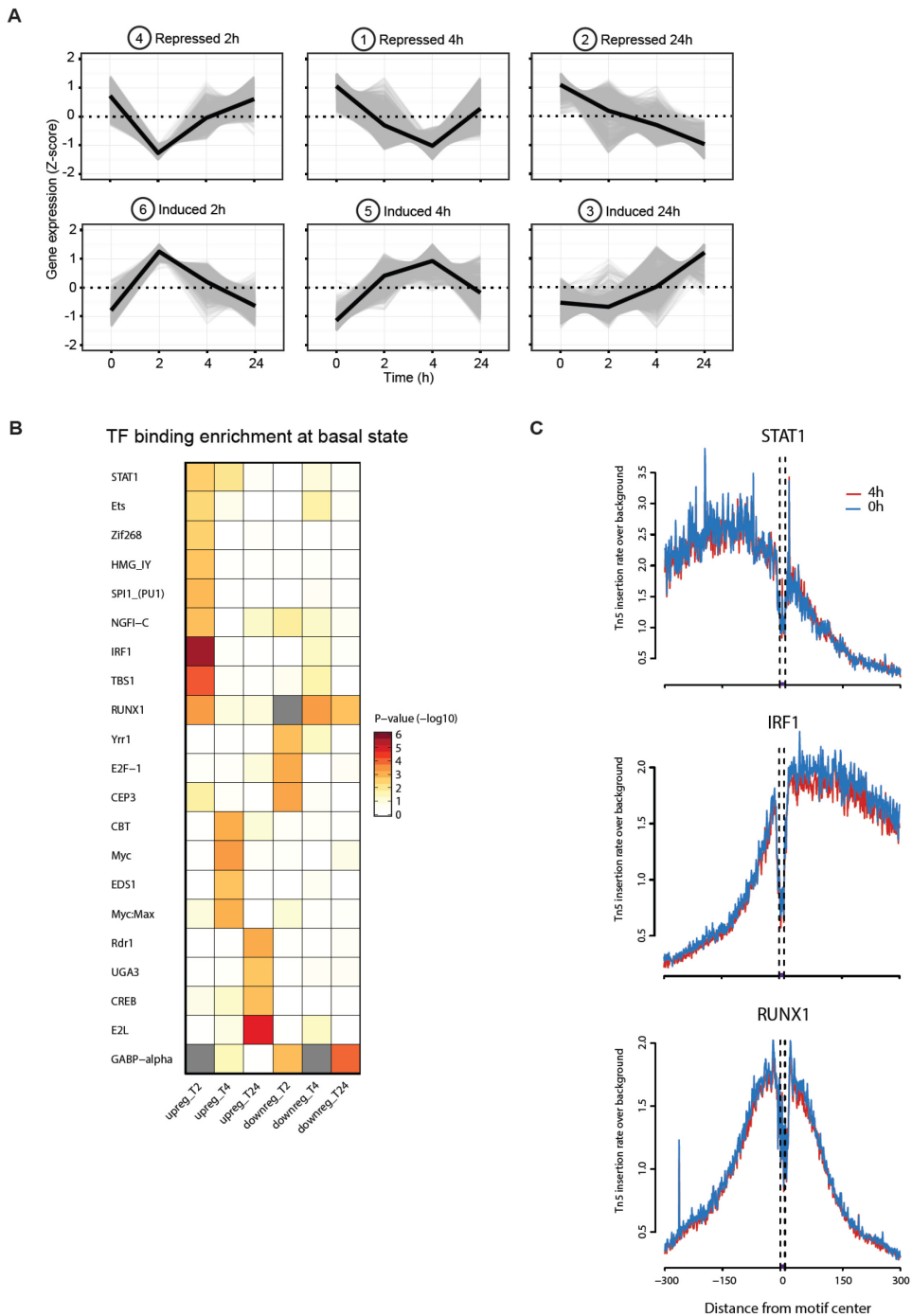


**Figure 10: Tn5 Footprinting analysis of different clusters of DEGs**

**A**, The six different clusters of differential expressed genes under IL15 signaling based on their temporal expression patterns. **B**, Motif analysis to identify distinct transcription factors bound at the promoters of each gene clusters at the steady state. **C**, Footprinting analysis of various transcriptional factors bound at the early induced genes (at 2h) – STAT1, IRF1, RUNX1.

#### 4.2 The dynamics of histone modifications during IL15 signaling

Having known that the chromatin accessibility was stable during the early time points during IL15 signaling, we examined the landscape of histone modifications in IELs. The various combinations of 4 histone marks H3K4me1, H3K4me3, H3K27Ac and H3K27me3 can characterize the regulatory regions of DNA as primed, poised, active, repressed, or latent enhancers / promoters<sup>76</sup>. We investigated if IL15 acted on histone modifications to introduce new regulatory elements, or change a preexisting regulatory elements (for example changing a poised enhancer to active enhancer) in order to carry out its diverse biological functions. In addition, histone modifications have been shown to have regulatory and biological consequences such as recruitment of chromatin modifying enzymes, stabilization of RNA polymerase II complex, crossing different chromatin domains and recruitment of chromatin remodeling complexes.

|            | Steady state<br># peaks | D.E. 4h post IL15<br># peaks (FDR < 0.05) | Percentage of<br>D.E. peaks |
|------------|-------------------------|---|-----------------------------|
| ATAC - Seq | 42,000                  | 0   | 0%                          |
| H3K4me3    | 62,661                  | 0   | 0%                          |
| H3K4me1    | 46,000                  | 1,528                                     | 3.3%                        |
| H3K27Ac    | 81,000                  | 510                                       | 0.6%                        |
| H3K27me3   | 10,000                  | 0   | 0%                          |

**Table 5: Number of total and differentially expressed peaks of Tn5 and various histone marks at 4h post IL15 stimulation**

In table 5, we summarized the total number of peaks per histone modification and the correspondent number of differential peaks at 4h post IL15 (FDR < 0.05, n = 3 biological replicates for H3K4me1 and H3K27Ac, and n = 1 for H3K27Ac and H3K4me3). For the first time, we obtained the histone modification map for human IELs, which provided insights on the histone code and the locations of various regulatory elements in IELs (classified based on histone marks). First, it became clear that the histone landscape did not change globally during IL15 stimulation. At 4h (at which there are 4000 differential

expressed genes based on RNA Seq), the histone modifications change very little. For H3K4me3, and H3K27me3, there were no differentially expressed peaks called. For H3K27Ac, there are 510 DE peaks among more than 81,000 existing peaks, made up only 0.6% change. For H3K3me1, there are 1528 DE peaks out of 46,000 peaks, made up around 3.3% change. Together with the ATAC data, we concluded that IL15 did not change the global histone modifications and chromatin accessibility landscape in order to induce major transcriptional changes. The data supported strongly the preset landscape hypothesis, in which the state of the chromatin was preset for terminally differentiated effector T cells. During IL15 signaling, there was no global epigenetic change, and the differential expression and binding of transcriptional factors (such as JAK/STAT, RUNX3, and SMAD3) are sufficient to induce broad transcriptional changes.

To understand the preset landscape of IELs at the steady state, prior to IL15 stimulation, we zoomed in different categories of genes based on their expression level under IL15. We overlaid all the epigenetic track along the genes, which included the ATAC peaks (Tn5 tracks) and 4 histone modifications at 0h and 4h. In figure 11, we showed the representative examples of non-differential, highly expressed genes in IELs such as CD8 and RUNX3. In addition, we showed the non-expressed genes such as transcriptional factors FOXP3 and TCF7 which were important in Treg and naïve T cells, but not in IELs. We started to see emerging patterns. At the steady state, non-expressed genes lack the activating mark H3K27Ac, and have low amount of Tn5 peaks or H3K4me3 peaks. Sometime, we observed the accumulation of repressive marks H3K27me3 across the gene body and promoters as in the case of TCF7. On the contrary, highly expressed genes have high amount of activating markers such as the combination of H3K4me3 and H3K27Ac on the promoters, or the combination of H3K4me1 and H3K27Ac on the enhancer sites. There is a lack of repressive mark H3K27me3 anywhere near the gene's location. In figure 12, we showed examples of differentially expressed genes, including the IL15-induced genes BCL2 and GZMB, and the IL15-repressed genes SMAD3 and FOXO3. Strikingly, both induced and repressed genes

share similar a pattern for Tn5 and H3K4me3 peaks, with strong signature for both at the promoter sites. H3K27me3 marks are absent in general. H3K27Ac seemed to be higher in the induced genes than repressed genes.

The observations of typical IL15 controlled genes beg the question if the histone landscape of IELs in the steady state are primed and preset. In other word, we asked if the steady state histone landscape can predict the gene expression patterns under IL15. To investigate further, we assigned each histone mark to the closest gene, keeping in mind the limitations of such analysis (some enhancer elements can be located far away from the regulated genes). In figure 13, we plotted the intensity of different histone marks and compared across different groups of genes: non differential expressed genes, induced genes at various times, and repressed genes at various time. Even at the steady state, the baseline levels of histone marks (H3K4me3, H3K4me1, H3K4Ac) are higher in early responded genes (both induced and repressed genes) than non-differentially expressed genes, or differentially expressed genes at 24h. In conclusion, it is indeed the case that at steady state, the IL15 DEGs may be primed, with higher level of activating histone marks and open chromatin accessibility.

Finally, among the four different histone marks, only H3K4me1 (enhancer associated marks) shows minor change (1528 DE peaks or 3.3%). Next, we analyzed the association of these dynamic H3K4me1 peaks. In figure 14, differential H3K4me1 peaks are preferentially enriched in both upregulated and downregulated genes at 2h, and to a smaller extent at 4h. H3K4me1 DE peaks are not enriched in late responded genes or non-differentially expressed genes. However, based on the experimental design, we could not conclude if the H3K4me1 changes are consequences of gene expression changes, or if H3K4me1 changes precede and cause gene expression changes.

Altogether, for the first time, we have obtained a full map of 4 different histone modification marks in human IELs prior and 4h post IL15 signaling. The histone modification landscape remains

relatively stable during the process. High level of H3K27Ac peaks, overlapping well with H3K4me1, H3K4me3 and Tn5 peaks are the signatures of highly expressed or differentially expressed genes. The number of repressive histone mark H3K27me3 is lowest among the marks (around 10,000 peaks), suggesting that IELs have a very “activating” chromatin and histone modification landscape. In turn, this preset, accessible and activated landscape can enable IELs to control a large amount of transcriptional program in a short amount of time. Finally, the histone modification marks at steady state together can predict if a particular gene will be expressed or not. Only H3K4me1 shows minor dynamic changes, and the changes are located primarily on genes that will be differentially expressed by IL15 at 2h.

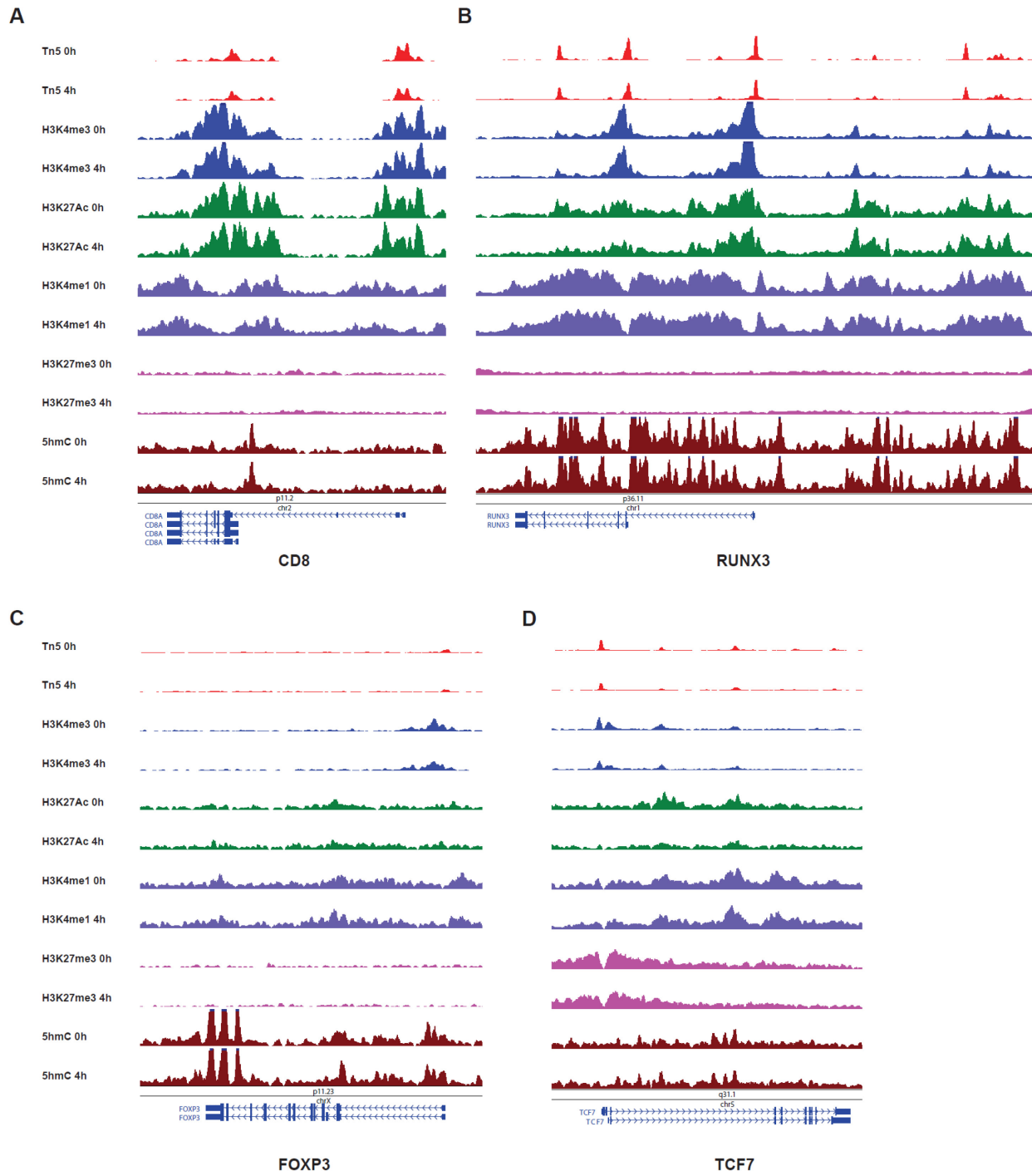


**Figure 11: The histone modifications, Tn5 and 5hmC landscape of non-differentially genes expressed at high level in steady state, and not expressed genes.**

**A, B**, The histone modifications, Tn5, 5hmC landscape of CD8 and RUNX3 – genes that are expressed at high level in steady state. **C, D**, The histone modifications, Tn5, 5hmC landscape of FOXP3 and TCF7 – genes that are not expressed in IELs.

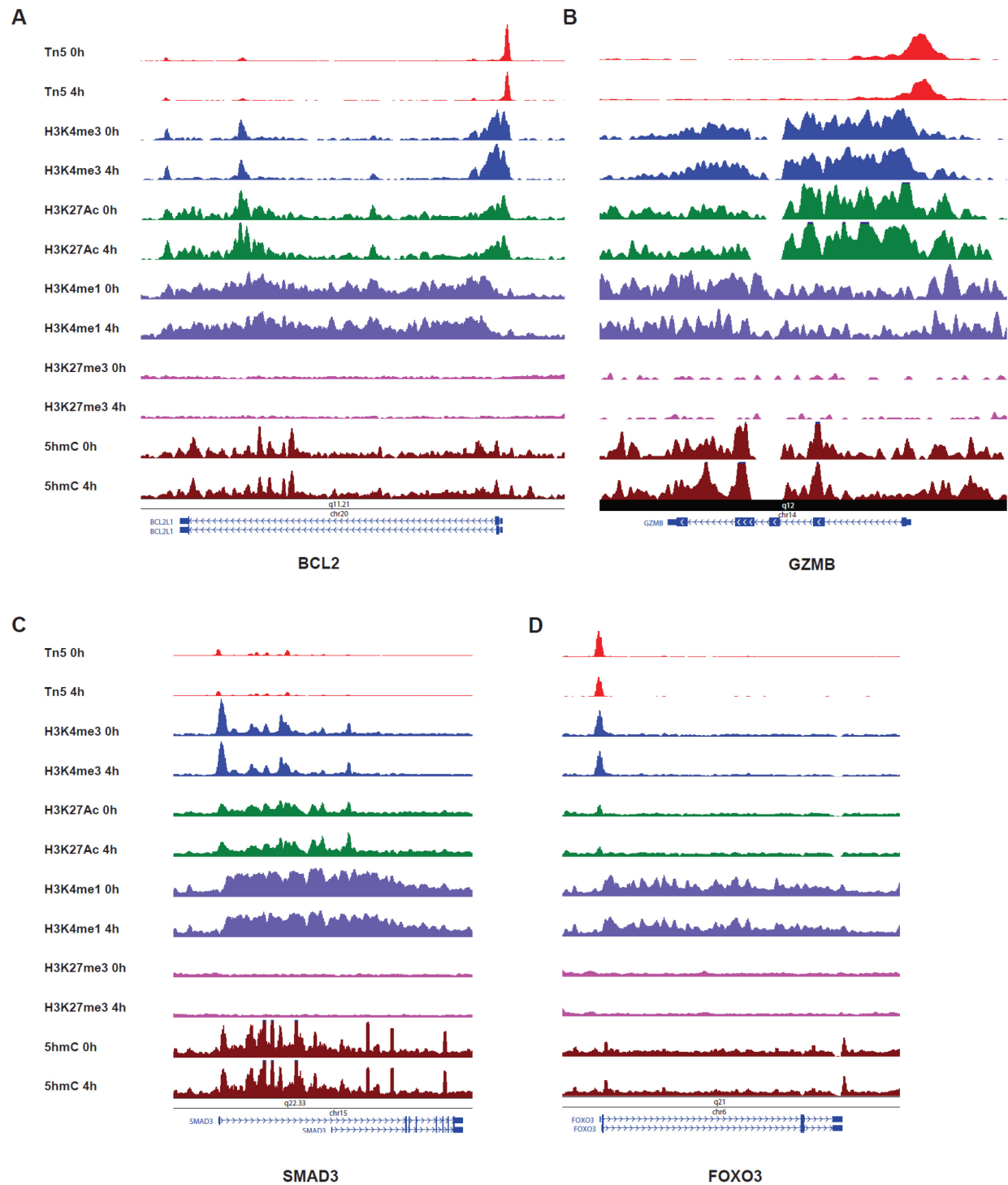


**Figure 12: Histone modifications landscape of induced and repressed genes during IL15 stimulation**

**A, B**, The histone modification, Tn5 and 5mC landscape of BCL2 and GZMB – induced genes post IL15 stimulation. **C, D**, The histone modification, Tn5 and 5mC landscape of SMAD3 and FOXO3 – repressed genes post IL15 stimulation.

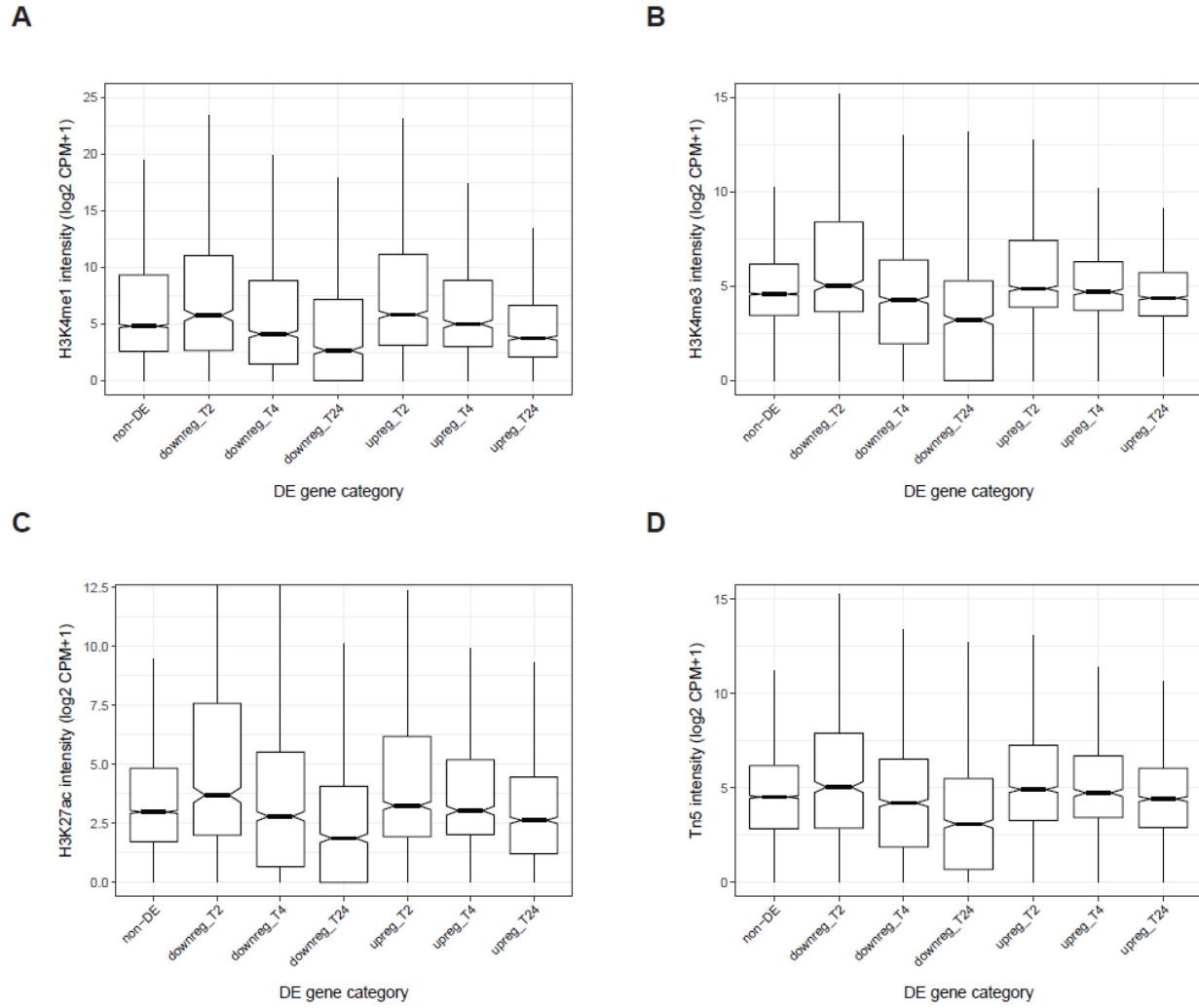


**Figure 13: Early differentiated genes show a higher than average number of activating histone modifications and Tn5 peaks count.**

**A**, Box plot representing the intensity of H3K4me1 (in term of  $\log_2 \text{CPM}+1$ ) of different categories of genes. **B**, Box plot representing the intensity of H3K4me3 (in term of  $\log_2 \text{CPM}+1$ ) of different categories of genes. **C**, Box plot representing the intensity of H3K27Ac (in term of  $\log_2 \text{CPM}+1$ ) of different categories of genes. **D**, Box plot representing the intensity of ATAC peaks (in term of  $\log_2 \text{CPM}+1$ ) of different categories of genes. Abbreviation: CPM – count per million. T2, T4, T24 – time 2h, 4h and 24h. Non-DE – None differentially expressed genes.

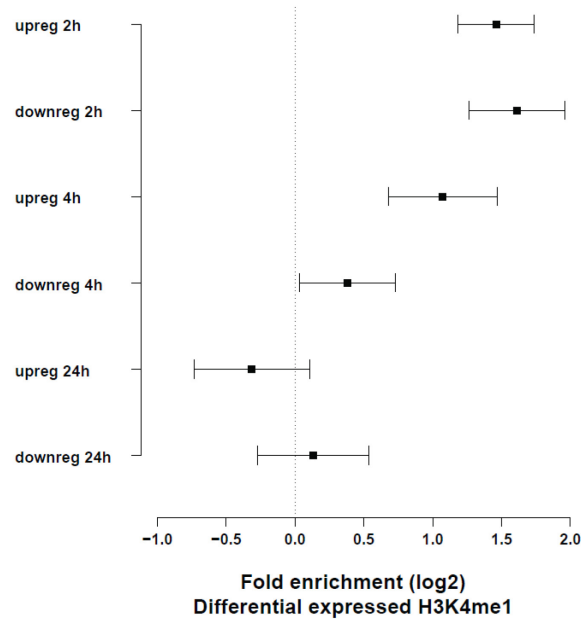


**Figure 14: H3K4me1 is enriched in early and intermediate differentially expressed genes**

The log<sub>2</sub> fold enrichment of H3K4me1 of different categories of genes. The histone peak is associated with the nearest gene. Gene segment is defined as +/- 5kb from TSS to TES.

#### 4.3 5-Hydroxymethylcytosines are abundant and change dynamically

Having understanding the chromatin accessibility and the dynamics of the histone marks, we sought to learn more about another type of epigenetic: methylation and demethylation. Methylation has long been known to be the “best studied epigenetic marks” in eukaryotic cells. Methylation has played important roles in genomic imprinting<sup>151</sup>, X chromosome inactivation<sup>152</sup>, transcriptional repression<sup>102</sup>, and generation of binding sites for important transcriptional factors<sup>151</sup>. In addition, methylation and demethylation has been shown to crosstalk with histone, affecting the recruitments of transcriptional complexes<sup>72</sup>. Methylation has been shown to be very stable, until recently, in which a demethylation pathway associated with the Tet family proteins has been discovered<sup>153</sup>. In the interest of understanding if demethylation processes involved in IL15 signaling pathway, we investigated the dynamics of 5hmC – the key intermediate mark of the demethylation process. In addition, 5hmC itself has been shown to be relatively stable, and can serve as the binding site for “readers” in stem cells. To obtain the map of 5hmC in IELs during IL15 signaling, we performed 5hmC-Seal – the IP in which 5hmC was labelled by  $\beta$ GT enzymes with modified azide sugars, and pulled down with streptavidin beads. The assay has been shown to have high sensitivity and selectivity<sup>127</sup>.

In figure 15A, we have performed 5hmC IP for 3 short termed IEL lines, and on average, we have 60,000 5hmC peaks at the baseline. Compared to 80,000 peaks of acetylation histone marks, one can see that 5hmC peaks are similar in term of abundance. The total number of peaks increases at 2h to 70,000 peaks, and gradually decreases at 4h and drastically decreases at 24h to around 40,000 total peaks. The dramatic loss of 5hmC at 24h can be due to two reasons. First, it may take 24h for some genes to lose their 5hmC peaks. Second, 24h post IL15 stimulation, the IELs enter cell division. During replication processes, the newly synthesize strands of DNA do not have time to regain the pattern of 5hmC; therefore, there is a global loss of 5hmC. In fact, this phenomenon has been observed before<sup>154</sup>. In figure 15B, we can bin the total number of genes into 4 different quantile based on their gene expression levels from

highest to lowest expression level. The 5hmC profile is as followed: 5hmC is mainly depleted at the TSS while high level of 5hmC can be find both before the TSS and on the gene body. The intensity of 5hmC correlates with the level of gene expression. The group of genes with highest expression levels also has highest level of 5hmC CHIP signal and vice versa. The profile of 5hmC distribution on the genomic region has been described before, and figure 15B in a sense is a quality control step. It confirms that the 5hmC IP has been working well and specific. In figure 15C, investigated the locations of the 5hmC peaks. As the data show, 5hmC peaks are found mainly in the intergenic regions. With the histone data to define regulatory genomic regions, 5hmC peaks overlap well with acetylation histone marks, and H3K4me1 marks, suggesting that 5hmC peaks are primarily located at enhancer sites. Next, we wanted to understand the dynamics of 5hmC. We searched for the differential 5hmC regions (DHMRs), and in contrast with the stability of both chromatin accessibility and histone marks, 5hmC exhibits robust dynamic changes.

At 2h post IL15 stimulation, there are more than 1700 differentially expressed 5hmC regions (DHMRs) with 1200 gain-of-5hmC peaks, and 500 loss-of-5hmC peaks. At 4h, there are 3000 DHMRs, with 2500 gain of 5hmC and 500 loss of 5hmC. At 24h time point, there are 1500 DHMRs with predominantly loss of 5hmC (1500 loss of 5hmC and 50 gain of 5hmC). Overall, at 2h and 4h, we have around 2795 DHMRs in a background of around 50,000-70,000 5hmC peaks. Therefore, around 4-5% of 5hmC changes. The changes are specific and reproducible with  $n = 3$  biological replicates. To understand better the roles of genes associated with dynamic 5hmC, we performed supervised hierarchical clustering analysis of all the dynamic 5hmC peaks. In figure 15E, the DHMRs cluster into three distinct groups based on the pattern of 5hmC changes: loss group in which 5hmC is lost over time, gain (2h) group in which 5hmC is gained mainly at 2h and gain (2-4h) group in which 5hmC is gained at 2h and maintained to 4h. There are 1966 peaks in the loss group, 1384 peaks in the gain (2h) group, 2069 peaks in the gain (2-4h). In figure 15F, the average

signal of 5hmC of each group is plotted to show the change over time. In figure 15G, representative examples are shown for each cluster.

Altogether, 4-5% of 5hmC peaks change dynamically; hence, epigenetic can be involved for these specific set of genes. Next, we will explore the potential functions of these dynamic 5hmC peaks.

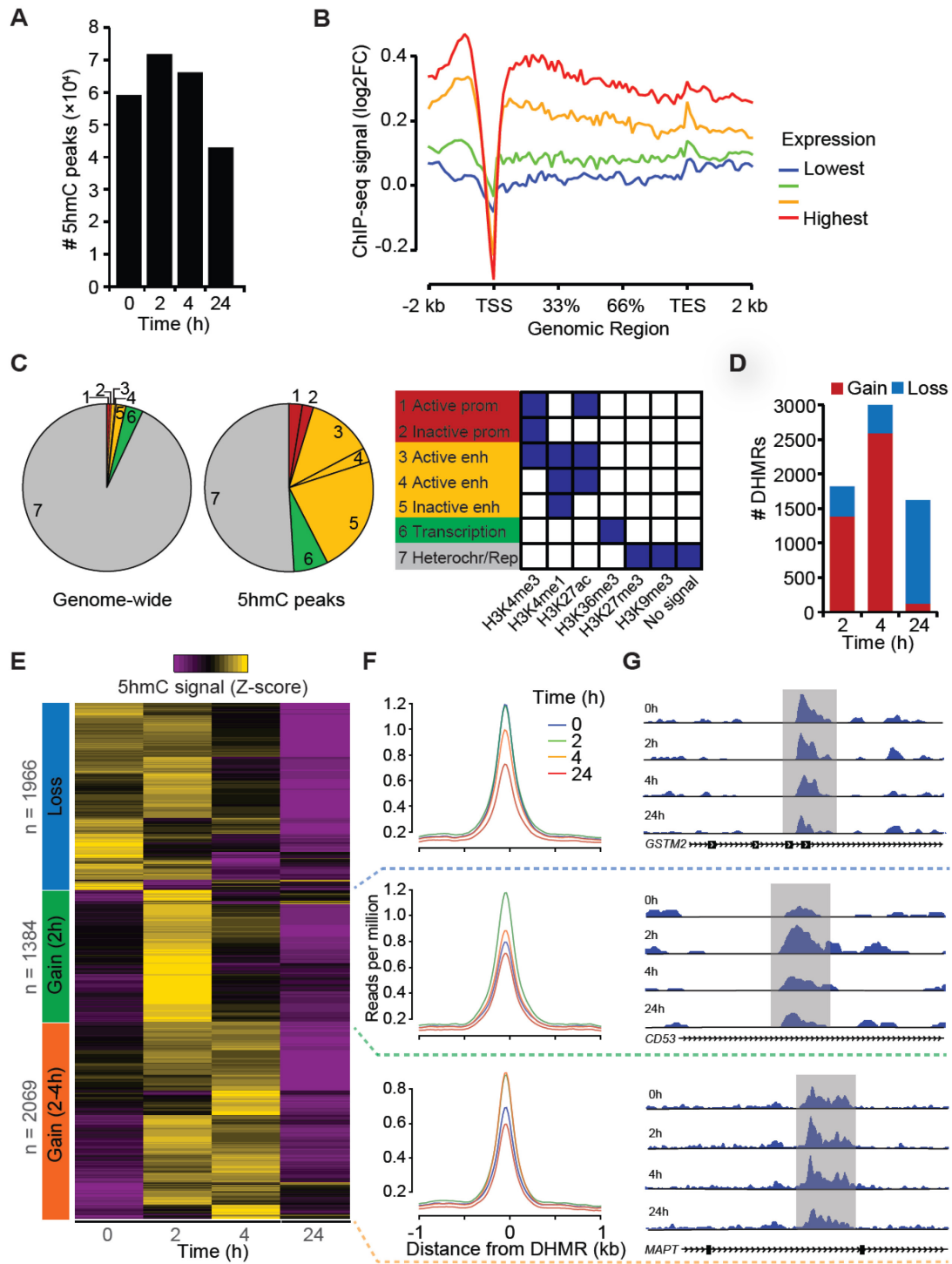


**Figure 15: IL15 induce dynamic 5hmC changes in IELs**

**A**, Quantification of the number of 5hmC peaks called at each time point during IEL stimulation (FDR < 0.05). n = 3 biological replicated. **B**, 5hmC profile across the gene body of all reference genes. The genes

**Figure 15, continued:** are color coded based on the quantile of their expression levels from RNA-Seq data. TSS, transcription start site; TES, transcription end site. **C**, Genomic distribution of all 5hmC peaks overlapping with UCSC RefGene database. Regulatory regions (promoters, active enhancers, etc....) are defined from ENCODE data of histone marks for CD8+ T cells. **D**, Differential 5hmC regions (DHMRs) at each time point. The gain and loss of 5hmC are based on the comparison to the 0h time point. **E**, Supervised hierarchical clustering analysis of all the 5hmC peaks based on the temporal pattern of the peaks. 5hmC DHMRs are clustered into 3 distinct groups: loss at 2h, gain at 2h and gain at 2-4h. **F**, The dynamic change of average 5hmC peaks for each cluster over time. **G**, Representative 5hmC peaks from each DHMR cluster.

#### 4.4 The correlation between DHMRs and DEGs

In order to understand the roles of 5hmC in transcriptional regulation of IL15 signaling, we carried out enrichment analysis to connect 5hmC dynamics to RNA expression levels. We investigated if any of the 6 clusters based on RNA expression (from figure 8B) is enriched for any category of 5hmC dynamics (from figure 15E). For example, for 5hmC loss categories: enrichment in 5hmC loss = (# induced 2h genes that are associated with 5hmC loss / # genes that are associated 5hmC loss) / (# induced 2h genes genome-wide / # genes genome-wide). In figure 16A, all the genes associated with dynamic 5hmC are more likely to be differentiated than genes without dynamic 5hmC. Therefore, differentially expressed 5hmC seems to be a good predictive mark for DEGs. Of note, genes with dynamic 5hmC are likely to be differentiated at early time points rather than at 24h. Next, DHMRs are classified as 5hmC loss, 5hmC gain at 2h, 5hmC gain at 2-4h. DEGs are classified as “induced 2h”, “induced 4h”, “induced 24h”, “repressed 2h”, “repressed 4h” and “repressed 24h” based on gene expression patterns. For the genes that loss 5hmC, especially loss 5hmC at 2h and 4h, they are more likely to be enriched in the categories “induced at 2h” and “induced at 4h”. There is slight enrichment (more than chance) for the “repressed at 2h”. However, there is no enrichment for DEGs at 24h time point. In figure 16B, for the genes that gain 5hmC, they are strongly enriched in “repressed at 2h” and “repressed at 4h”, and slight enriched in “induced at 2h” and “induced at 4h”. There is no enrichment for DEGs at 24h time point.

Generally, 5hmC has been shown to act via two distinct mechanisms<sup>102</sup>. First, 5hmC can be an intermediate marker for the demethylation process, in which 5mC can be oxidized to 5hmC, 5fC and 5caC and be excised out via TDG/BER<sup>155</sup>. However, 5hmC can also be a stable epigenetic mark for binding of transcriptional factors, histone remodifying enzymes or “readers”<sup>93,156</sup>. 5hmC can also act to disrupt the 5mC patterns, and 5mC binding proteins<sup>157</sup>. For example, 5hmC peaks can act as binding sites to recruit HDAC2 complexes to repress the expression of IL6 in macrophage, and there has been no demethylated regions detected in that system<sup>158</sup>. In our dataset, there are two emerging categories of dynamic 5hmC in

figure 17. The genes that loss 5hmC are enriched for induced genes at early time point. On the contrary, genes that gain 5hmC are enriched for repressed genes at early time point. The observations can be explained based on the how 5hmC can act to affect gene expression. For the genes that loss 5hmC, they may undergo demethylation process in which 5hmC is oxidized further and lost. Demethylation removes repressive 5mC marks, and opens up the genes for transcription. Hence, loss of 5hmC can be associated with induced genes. Now, on the other end, genes that gain 5hmC may gain and maintain the marks. In fact, many genes in our data set has gained these 5hmC at 2h, and still have them at 4h and 24h. These 5hmC peaks may be stable, and function as binding sites of repressive transcriptional factors to shut down gene expression. In such mechanism, gain in 5hmC can be associated with repressed genes. Of course, many genes that gain 5hmC can also be at the early stage of demethylation. In fact, gain in 5hmC is also enriched for induced genes, but not as strongly as repressive genes.

Altogether, our data indicate important trends of differential 5hmC peaks. Loss in 5hmC associates with early induced genes, suggesting demethylation at these loci. Gain in 5hmC associates with repressed genes, suggesting a different mechanism: 5hmC can be used as binding sites for repressive complex or to inhibit gene expression. Finally, change in 5hmC predicts well change in gene expression.

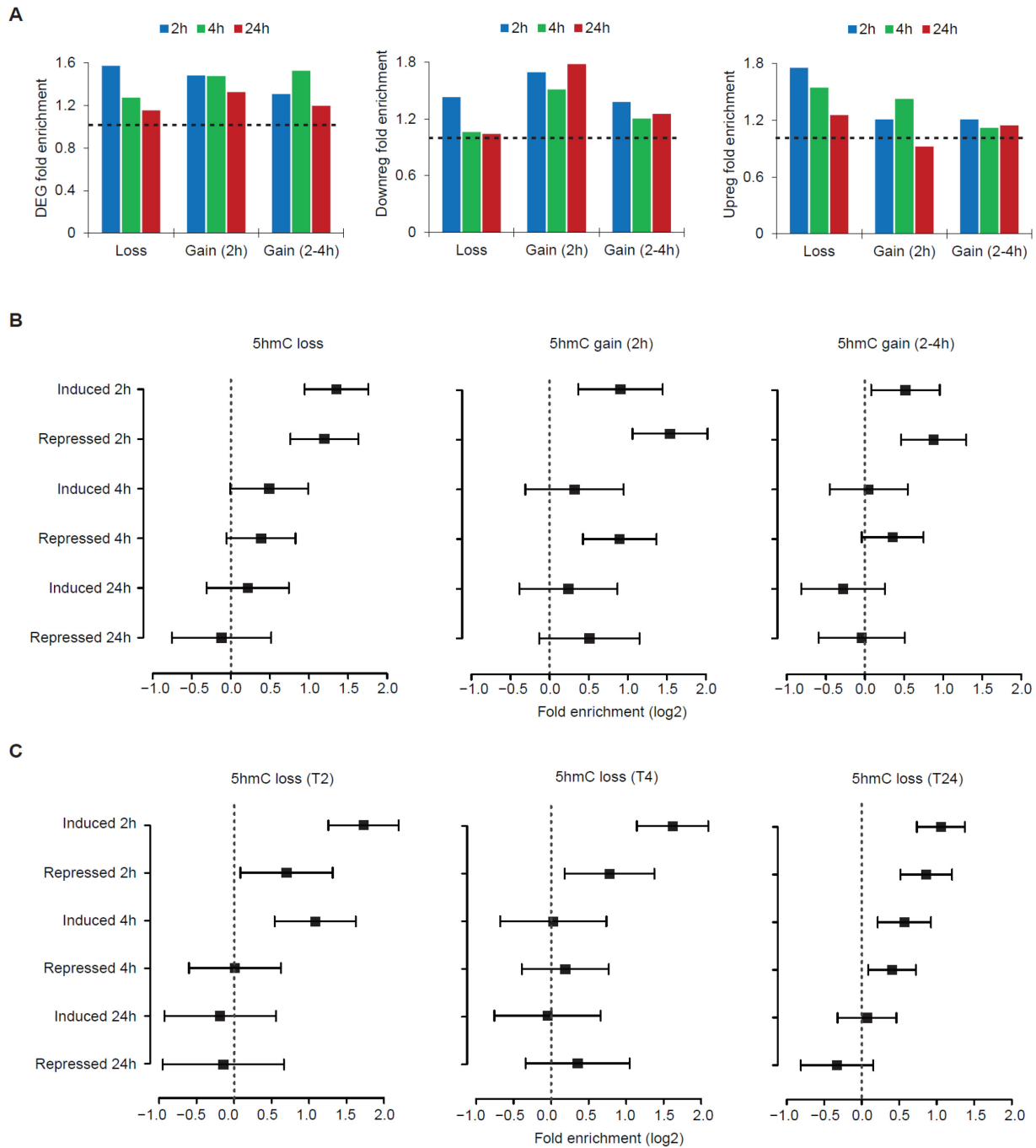


**Figure 16: Enrichment analysis of 5hmC DHMRs**

**A**, Genes with dynamic 5hmC are more likely to be differentially expressed. **B**, Enrichment analysis on loss vs. gain 5hmC peaks. Formula: calculated fold enrichment of induced 2h genes that are associated with 5hmC loss = (# induced 2h genes that are associated with 5hmC loss / # genes that are associated 5hmC loss) / (# induced 2h genes genome-wide / # genes genome-wide). **C**, Enrichment analysis on loss at 2h vs. loss at 4h vs. loss at 24h.

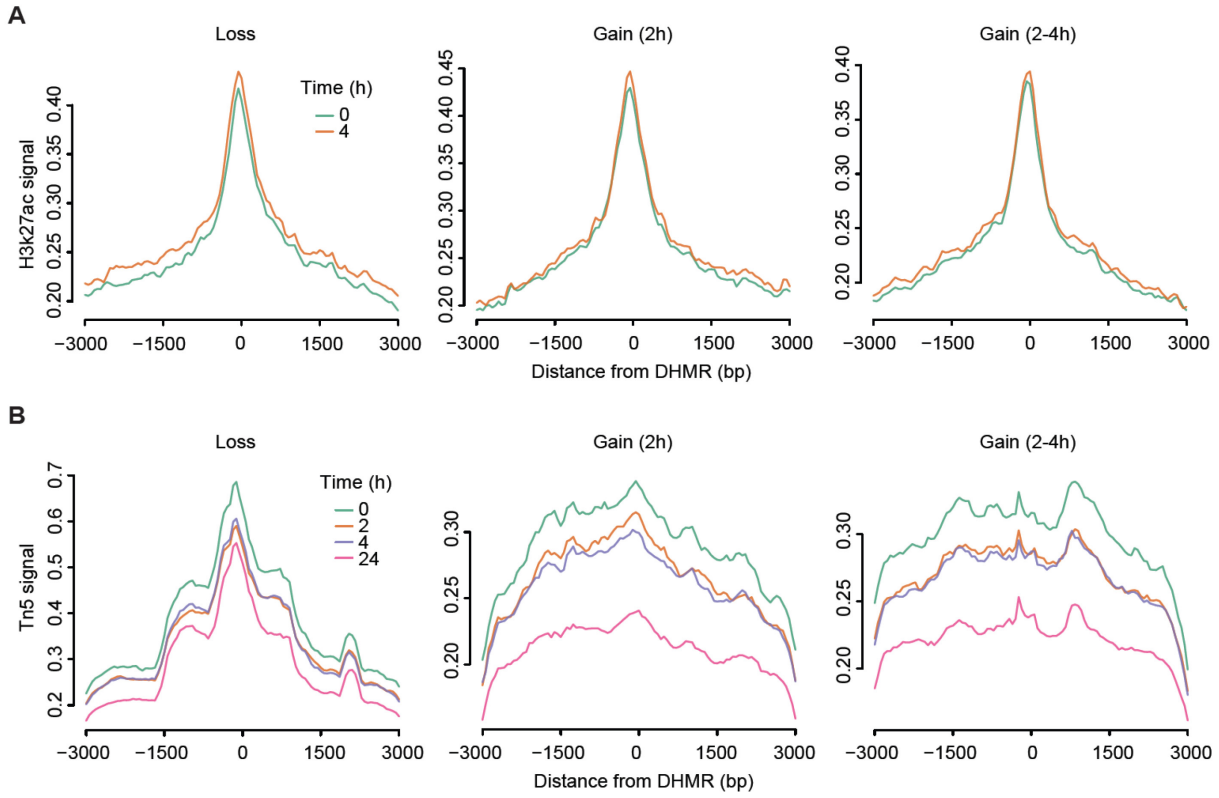


**Figure 17: The overlap between 5hmC dynamic peaks, H3K27Ac and ATAC peaks**

**A**, The average signal of H3K27Ac at 0h or 4h post IL15 stimulation when overlapped and centered on dynamic 5hmC peaks. The dynamic 5hmC peaks are classified into loss of 5hmC, gain of 5hmC at 2h and gain of 5hmC at 2h and 4h. **B**, The average signal of ATAC peaks when overlapped and centered on dynamic 5hmC peaks. The dynamic 5hmC peaks are classified similar as in A.

## CHAPTER 5: THE ROLES OF TET 2 DEMETHYLASE AND 5-HYDROXYMETHYLcytosine

### 5.1 Tet family in IELs and their expression levels during the signaling cascade

Due to the dynamic changes that we observed in 5hmC, we decided to investigate the molecular mechanism in which 5hmC was generated in IELs. Currently, there has been only one known mechanism in which 5hmC is generated: through the Tet family of demethylases. In order to zoom in to the relevant Tet in the system, we performed qPCR to learn the baseline expression of each Tet in the family. In figure 18, Tet1 is the Tet with the lowest expression. During the course of IL15 stimulation, Tet1 is strongly repressed, and the repression of Tet1 has been maintained throughout 24h. Therefore, Tet1 does not have the sufficient expression to drive the generation of new 5hmC. We shifted our focuses to the other members of the family: Tet2 and Tet3. Tet2 is expressed at highest level among the Tet proteins, 4 folds more abundant than the Tet3 transcripts. During IL15 stimulation, both Tet2 and Tet3 are slightly upregulated at 2h, and the expression levels of both Tets are quickly restored back to the baseline at 4h. At 24h post IL15 stimulation, both Tet2 and Tet3 are slightly repressed.

On the other hand, the family of Dnmt proteins are methylases, which capable of methylating the DNA. During IL15 signaling, Dnmt 3a is upregulated early on, peaking at 4h. Dnmt3b and Dnmt1 is not upregulated until after 24h. Dnmt 1 is a maintenance methylase. During cell division, the new strands of DNA are synthesized without methylation marks on them. Therefore, Dnmt1 may be upregulated to establish the 5mC patterns on newly synthesized DNA strand. Altogether from the data, we can see both the demethylases and methylases' expression levels altered during IL15 signaling – signifying that Tet and Dnmt families may be involved under IL15 signaling.

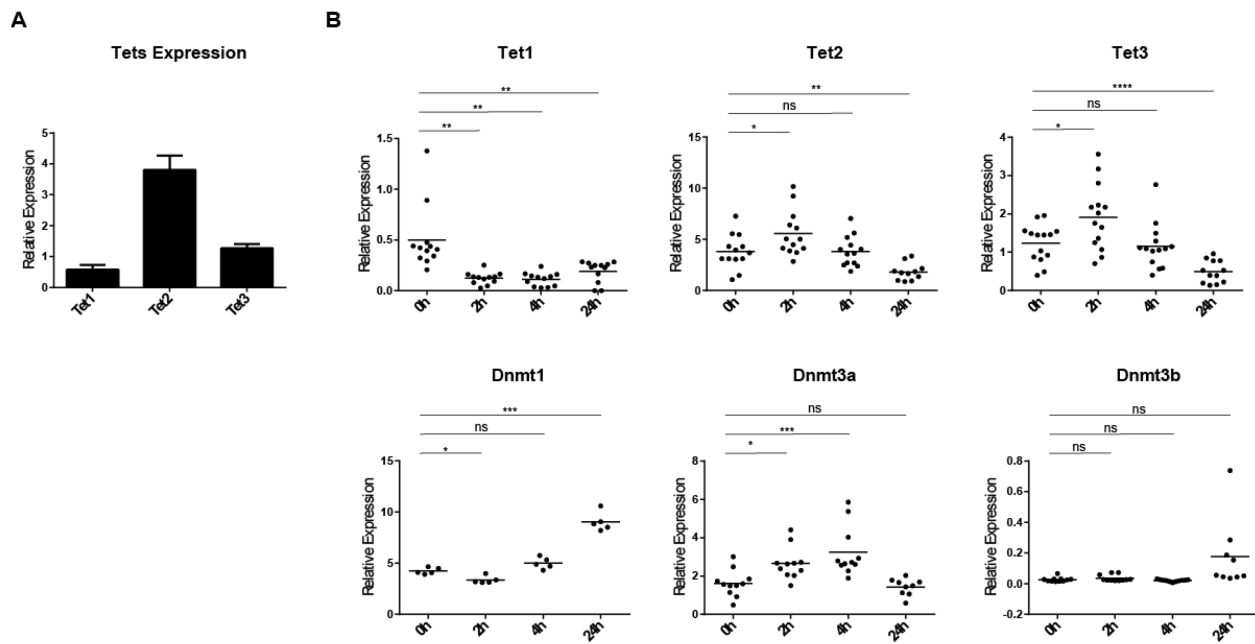


**Figure 18: Expression of Tet family at base line and during the course of IL15 stimulation in IELs**

**A**, The expression levels of Tet1, Tet2, Tet3 at base line level in IELs. The relative expressions are measured by qPCR and normalized to GAPDH. **B**, The expression levels of Tets and Dnmts during the course of IL15 stimulation.

## 5.2 Tet2 knock down (siTet2) and the baseline differential expressed genes

In order to learn the direct role of Tet protein in the generation of 5hmC and the regulatory roles of Tet in controlling transcriptions under IL15, we knocked down Tet2 via siRNA. Tet2 is the most expressed among the Tet protein, and Tet2 has been implicated in various biological processes involved 5hmC, making Tet2 the ideal target to investigate. To investigate DEGs in siTet2 versus siCtrl, we performed RNA-Seq for 5 biological replicates (5 short termed IEL lines) at 4 different time points (0h, 2h, 4h and 24h). In figure 19, we observed 1170 DEGs due to siTet2 at the baseline prior to IL15 stimulation. These DEGs are Tet2 regulated genes, independent with IL15. Tet2 is an important epigenetic regulator; therefore, it has not been a surprise to see 1170 DEGs due to the lack of Tet2. In figure 19A, gene ontology analysis of these DEGs points to important processes necessary for the package and maintenance of DNA's

integrity and structure. In addition, lacking Tet2 affects many DEGs in cell cycles such as those necessary for cell cycle check points, cell cycle phase transition, replication, regulation of cyclin dependent activity, mitotic nuclear division. Interestingly, iNKT and CD4<sup>+</sup> T cells in Tet2 knock out mice has been shown to be defective in cell cycle regulators<sup>106</sup>, DNA structure, and histone modifications<sup>105</sup>. Therefore, Tet2 may be fundamental important for DNA structure and cell cycle related genes in many cell types. In figure 19B, we list the top DEGs at baseline in siControl and siTet2 as representative examples.

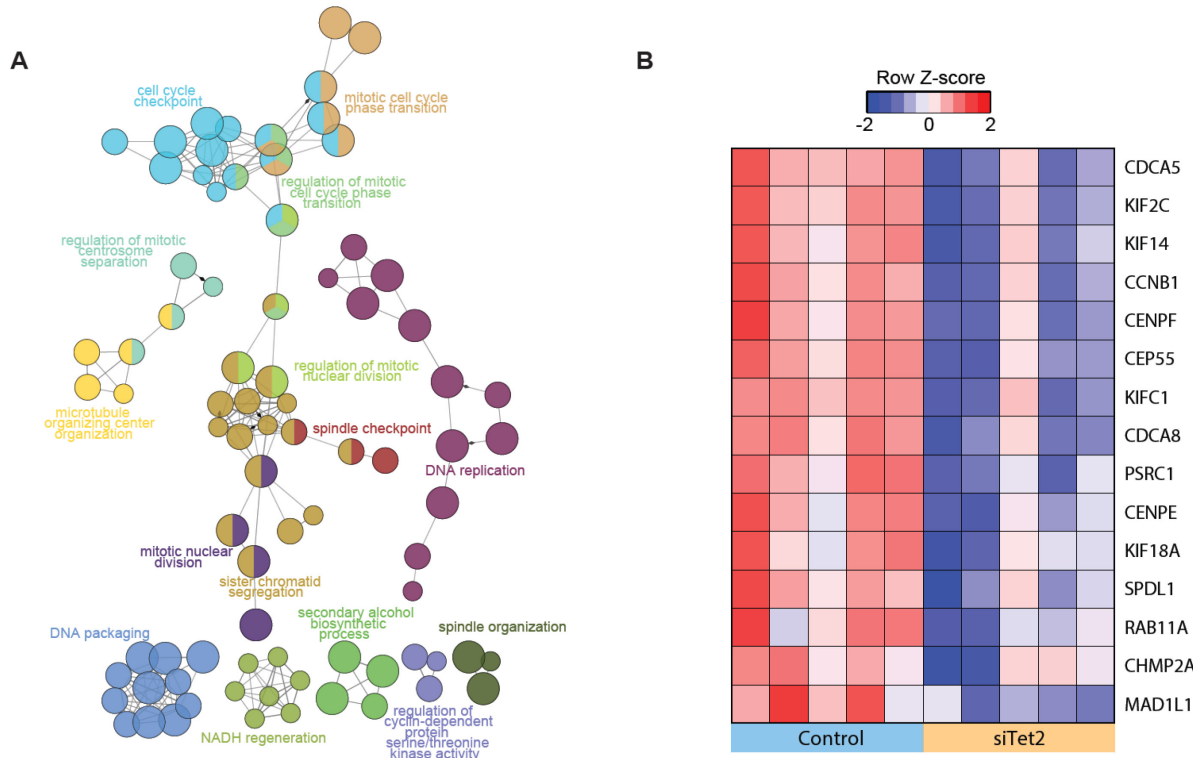


**Figure 19: The baseline effects of siTet2 in IELs**

**A**, The gene ontology of pathways affected due to the knock down of Tet2 at the baseline condition compared to scramble siControl construct. **B**, Representative differential expressed genes between siCtrl and siTet2. Each column is one short term IEL line. Each line is a DEG. N = 5 biological replicates.

### 5.3 Tet2 knock down (siTet2) and the roles of Tet2 in IL15 signaling

After understanding the baseline consequences of Tet2 knock down, we investigated the possible roles of Tet2 in IL15 signaling. We performed RNA sequencing for both siCtrl and siTet2 for n = 5 shorted term IELs cell lines in all 4 time points: at 0h, 2h, 4h and 24h. From Figure 20B, at 0h, baseline, we had 1170 DEGs between siCtrl and siTet2. At 2h, the difference was 172 DEGs. At 4h, there was 125 DEGs. Finally, at 24h there was no difference between the siCtrl and siTet2. From the data, the impact of Tet2 knock down is primarily on the transcriptional program of the early time points at 2h and 4h and not at the 24h. In addition, from figure 20B, we observed that there were more downregulated genes than upregulated genes. In order to understand better the Tet2 dependent genes in IL15 signaling pathway, we performed GO and KEGG analysis for these DEGs at 2h and 4h.

At 2h, the primary role of IL15 (from RNA-Seq data) is to mount an immune response to IL15 ligand. With Tet2 reduction, interestingly, the differential pathways between siCtrl and siTet2 are interferon gamma mediated signaling pathway, chemotaxis, leukocyte chemotaxis, and defense response. We looked deeply at the DEGs, and from figure 20D, in interferon gamma pathway, we saw higher level of relevant genes in this particular pathway: IFNG, IRF7, IRF5, MX1, ISG20, and MYD88. All the IFNg related genes are normally upregulated during IL15 signaling. In the knock down of Tet2, these genes are upregulated even further – for example, at the transcript level, IFNG has twice as much transcript in the siTet2 condition relative to the siCtrl at 2h. The evidences pointed to a hyper responsive state of IELs, in which they started to upregulate IFNg related genes at abnormally high levels. In similar fashion, many chemotaxis receptors have been upregulated at a higher level in Tet2 knockdown than the control: CCR1, CCR5, CCL3, and IL2RB. Of note, none of the anti-apoptotic genes regulated by IL15 were disturbed by the knock down of Tet2. The levels of BCL2, BCL-XL, and MCL1 remained the same in siTet2 versus siCtrl IELs. The data suggests Tet2 may be important specifically in immune related pathways like chemotaxis, IFNg related pathway or defense response and not important for survival pathways. On the other hand, in

siTet2 IELs, the downregulated genes are mainly cell cycle regulators and microtubule regulators such as WEE1 (G2 check point kinase), SKP2, APC, CKAP2 and TPPP. With many cell cycle regulators downregulated, the siTet2 IELs should be susceptible to a higher level of uncontrolled proliferation. This hypothesis will be tested in the next session. At 4h, there were 125 DEGs between the siTet2 and siCtrl. Most of the DEGs were downregulated and belong to cell cycle regulators – confirming the importance of Tet2 in controlling cell cycle check points such as CENPE, CENPF, KIF11, and PSRC1.

Altogether, in IL15 stimulated CD8+ T cells, 296 genes (1.8% of total IL15 regulated genes) are differentially expressed upon siTet2 knockdown (FDR<0.5). Of note, the knock down level of Tet2 is from 28% to 33%. Therefore, the number of IL15 regulated and Tet2 dependent genes may be underestimated. Genes that are upregulated upon siTet2 are pro-inflammatory genes. In particular, genes associated with IFN pathway (IFNg, IRF7), and defense responses pathway (Gzmb). Genes that are downregulated upon siTet2 knock down are cell cycle related genes.

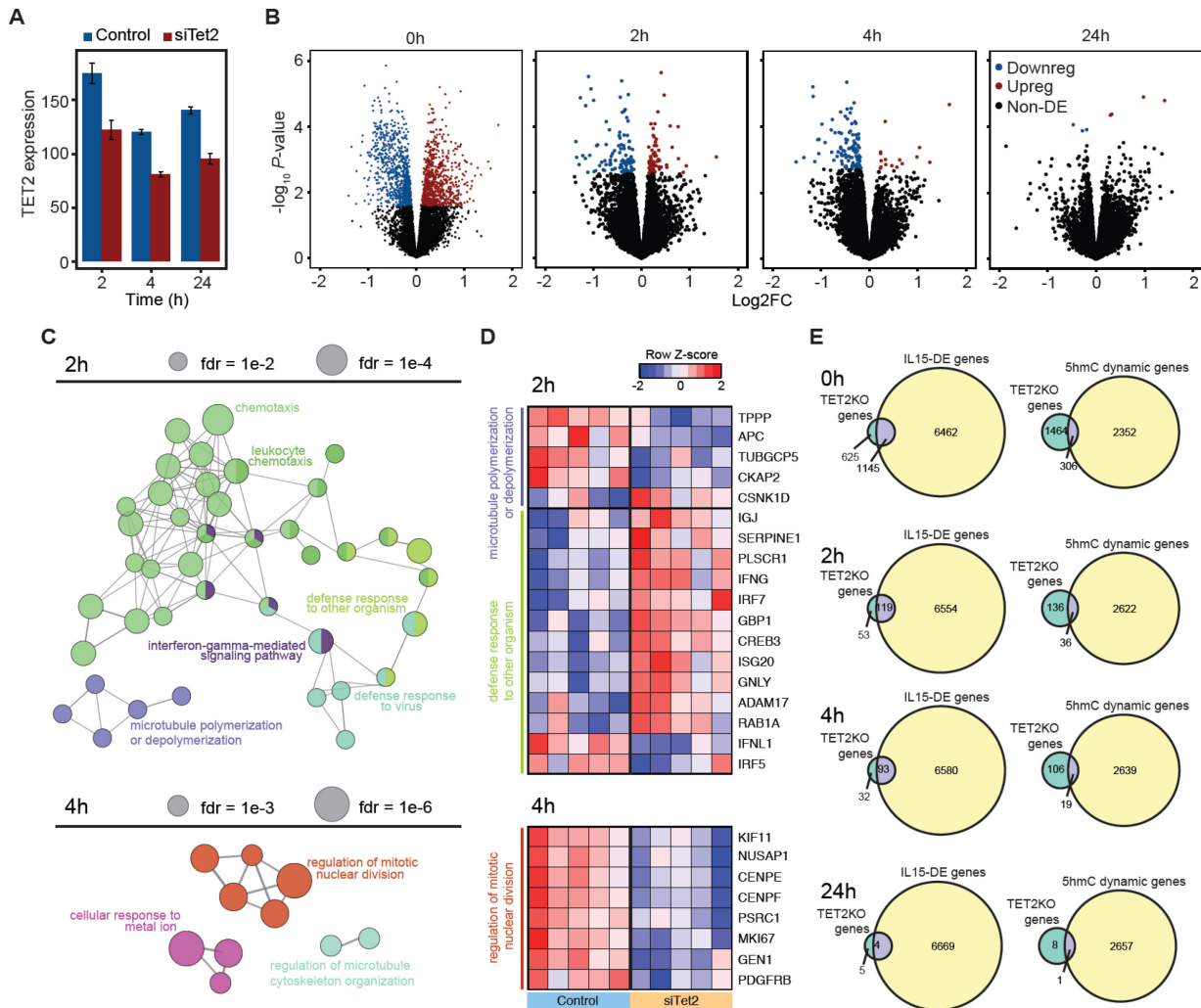


**Figure 20: The role of Tet2 in IL15 signaling pathway of IELs**

**A**, The level of knock down of Tet2 by Accell siRNA at each time point (2h, 4h, and 24h post IL15 stimulation). **B**, Volcano plots to represent the differentially expressed genes (DEGs) in siTet2 compared to siCtrl at each time point. Black dots represent non-differentially expressed genes, blue dots represent down regulated genes, and red dots represent up regulated genes (FDR < .01). **C**, GO analysis for DEGs in siTet2 compared to siCtrl at 2h and 4h post IL15 stimulation. **D**, Heat map of top DEGs at 2h and 4h. Each column represents one short termed IEL line. Each line represents one DE gene. N = 5 biological replicates for siCtrl and for siTet2. **E**, The overlaps between the DEGs in siTet2 at each time point with the total genes differentially regulated by IL15, and with the set of 5hmC dynamic genes.

#### 5.4 Functional consequences of Tet2 knockdown in IELs

Due to the downregulation of many cell cycle regulators such as P53, CCNK1A, and CCNK1C in the Tet2 knock down conditions, we investigated the functional consequence of knocking down Tet2 in term of proliferative capability of IELs. We stained the actively divided cells with edU (5-ethynyl-2'-deoxyuridine), an analog of thymidine. During the synthesis of new strands of DNA in actively dividing cells, edU will be incorporated into the DNA, and these cells can be stained and detected via flow cytometry. In figure 21A, without the presence of IL15, both siCtrl and siTet2 IELs did not enter division, and the percentages of edU+ cells were at background levels at 1.25% and 1.07% respectively. Upon IL15 stimulation, after 48h of incubation with IL15, the cells were stained for edU to look at the percentage of cells that were actively dividing at that particular time. For siCtrl IELs, 21.0% of the total cells were synthesizing new DNA strands. The correspondent percentage for siTet2 IELs was 29.4%. Therefore, 48h post IL15 stimulation, siTet2 IELs proliferated at higher rate than siCtrl IELs. In figure 21B, we repeated the experiments for  $n = 8$  replicates, and siTet2 IELs did proliferated statistically faster. In figure 21C, we also looked at the absolute number of cells post 48h of IL15 stimulation. The total numbers of siTet2 IELs were also higher than siCtrl IELs 48h post IL15 stimulation. Of note, the amount of final cell counts of both siTet2 and siCtrl did not differ much from the starting amount of IELs prior to IL15. It was due to the fact that many IELs died during the initial exposure to IELs. Only the survived IELs started to divide and increase in number. Altogether, it seemed that the loss of cell cycle regulators translated into a faster proliferative rate for siTet2 IELs. With reduced levels of cell cycle regulators in siTet2, the IELs presumably can enter S phase and G1 phase easier, and divide at a faster rate. The observation has been in according to the literatures. Tet2 knockout mice are susceptible to develop T cells lymphoma<sup>159</sup>. Loss of Tet2 in hematopoietic cells can also lead to hypermethylated enhancers on crucial tumor suppressor genes, leading to the loss of these regulators and the faster rate of population doubling<sup>160</sup>. Further investigation

needs to be done to examine the mechanism in which the knock down of Tet2 affected the expression of these cell cycle regulators, and if hypermethylation played any role in silencing these regulators.

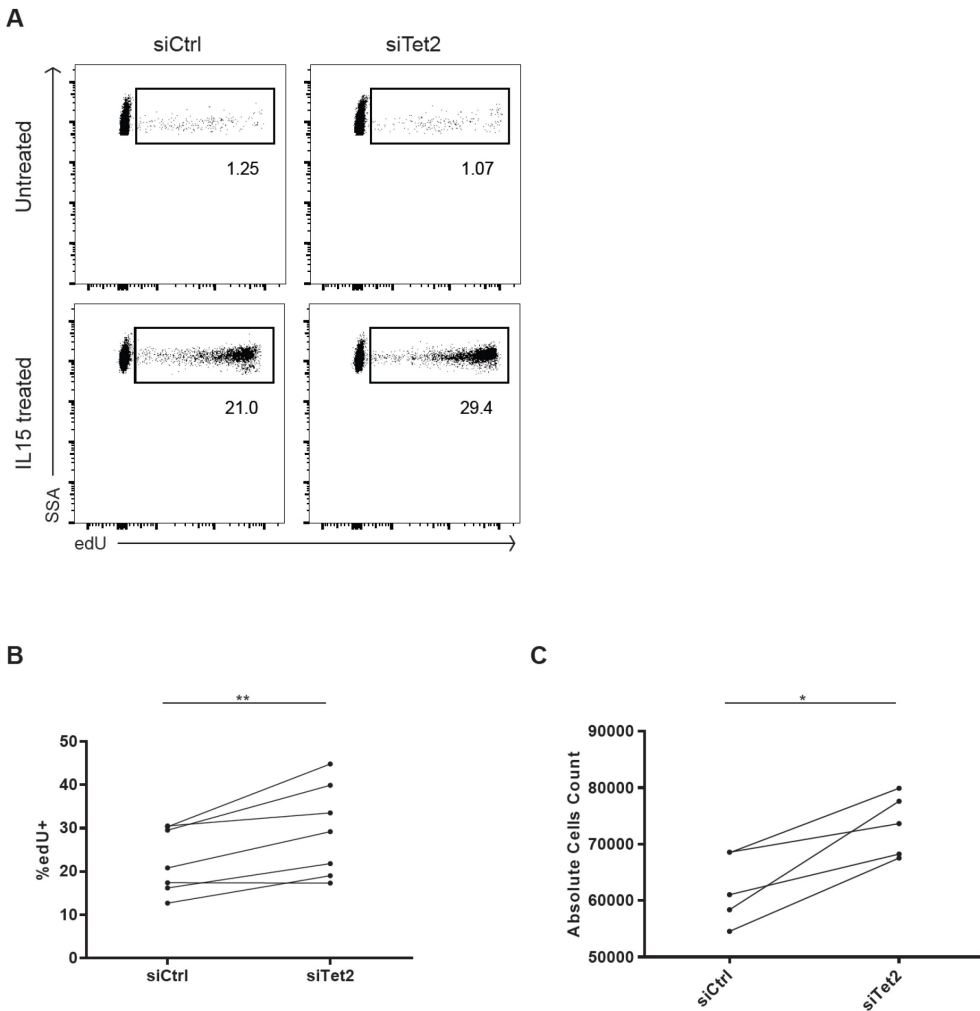


**Figure 21: Proliferation rate of siTet2 IELs**

**A**, The proliferation rate of untreated and IL15 treated (48h post stimulation) IELs in either siCtrl or siTet2 background. EdU is the nucleoside analog of thymidine and is incorporated to newly synthesized DNA. **B**, The percentage of edU+ IELs 48h post IL15 treated IELs in either siCtrl or siTet2 background for n = 7 biological replicates. **C**, The absolute number of cells 48h post IL15 stimulation in either siCtrl or siTet2 background. n = 5 biological replicates. The number of starting IELs is 50,000 cells.

## CHAPTER 6: DISCUSSION AND FUTURE DIRECTIONS

### 6.1 Overview

We began our studies by examining the transcriptomic changes during the course of IL15 signaling in IELs. By using short termed IEL cell lines generated from patients' biopsies, we demonstrated that IL15 was a potent cytokine, capable of controlling as much as 6462 genes during a 24h period. Beside known roles in anti-apoptosis, cytotoxicity, proliferation, we showed that IL15 was involved in the regulation of metabolism and the processing of various RNA species (including long noncoding RNAs). Since the mapping of IL15-mediated transcriptomic changes in the mouse peripheral blood CD8<sup>+</sup> T cells<sup>32</sup>, this is the first transcriptomic map of *in vitro* IL15 signaling in human intestinal CD8<sup>+</sup>TCR $\alpha\beta$ <sup>+</sup> T cells.

There is a large body of literature that demonstrated the roles of epigenetic during T cells' development, differentiation and responses to pathogens<sup>59,104,149</sup>. However, T cells do not stop functioning after the activation and differentiation processes. IELs are the prototypical cells of tissue resident, terminally differentiated CD8<sup>+</sup> T cells. At this stage, IELs no longer differentiate, but they continue to encounter the changing local mucosal environment with various immunological or stress signals such as IL15. By performing ATAC-Seq on IELs, we demonstrated that the chromatin accessibility of IELs is stable, with no change during the short time period after IL15 signaling. At 24h, the whole IEL's chromatin landscape is altered nonspecifically due to cell division. Using native histone pull down, followed by next gen sequencing, we demonstrated that the 4 histone marks (H3K4me1, H3K4me3, H3K27Ac, and H3K27me3) are mainly preset, and stable during the course of IL15 stimulation. Different combinations of these 4 histone marks can have predictive power on how the correspondent genes would change during the IL15 signaling, similar to what have been known about the histone code<sup>74,75</sup>.

Next, by using modified sugar to label and pull down 5hmC, for the first time, we obtained 5hmC map in IELs during IL15 signaling. We demonstrated that 5hmC peaks are widespread in IELs with around 70,000 total 5hmC peaks on average. 5hmC peaks locate mostly in the enhancer elements, and 5hmC levels on gene body correlate well with gene expression levels. We then demonstrated that 4.6% of total 5hmC peaks change dynamically during the course of IL15 signaling. Loss of 5hmC is associated with induced genes, and gain of 5hmC is associated with repressed genes, suggesting different mechanisms may operate via 5hmC to regulate gene expression. Lastly, we investigated the role of Tet2 in IL15 signaling. We demonstrated that by knocking down of Tet2, many important pathways associated with DNA packaging, and chromatin integrity were affected. During the response to IL15, Tet2 knockdown IELs have more proliferative capability due to the reduction of cell cycle regulators. Furthermore, in term of the magnitude of the response to IL15, Tet2 knockdown IELs upregulate higher level of transcriptions of IFN related pathway compared to the control IELs. Altogether, the data suggest that there are a subset of genes, mainly cell cycle related and IFN related are controlled both by Tet2 and IL15.

## **6.2 The model: preset versus altered epigenetic landscape in IL15 signaling**

We set out to explore possible epigenetic changes when IELs responded to IL15. At the end, our data and analysis reveal a model in which the chromatin and histone modifications on IELs are mostly preset and do not change significantly in response to IL15. Among all the epigenetic marks, 5hmC is the one that changes the most. Yet, even this change is small – 4.6% of total 5hmC peaks. Therefore, we can conclude that on the global scale, the epigenetic landscape (in term of chromatin accessibility, histone modifications and 5hmC) is stable and preset in IELs during IL15 signaling. However, we do not rule out the involvement of epigenetic regulation in a small subset of important genes such as cell cycle related and IFN related genes. The impact of Tet2 knockdown on the transcription levels of this subset of genes suggests that these genes may be indeed regulated via Tet and 5hmC.

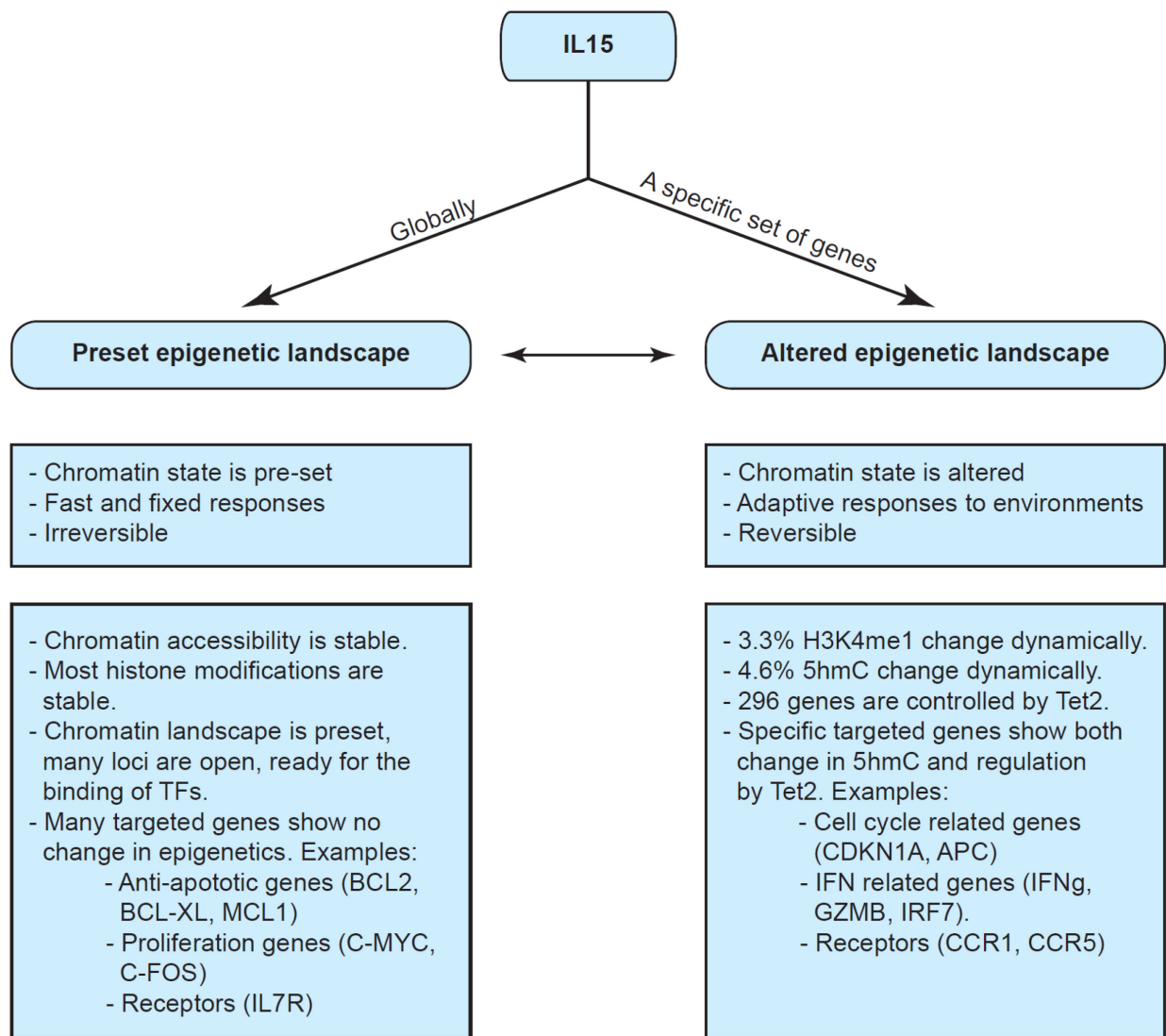


**Figure 22: Model - Epigenetic landscape during IL15 signaling in IELs**

Our results are in agreement with previous reports on similar systems. Epigenetic seems to be mostly important for differentiating system, in which cells undergo identity change<sup>108</sup>. When the differentiation ends, the epigenetic landscape seems to be stable and one may consider the epigenetic landscape as a part of molecular signatures made up the identity of the cells. For example, the chromatin

landscape (revealed by ATAC seq) is changed most significantly during the activation of naïve T cells into effector T cells<sup>149</sup>. In vitro differentiation assays of Th0 into Th1 and Th2 reveal significant changes in 5hmC and 5mC, with demethylation occurs at specific loci: IFNg for Th1 differentiation, an IL4 for Th2 differentiation<sup>104</sup>. The phenomenon is not limited to T cells as naïve dendritic cells show global demethylation and alteration of histone modifications upon tuberculosis infection<sup>150</sup>. On the other hand, once the cells are terminally differentiated, the chromatin accessibility seem to be stable. During the course of chronic viral infection, the ATAC landscape does not vary between day 8 and day 27 post infection<sup>122</sup>. Furthermore, there are evidences that the epigenetic landscape is also maintained by complex machinery to establish the necessary stability for differentiated T cells to function<sup>121</sup>. In this study, we demonstrated that in IELs, as terminally differentiated T cells, the response to IL15, a cytokine, does not involve global changes of epigenetic landscape.

In term of evolutionary viewpoint, there are advantages associated with operating on a preset epigenetic landscape. IELs are tissue resident CD8<sup>+</sup> T cells at the front line of the immune system to protect the integrity of the mucosal barrier and the surrounding epithelial cells<sup>7</sup>. IL15 has been thought as a stress signal, presented by antigen presenting cells and epithelial cells to activate IELs and license them to kill<sup>11,14</sup>. Therefore, acting on a preset landscape, the IELs can control its transcriptomic program quickly to mount fast proinflammatory responses to protect the intestinal environment. Our data indicate that for important effector genes such as BCL2, BCL-XL, IFNG, GZMB, and PRF1, there are strong ATAC-Seq peaks at the promoter sites with relevant activating histone marks: H3K4me3 and H3K27Ac. The epigenetic signatures point toward accessible chromatin at steady state, ready for the binding of STAT3/STAT5 transcriptional factors upon the binding of IL15 to its receptors. Phosphorylation of JAK/STAT can occur within minutes of ligand-receptor interaction<sup>161</sup>, and in combination with a preset chromatin landscape, the signal cascade can be fully activated rapidly. As a result, IELs can react and protect in a timely manner.

There are apparent limitations to our *in vitro* system: the fact that the short term IELs are not *ex vivo* cells, and they are cultured in 100u of IL2. We performed experiments on short term IELs (as opposed to long term IELs in culture medium) to preserve as much as possible the epigenetic of *in vivo* IELs. Freshly isolated and sorted IELs from patients' biopsies were stimulated one time to make short term IEL cell lines. All subsequent experiments were done on these cell line stocks. We had done quality controls to investigate the difference between the short termed IEL lines and the *ex vivo* IELs counterpart in term of ATAC-Seq data. There are more ATAC-Seq peaks on the *ex vivo* IELs, especially on the enhancer sites, reflecting the loss of a portion of epigenetic signatures during the course of making short termed IEL lines. However, there are a large percentage of overlapped and conserved ATAC peaks (>70%) between the *ex vivo* and *in vitro* IELs, reflecting the preservation of the chromatin accessibility landscape (unpublished data). Due to the requirement of large amount of cells as starting materials, we cannot compare the 5hmC and the histone landscapes between the *ex vivo* and *in vitro* short termed IELs. Next, in order to culture the IELs and ensure their survival, we used medium with 100 units of interleukin 2. In the absence of IL2 or IL15, CD8<sup>+</sup> TCR $\alpha\beta$  T cells will start to enter apoptosis and die. However, IL2 does have overlapping functions with IL15<sup>32</sup>, and the exposure of IELs to IL2 raise the possibility that the epigenetic has already been changed in culture prior to the stimulation of IL15. To address this concern, first, the *in vitro* system is still relevant because in the physiological conditions, IELs have been shown to exist in the intestinal environment with low level of IL15 (similar to the exposure to low dose of IL2 in culture medium)<sup>44</sup>. Second, there was a starvation period of 48h to remove all the effect of IL2 prior to the addition of IL15. However, to truly address this problem, future experiments should be done on *ex vivo* IELs to show that the chromatin accessibility, 5hmC and histone landscape of *ex vivo* IELs does not change much upon IL15 stimulation, similar to the *in vitro* short term IELs.

### 6.3 The roles of 5hmC – demethylation intermediate or stable epigenetic mark?

Since the discovery that the Tet proteins can oxidize 5mC to 5hmC, 5fC and 5caC in the progressive steps of demethylation, 5hmC is traditionally thought as a transient intermediate mark of demethylation<sup>86,162</sup>. The gain and the loss of 5hmC are thought to be direct consequences of Tet mediated demethylation on specific loci, for example the NANOG locus in stem cells<sup>163,164</sup>. However, recent biochemical studies on the half-life of 5hmC, the dynamics of Tet2 – 5hmC complex, and the independent roles of Tets from demethylation have revealed an alternative function for 5hmC<sup>93,99,158,165</sup>. 5hmC can act as a stable epigenetic mark, and a binding site for multimeric protein complexes, including the binding of TET2, SALL4A or HDAC proteins<sup>99,158</sup>. In the context of IL15 signaling, we demonstrated that there were two distinct categories of dynamic 5hmC: dynamic gain and dynamic loss of 5hmC. The locations and the potential roles of these two classes of dynamic 5hmC are distinct, suggesting that 5hmC can indeed be a marker of two different mechanisms.

The loss of 5hmC has occurred primarily on open chromatin, evident in the overlap between 5hmC peaks and ATAC peaks. The loss of 5hmC also occurred at poised or activated regulatory sites, evident in the overlap with the H3K27 acetylation marks. Finally, the loss of 5hmC was associated with early induced genes, suggesting that losing 5hmC could promote transcription. The observation fit the concept of 5hmC as an intermediate mark of demethylation. Loss of 5hmC can be the result of further oxidation to 5fC and 5caC and subsequent removal of 5mC. Therefore, loss of 5hmC can signify the concurrent removal of suppressive methylation marks. Happening on primed locations with euchromatin landscape and activating histone mark H3K27Ac, demethylation can promote the binding of RNA polymerase II machinery and initiate the transcription. However, with our current data, we cannot make the full statement here without further experiments. Specifically, for these loci, a site specific methylation assay such as bisulfite sequencing is needed to pinpoint with base resolution the demethylated cytosine. In

addition, POLR2 CHIP-Seq can be done to show the differential binding of POLR2 in these loci before and after the loss of 5hmC.

On the other hand, the gain of 5hmC has different and distinct features. Gain of 5hmC did not occur on open chromatin, but on heterochromatin, evident in the lack of overlap with ATAC peaks. These loci did not enrich for induced genes, but they did for early repressed genes. How can one make the connection between 5hmC and repression of gene expression? If 5hmC can be a stable epigenetic mark, gain in 5hmC would generate binding sites for 5hmC “readers”. These readers can be repressive transcriptional factors which in turn can shut down transcription. Indeed in a study, 5hmC acted to recruit the binding of HDACs to repress IL6 expression post lipopolysaccharide (LPS) stimulation in macrophages<sup>158</sup>. In addition, Tet2 has been shown to be a tumor suppressor gene in hematopoietic disorders<sup>166</sup>. The binding of Tet2 on 5hmC sites in these system does not initiate, but repress transcription presumably through the recruit of other Tet2 partners that are repressive transcriptional factors. Alternatively, the gain of 5hmC can be simply the first step prior to the loss of 5hmC due to further oxidation to 5fC and 5caC. However, we did not observe any changed in ATAC peaks associated with gain of 5hmC. Demethylation has been shown to open up chromatin, and preferentially occur at euchromatin. Therefore, it is unlikely that these gain of 5hmC can lead to demethylation. However, similar to the case of 5hmC loss, one can only reach a definite answer after performing experiments to quantify the methylation status of these loci at base resolution, presumably through whole genome or site specific bisulfite sequencing.

#### 6.4 Tet2 and Tet3 in IL15 signaling cascade

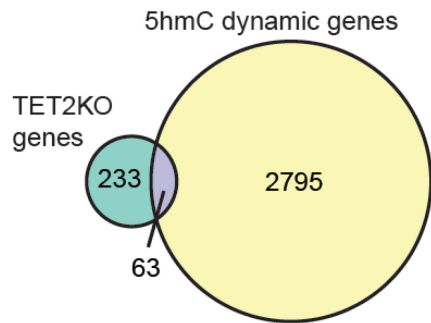


**Figure 23: The overlap between Tet2 controlled genes and dynamic 5hmC genes**

Having established the dynamics and locations of 5hmC, we also connected the 5hmC epigenetic mark to Tet proteins. Reduction in the level of Tet2 (by siTet2) impacted as much as 296 genes (FDR < 0.05, n = 5 biological replicates), confirming the importance of Tet2 in the signaling cascades of IL15. However, considering that IL15 controls as much as 6462 DEGs, the 296 Tet2-regulated DEGs seem to be a small amount of genes. 212 out of 296 genes are controlled by both IL15 and Tet2, representing 71% of Tet2-regulated genes in IELs, yet only 3.2% IL15-regulated genes. In order to understand the experimental results, we took into account the following limitations and interpretations. First, in many literatures, there have been reports of redundancy between Tet2's and Tet3's functions in normal development and hematopoietic stem cell emergence<sup>167-169</sup>. Both Tet2 and Tet3 are expressed at high levels in IELs. Reducing only Tet2 will most likely not be able to reveal all the DEGs controlled via 5hmC and Tets because Tet3 can still compensate the loss of Tet2. Second, the loss of Tet2 is not complete. Due to the difficulties in transfecting short termed cell lines (made from primary IELs from biopsies), the maximum level of Tet2 reduction was only around 25-33%. Therefore, the number of 296 DEGs due to siTet2 was an underestimation from the actual number of total Tet2-regulated genes. The fact that we underestimated

the total number of Tet2 controlled genes, and we still observed 296 Tet2 dependent genes reflects the importance of Tet2 in IL15 signaling.

Next, we asked if Tet2 operated through dynamic 5hmC, or through pre-existed 5hmC. We overlaid the Tet2-regulated DEGs with dynamic 5hmC peaks, and we saw little overlap: 63 genes out of 296 genes. Or in other words, 21% of Tet2 regulated genes showed dynamic 5hmC. 79% of Tet2 regulated genes did not show any change in 5hmC. How did we integrate this information to reflect the potential functions of 5hmC? First, the 63 genes that were both Tet2 dependent and had dynamic 5hmC (purple session in figure 23) may depend on Tet2 to generate these necessary dynamic 5hmC for transcription. They could be genes that were demethylated post IL15. Without Tet2, the 5hmC patterns could not be change, and demethylation could not occur, and the transcription of these genes was suppressed. However, to provide direct evidence for this mechanism, one will need to do 5mC profiling and show active demethylation post IL15 on these loci. Yet, demethylation could be a sound explanation on why these genes were both dependent on Tet2 and dynamic 5hmC.

In contrary, 233 out of 296 genes, or 79% of Tet2 regulated gene did not show dynamic 5hmC patterns (blue session in figure 23). These genes were dependent on Tet2 for proper transcription, yet without Tet2, the 5hmC did not change. Therefore, for these genes, Tet2 did not act through alteration of 5hmC or in other word, Tet2 did not act through demethylation and oxidation of 5hmC. To explain this fact, these may be the sites in which Tet2 was important as “a reader” to bind to 5hmC and recruit other transcriptional factors without exerting any demethylation activity. Without Tet2, transcriptional factors may not be properly recruited, and transcription was impacted. Yet, because Tet2 acted as recruiting or adapter protein, the 5hmC pattern was not necessarily altered by Tet2. To understand better, we attempted Tet2 CHIP-Seq to identify Tet2 binding sites throughout IELs genome. We also attempted Tet2 IP followed by mass spec to identify Tet2 binding partners. However, both attempts were unsuccessful due to the unavailability of good CHIP graded Tet2 antibodies at the current time. Future experiments

would need to be done to fully understand if indeed Tet2 bind to these sites, and methylation assay could be done to prove that the binding of Tet2 did not necessary mean demethylation for such sites. Finally, there was a novel interesting observation in the literature that may explain these Tet2 dependent genes with no dynamic 5hmC. Tet2 may act on RNA instead of DNA for certain genes. In fact, Tet2 had been shown to generate 5hmC on RNA<sup>170</sup>. Therefore, certain genes may be Tet2 dependent when we could not observe any impact of Tet2 on 5hmC on the DNA level.

Finally, there were 2499 genes with dynamic 5hmC peaks and they were not dependent on Tet2 at all (yellow session in figure 23). To explain them, these genes may be dependent on Tet3, and Tet3 could potentially be the enzymes that generate the dynamic 5hmC on these genes. Another explanation may be due to the fact that our Tet2 knock down was incomplete. The number of siTet2 DEGs may underestimate the real number of Tet2 dependent genes. Many of the 2499 genes may still dependent on Tet2, yet only with full knockdown of Tet2 or even with the double knock down of Tet2/Tet3 that we may observe the impact of siTets on the transcription of these genes. Finally, 5hmC may be an epigenetic marker that correlate well with gene expression, yet plays no regulatory role. The appearance of dynamic 5hmC does not necessary mean that these genes were dependent on Tet2 for their transcriptional activation and progression.

## 6.5 Future directions

While our work addressed the question if certain epigenetic markers such as 5hmC, histone modifications or chromatin accessibility were involved in IL15 signaling process, it also raised a new set of important questions.

First, what exactly is the mechanism in which Tet2 and 5hmC control gene expression? We have identified the subset of genes that are controlled by Tet2 and have 5hmC peaks. However, we have not pinpointed if 5hmCs act as a demethylation intermediates or binding sites for transcriptional factors to

regulate gene expression. In order to answer these questions, one needs to perform whole genome methylation assays such as bisulfite whole genome sequencing or 5mC IP (MeDIP) at various time points. One can overlap and track the changes in 5hmC and observe the pattern of 5mC. If 5hmCs act as intermediate markers for demethylation, one would expect to see change in methylation at these specific loci, and without Tet or 5hmC, there would be no change in methylation, and subsequently gene expression. Candidates for methylation tests can be genes that are Tet2 dependent and dynamic 5hmC dependent such as IFNg, GZMB and cell cycled related genes. On the other hand, if there is no change in 5mC even though the genes are Tet2 dependent, 5hmCs can be marks to recruit transcriptional factors. In this case, further assays need to be performed to identify the 5hmC binding proteins. Alternatively, one can look at our dynamic 5hmC data, and perform CHIP for candidate TFs (such as IRF1 or RUNX1), and then overlap the TFs binding sites, 5hmC sites, TET2 binding sites to prove the presence of such TFs at the dynamic 5hmC loci.

Second, what are the roles of Tet2 and possibly Tet3 in generating these 5hmC patterns? In order to answer this question, one needs to perform 5hmC IP in the siTet2 and siTet3 IELs. With the reduction on level of Tet2 or Tet3, one can expect alterations in the 5hmC landscape. Then one can attribute specific dynamic 5hmC loci to either Tet2 mediated, Tet3 mediated or both. It would be interesting to correlate such 5hmC alterations to change in gene expression changes in siTet2 and siTet3. How much would a change in 5hmC necessary to alter gene expression? We have siTet2 upregulated gene sets (IFN and defense related genes), and siTet2 down regulated genes (cell cycle specific). Lacking Tet2 altered the gene expression levels of these two sets of genes in opposite directions. Would the altered 5hmC landscape in siTet2 explain this phenomenon? In addition, there are many literatures that reveal the redundancy of Tet2 and Tet3<sup>106,167</sup>. One would be able to answer if Tet2 and Tet3 operate on largely overlapping sets of genes in the context of IL15 and IELs as well.

Third, our *in vitro*, short termed IEL cell lines are crucial for the study of IL15 signaling and epigenetic because the system can provide enough materials for CHIP-Seq and 5hmC-Seq (10ug in term of DNA required), it has its own limitation: the need to culture IELs in IL2 contained medium, and the potential epigenetic changes from the *ex vivo* IELs. Therefore, in the future, we must establish the difference and similarity between *in vitro* and *ex vivo* IELs in term of gene expression, and epigenetics (when the technology allows us to sequence histone marks and 5hmC marks with low amount of DNA inputs from *ex vivo* cells). Because in *ex vivo*, IELs were naturally exposed to steady state low level of IL15 in the intestinal tract, it would be important to see if that would make the IELs primed to IL15 response similar to our *in vitro* system.

Forth, one of the limitation of the study is the difficulty to transfect short term IELs and knock down Tet2 to a significantly low level. Therefore, our identification of 296 Tet2 dependent genes may underestimate the true number of genes. In addition, our system is an *in vitro* system; therefore, it is hard to put the relevant of Tet2 knock down IELs in the context of a full physiological system. The next logical step would be to use mouse models to further investigate 5hmC, IELs and IL5. With a Tet2, Tet3 or Tet2/Tet3 knock out mice, we can explore the redundancy and unique roles of each Tet in the physiological function of IELs. In addition, we have the mouse model of celiac disease, in which IL15 is expressed at a high level in the intestinal compartment. It will be valuable to understand if the IELs in IL15 high, Tet2 knock down mice have more proliferative capability and hyperactive immune response. It would also be interesting to see how these phenotypes would affect the whole intestinal compartment as a whole. Such study can further expand the impact of the research and answer relevant questions.

Fifth, we have studied and proved that during the short term of 4h post IL15 stimulation, even though the list of IL15 mediated, differential expressed genes is vast and diverse, the epigenetics in term of histone modification, chromatin accessibility and 5hmC seem to be stable. We have not addressed if epigenetic changes can occur during long time exposure with IL15. In fact, a recent

publication has shown that genomic instability and hypermethylation can occur after a month of constant exposure to high level of IL15<sup>123</sup>. As in many disease models, IL15 has been dysregulated for a long time prior to the onset of the diseases such as the cases of celiac disease and type 1 diabetes<sup>44</sup>. Therefore, it is valuable to look at the long term changes caused by IL15 to IELs in both gene expression and epigenetic landscape. Only then we may gain valuable insights on how IL15, long term epigenetic changes and disease development can be related.

Last but not least, we have demonstrated that for control patients, IELs chromatin and epigenetic are mostly stable during IL15 signaling. It would be interesting to push this one level further, and look at the epigenetic landscape at steady state and during IL15 signaling from IELs of patients from celiac disease, the autoimmune disorder in which the self-destruction of the villi are carried out by IELs. Celiac disease is a complex autoimmune disorder in which environments and epigenetics may play important roles in disease development and progression<sup>171</sup>. By obtaining the differences in gene expression, chromatin accessibility, histone modifications, and methylation associated marks, we may be able to understand if there are disease specific, epigenetic changes that enable the IELs to kill nonspecifically in celiac disease. Ideally, we can also perform gene expression and epigenetic analysis on *ex vivo* control IELs versus disease specific IELs to reserve best the epigenetic landscape of the *in vivo* IELs.

## 6.6 Conclusion

There has never been transcriptomic and epigenetic maps of human intestinal IELs at steady state and during IL15 signaling. In our work, we generated short term IEL cell lines, and used a combination of RNA-Seq, histone ChIP-Seq, ATAC-Seq and 5hmC-Seq to map out various epigenetic marks, and characterize the epigenetic changes and transcriptomic changes occurred in IELs during IL15 stimulation. We demonstrate that on a global level, the histone marks and the chromatin accessibility are stable throughout IL15 signaling process. Yet, a small fraction of genes have dynamic 5hmC, dynamic H3K4me1

and altered expression levels upon Tet2 knockdown, suggesting the involvement of epigenetic controlled for these specific gene sets (cell cycle related and IFN related genes). Finally, the steady state histone landscape of IELs is marked with activating marks such as the combination of Tn5, H3K4me3 and H3K27Ac that enable IELs to stay in an activating and primed state of cytotoxic effector T cells.

## REFERENCES

- 1 Perez-Lopez, A., Behnsen, J., Nuccio, S.-P. & Raffatellu, M. Mucosal immunity to pathogenic intestinal bacteria. *Nature reviews. Immunology* 16, 135-148, (2016).
- 2 Cheroutre, H. IEIs: enforcing law and order in the court of the intestinal epithelium. *Immunological reviews* 206, 114-131, (2005).
- 3 van der Poll, T., van de Veerdonk, F. L., Scicluna, B. P. & Netea, M. G. The immunopathology of sepsis and potential therapeutic targets. *Nature reviews. Immunology* 17, 407-420, (2017).
- 4 de Souza, H. S. P. & Fiocchi, C. Immunopathogenesis of IBD: current state of the art. *Nat Rev Gastroenterol Hepatol* 13, 13-27, (2016).
- 5 Baumgart, D. C. & Sandborn, W. J. Crohn's disease. *The Lancet* 380, 1590-1605.
- 6 Zhang, N. & Bevan, M. J. CD8(+) T cells: foot soldiers of the immune system. *Immunity* 35, 161-168, (2011).
- 7 Cheroutre, H., Lambolez, F. & Mucida, D. The light and dark sides of intestinal intraepithelial lymphocytes. *Nature reviews. Immunology* 11, 445-456, (2011).
- 8 Fuchs, A. *et al.* Intraepithelial type 1 innate lymphoid cells are a unique subset of IL-12- and IL-15-responsive IFN-gamma-producing cells. *Immunity* 38, 769-781, (2013).
- 9 Thome, J. J. C. & Farber, D. L. Emerging concepts in tissue-resident T cells: lessons from humans. *Trends in Immunology* 36, 428-435.
- 10 Farber, D. L., Yudanin, N. A. & Restifo, N. P. Human memory T cells: generation, compartmentalization and homeostasis. *Nature reviews. Immunology* 14, 24-35, (2014).
- 11 Jabri, B. & Ebert, E. Human CD8+ intraepithelial lymphocytes: a unique model to study the regulation of effector cytotoxic T lymphocytes in tissue. *Immunological reviews* 215, 202-214, (2007).
- 12 Masopust, D., Vezys, V., Wherry, E. J., Barber, D. L. & Ahmed, R. Cutting edge: gut microenvironment promotes differentiation of a unique memory CD8 T cell population. *Journal of immunology* 176, 2079-2083, (2006).
- 13 Masopust, D., Jiang, J., Shen, H. & Lefrancois, L. Direct analysis of the dynamics of the intestinal mucosa CD8 T cell response to systemic virus infection. *Journal of immunology* 166, 2348-2356, (2001).
- 14 Jabri, B. & Abadie, V. IL-15 functions as a danger signal to regulate tissue-resident T cells and tissue destruction. *Nature reviews. Immunology* 15, 771-783, (2015).
- 15 Bamford, R. N. *et al.* The interleukin (IL) 2 receptor beta chain is shared by IL-2 and a cytokine, provisionally designated IL-T, that stimulates T-cell proliferation and the induction of lymphokine-

activated killer cells. *Proceedings of the National Academy of Sciences of the United States of America* 91, 4940-4944, (1994).

16 Tagaya, Y., Bamford, R. N., DeFilippis, A. P. & Waldmann, T. A. IL-15: a pleiotropic cytokine with diverse receptor/signaling pathways whose expression is controlled at multiple levels. *Immunity* 4, 329-336, (1996).

17 Wang, X., Lupardus, P., Laporte, S. L. & Garcia, K. C. Structural biology of shared cytokine receptors. *Annual review of immunology* 27, 29-60, (2009).

18 Mishra, A., Sullivan, L. & Caligiuri, M. A. Molecular pathways: interleukin-15 signaling in health and in cancer. *Clinical cancer research : an official journal of the American Association for Cancer Research* 20, 2044-2050, (2014).

19 Tagaya, Y. *et al.* Generation of secretable and nonsecretable interleukin 15 isoforms through alternate usage of signal peptides. *Proceedings of the National Academy of Sciences of the United States of America* 94, 14444-14449, (1997).

20 Kury, G., Tagaya, Y., Bamford, R., Hanover, J. A. & Waldmann, T. A. The long signal peptide isoform and its alternative processing direct the intracellular trafficking of interleukin-15. *The Journal of biological chemistry* 275, 30653-30659, (2000).

21 Waldmann, T. A. The biology of interleukin-2 and interleukin-15: implications for cancer therapy and vaccine design. *Nature reviews. Immunology* 6, 595-601, (2006).

22 Mention, J.-J. *et al.* Interleukin 15: a key to disrupted intraepithelial lymphocyte homeostasis and lymphomagenesis in celiac disease. *Gastroenterology* 125, 730-745, (2003).

23 Cui, G. *et al.* Characterization of the IL-15 niche in primary and secondary lymphoid organs in vivo. *Proceedings of the National Academy of Sciences* 111, 1915-1920, (2014).

24 Doherty, T. M., Seder, R. A. & Sher, A. Induction and regulation of IL-15 expression in murine macrophages. *The Journal of Immunology* 156, 735, (1996).

25 Dubois, S. P., Waldmann, T. A. & Müller, J. R. Survival adjustment of mature dendritic cells by IL-15. *Proceedings of the National Academy of Sciences of the United States of America* 102, 8662-8667, (2005).

26 Schneider, R. *et al.* B Cell-Derived IL-15 Enhances CD8 T Cell Cytotoxicity and Is Increased in Multiple Sclerosis Patients. *The Journal of Immunology* 187, 4119, (2011).

27 Reinecker, H. C., MacDermott, R. P., Mirau, S., Dignass, A. & Podolsky, D. K. Intestinal epithelial cells both express and respond to interleukin 15. *Gastroenterology* 111, 1706-1713, (1996).

28 Mattei, F., Schiavoni, G., Belardelli, F. & Tough, D. F. IL-15 Is Expressed by Dendritic Cells in Response to Type I IFN, Double-Stranded RNA, or Lipopolysaccharide and Promotes Dendritic Cell Activation. *The Journal of Immunology* 167, 1179, (2001).

29 Ogasawara, K. *et al.* Requirement for IRF-1 in the microenvironment supporting development of natural killer cells. *Nature* 391, 700-703, (1998).

30 Waldmann, T. A. The shared and contrasting roles of interleukin-2 (IL-2) and IL-15 in the life and death of normal and neoplastic lymphocytes: implications for cancer therapy. *Cancer immunology research* 3, 219-227, (2015).

31 Chirifu, M. *et al.* Crystal structure of the IL-15-IL-15Ralpha complex, a cytokine-receptor unit presented in trans. *Nature immunology* 8, 1001-1007, (2007).

32 Ring, A. M. *et al.* Mechanistic and structural insight into the functional dichotomy between IL-2 and IL-15. *Nature immunology* 13, 1187-1195, (2012).

33 Berard, M., Brandt, K., Paus, S. B. & Tough, D. F. IL-15 Promotes the Survival of Naive and Memory Phenotype CD8<sup>+</sup> T Cells. *The Journal of Immunology* 170, 5018, (2003).

34 Gordy, L. E. *et al.* IL-15 regulates homeostasis and terminal maturation of NKT cells. *Journal of immunology* 187, 6335-6345, (2011).

35 Ranson, T. *et al.* IL-15 is an essential mediator of peripheral NK-cell homeostasis. *Blood* 101, 4887, (2003).

36 Surh, C. D. & Sprent, J. Homeostasis of naive and memory T cells. *Immunity* 29, 848-862, (2008).

37 Becknell, B. & Caligiuri, M. A. Interleukin-2, Interleukin-15, and Their Roles in Human Natural Killer Cells. *Advances in Immunology* 86, 209-239, (2005).

38 Ohteki, T., Suzue, K., Maki, C., Ota, T. & Koyasu, S. Critical role of IL-15-IL-15R for antigen-presenting cell functions in the innate immune response. *Nature immunology* 2, 1138-1143, (2001).

39 Czabotar, P. E., Lessene, G., Strasser, A. & Adams, J. M. Control of apoptosis by the BCL-2 protein family: implications for physiology and therapy. *Nature reviews. Molecular cell biology* 15, 49-63, (2014).

40 Dubois, S., Mariner, J., Waldmann, T. A. & Tagaya, Y. IL-15R $\alpha$  Recycles and Presents IL-15 In trans to Neighboring Cells. *Immunity* 17, 537-547, (2002).

41 Liao, W., Lin, J. X. & Leonard, W. J. Interleukin-2 at the crossroads of effector responses, tolerance, and immunotherapy. *Immunity* 38, 13-25, (2013).

42 Chen, L. & Flies, D. B. Molecular mechanisms of T cell co-stimulation and co-inhibition. *Nature reviews. Immunology* 13, 227-242, (2013).

43 Gascoigne, N. R. J. Do T cells need endogenous peptides for activation? *Nature reviews. Immunology* 8, 895-900, (2008).

44 Abadie, V. & Jabri, B. IL-15: a central regulator of celiac disease immunopathology. *Immunological reviews* 260, 221-234, (2014).

45 Strid, J., Sobolev, O., Zafirova, B., Polic, B. & Hayday, A. The intraepithelial T cell response to NKG2D-ligands links lymphoid stress surveillance to atopy. *Science* 334, 1293-1297, (2011).

46 Hüe, S. *et al.* A Direct Role for NKG2D/MICA Interaction in Villous Atrophy during Celiac Disease. *Immunity* 21, 367-377, (2004).

47 Jabri, B. *et al.* TCR Specificity Dictates CD94/NKG2A Expression by Human CTL. *Immunity* 17, 487-499, (2002).

48 Bauer, S. *et al.* Activation of NK Cells and T Cells by NKG2D, a Receptor for Stress-Inducible MICA. *Science* 285, 727, (1999).

49 Zhang, C., Zhang, J., Niu, J., Zhang, J. & Tian, Z. Interleukin-15 improves cytotoxicity of natural killer cells via up-regulating NKG2D and cytotoxic effector molecule expression as well as STAT1 and ERK1/2 phosphorylation. *Cytokine* 42, 128-136, (2008).

50 Xing, L. *et al.* Alopecia areata is driven by cytotoxic T lymphocytes and is reversed by JAK inhibition. *Nature medicine* 20, 1043-1049, (2014).

51 Rückert, R. *et al.* Inhibition of Keratinocyte Apoptosis by IL-15: A New Parameter in the Pathogenesis of Psoriasis? *The Journal of Immunology* 165, 2240, (2000).

52 Bo, H. *et al.* Elevated expression of transmembrane IL-15 in immune cells correlates with the development of murine lupus: a potential target for immunotherapy against SLE. *Scandinavian journal of immunology* 69, 119-129, (2009).

53 Maiuri, L. *et al.* Interleukin 15 mediates epithelial changes in celiac disease. *Gastroenterology* 119, 996-1006, (2000).

54 Kirman, I. & Nielsen, O. H. Increased numbers of interleukin-15-expressing cells in active ulcerative colitis. *The American journal of gastroenterology* 91, 1789-1794, (1996).

55 Liu, Z. *et al.* IL-15 Is Highly Expressed in Inflammatory Bowel Disease and Regulates Local T Cell-Dependent Cytokine Production. *The Journal of Immunology* 164, 3608, (2000).

56 Farh, K. K.-H. *et al.* Genetic and epigenetic fine mapping of causal autoimmune disease variants. *Nature* 518, 337-343, (2015).

57 Jeffries, M. A. & Sawalha, A. H. Autoimmune disease in the epigenetic era: how has epigenetics changed our understanding of disease and how can we expect the field to evolve? *Expert review of clinical immunology* 11, 45-58, (2015).

58 Waldmann, T. A. & Tagaya, Y. The multifaceted regulation of interleukin-15 expression and the role of this cytokine in NK cell differentiation and host response to intracellular pathogens. *Annual review of immunology* 17, 19-49, (1999).

59 Yu, B. *et al.* Epigenetic landscapes reveal transcription factors that regulate CD8+ T cell differentiation. *Nature immunology* 18, 573-582, (2017).

60 Miyazaki, T. *et al.* Functional activation of Jak1 and Jak3 by selective association with IL-2 receptor subunits. *Science* 266, 1045, (1994).

61 Johnston, J. A. *et al.* Tyrosine phosphorylation and activation of STAT5, STAT3, and Janus kinases by interleukins 2 and 15. *Proceedings of the National Academy of Sciences of the United States of America* 92, 8705-8709, (1995).

62 Lin, J. X. *et al.* The role of shared receptor motifs and common Stat proteins in the generation of cytokine pleiotropy and redundancy by IL-2, IL-4, IL-7, IL-13, and IL-15. *Immunity* 2, 331-339, (1995).

63 Miyazaki, T. *et al.* Three distinct IL-2 signaling pathways mediated by *bcl-2*, *c-myc*, and *lck* cooperate in hematopoietic cell proliferation. *Cell* 81, 223-231.

64 Martini, M., De Santis, M. C., Braccini, L., Gulluni, F. & Hirsch, E. PI3K/AKT signaling pathway and cancer: an updated review. *Annals of Medicine* 46, 372-383, (2014).

65 Hand, T. W. *et al.* Differential effects of STAT5 and PI3K/AKT signaling on effector and memory CD8 T-cell survival. *Proceedings of the National Academy of Sciences* 107, 16601-16606, (2010).

66 Steelman, L. S. *et al.* JAK/STAT, Raf/MEK/ERK, PI3K/Akt and BCR-ABL in cell cycle progression and leukemogenesis. *Leukemia* 18, 189-218, (2004).

67 Adunyah, S. E., Wheeler, B. J. & Cooper, R. S. Evidence for the Involvement of LCK and MAP Kinase (ERK-1) in the Signal Transduction Mechanism of Interleukin-15. *Biochemical and biophysical research communications* 232, 754-758, (1997).

68 Waddington, C. H. The Epigenotype. *International Journal of Epidemiology* 41, 10-13, (2012).

69 Waddington, C. H. Canalization of development and genetic assimilation of acquired characters. *Nature* 183, 1654-1655, (1959).

70 Mapping the epigenome. *Nat Meth* 12, 161-161, (2015).

71 Clapier, C. R., Iwasa, J., Cairns, B. R. & Peterson, C. L. Mechanisms of action and regulation of ATP-dependent chromatin-remodelling complexes. *Nature reviews. Molecular cell biology* 18, 407-422, (2017).

72 Du, J., Johnson, L. M., Jacobsen, S. E. & Patel, D. J. DNA methylation pathways and their crosstalk with histone methylation. *Nature reviews. Molecular cell biology* 16, 519-532, (2015).

73 Jaenisch, R. & Bird, A. Epigenetic regulation of gene expression: how the genome integrates intrinsic and environmental signals. *Nature genetics* 33 Suppl, 245-254, (2003).

74 Bannister, A. J. & Kouzarides, T. Regulation of chromatin by histone modifications. *Cell research* 21, 381-395, (2011).

75 Wang, Z. *et al.* Combinatorial patterns of histone acetylations and methylations in the human genome. *Nature genetics* 40, 897-903, (2008).

76 Shlyueva, D., Stampfel, G. & Stark, A. Transcriptional enhancers: from properties to genome-wide predictions. *Nature reviews. Genetics* 15, 272-286, (2014).

77 Smith, Z. D. & Meissner, A. DNA methylation: roles in mammalian development. *Nature reviews. Genetics* 14, 204-220, (2013).

78 Panning, B. & Jaenisch, R. RNA and the epigenetic regulation of X chromosome inactivation. *Cell* 93, 305-308, (1998).

79 Jeschke, J., Collignon, E. & Fuks, F. Portraits of TET-mediated DNA hydroxymethylation in cancer. *Current opinion in genetics & development* 36, 16-26, (2016).

80 Feinberg, A. P. & Vogelstein, B. Hypomethylation of Ras Oncogenes in Primary Human Cancers. *Biochemical and biophysical research communications* 111, 47-54, (1983).

81 Goelz, S. E., Vogelstein, B., Hamilton, S. R. & Feinberg, A. P. Hypomethylation of DNA from Benign and Malignant Human-Colon Neoplasms. *Science* 228, 187-190, (1985).

82 Sasaki, H. & Matsui, Y. Epigenetic events in mammalian germ-cell development: reprogramming and beyond. *Nature reviews. Genetics* 9, 129-140, (2008).

83 Oswald, J. *et al.* Active demethylation of the paternal genome in the mouse zygote. *Current biology : CB* 10, 475-478, (2000).

84 Hajkova, P. *et al.* Epigenetic reprogramming in mouse primordial germ cells. *Mechanisms of development* 117, 15-23, (2002).

85 He, Y. F. *et al.* Tet-mediated formation of 5-carboxylcytosine and its excision by TDG in mammalian DNA. *Science* 333, 1303-1307, (2011).

86 Ito, S. *et al.* Tet proteins can convert 5-methylcytosine to 5-formylcytosine and 5-carboxylcytosine. *Science* 333, 1300-1303, (2011).

87 Pfaffeneder, T. *et al.* The discovery of 5-formylcytosine in embryonic stem cell DNA. *Angewandte Chemie* 50, 7008-7012, (2011).

88 Maiti, A. & Drohat, A. C. Thymine DNA glycosylase can rapidly excise 5-formylcytosine and 5-carboxylcytosine: potential implications for active demethylation of CpG sites. *The Journal of biological chemistry* 286, 35334-35338, (2011).

89 Zhang, L. *et al.* Thymine DNA glycosylase specifically recognizes 5-carboxylcytosine-modified DNA. *Nature chemical biology* 8, 328-330, (2012).

90 Guo, J. U., Su, Y., Zhong, C., Ming, G. L. & Song, H. Hydroxylation of 5-methylcytosine by TET1 promotes active DNA demethylation in the adult brain. *Cell* 145, 423-434, (2011).

91 Cortellino, S. *et al.* Thymine DNA glycosylase is essential for active DNA demethylation by linked deamination-base excision repair. *Cell* 146, 67-79, (2011).

92 Schiesser, S. *et al.* Mechanism and stem-cell activity of 5-carboxycytosine decarboxylation determined by isotope tracing. *Angewandte Chemie* 51, 6516-6520, (2012).

93 Kohli, R. M. & Zhang, Y. TET enzymes, TDG and the dynamics of DNA demethylation. *Nature* 502, 472-479, (2013).

94 Blaschke, K. *et al.* Vitamin C induces Tet-dependent DNA demethylation and a blastocyst-like state in ES cells. *Nature* 500, 222-226, (2013).

95 Yu, M. *et al.* Base-resolution analysis of 5-hydroxymethylcytosine in the mammalian genome. *Cell* 149, 1368-1380, (2012).

96 Song, C. X. *et al.* Genome-wide profiling of 5-formylcytosine reveals its roles in epigenetic priming. *Cell* 153, 678-691, (2013).

97 Li, W. & Liu, M. Distribution of 5-Hydroxymethylcytosine in Different Human Tissues. *Journal of Nucleic Acids* 2011, (2011).

98 Wu, X. & Zhang, Y. TET-mediated active DNA demethylation: mechanism, function and beyond. *Nature reviews. Genetics*, (2017).

99 Xiong, J. *et al.* Cooperative Action between SALL4A and TET Proteins in Stepwise Oxidation of 5-Methylcytosine. *Molecular cell* 64, 913-925, (2016).

100 Lee, H. J., Hore, T. A. & Reik, W. Reprogramming the methylome: erasing memory and creating diversity. *Cell stem cell* 14, 710-719, (2014).

101 Saitou, M., Kagiwada, S. & Kurimoto, K. Epigenetic reprogramming in mouse pre-implantation development and primordial germ cells. *Development* 139, 15-31, (2012).

102 Wu, H. & Zhang, Y. Reversing DNA methylation: mechanisms, genomics, and biological functions. *Cell* 156, 45-68, (2014).

103 Zhang, X. *et al.* DNMT3A and TET2 compete and cooperate to repress lineage-specific transcription factors in hematopoietic stem cells. *Nature genetics* 48, 1014-1023, (2016).

104 Nestor, C. E. *et al.* 5-Hydroxymethylcytosine Remodeling Precedes Lineage Specification during Differentiation of Human CD4+ T Cells. *Cell reports* 16, 559-570, (2016).

105 Ichiyama, K. *et al.* The methylcytosine dioxygenase Tet2 promotes DNA demethylation and activation of cytokine gene expression in T cells. *Immunity* 42, 613-626, (2015).

106 Tsagaratou, A. *et al.* TET proteins regulate the lineage specification and TCR-mediated expansion of iNKT cells. *Nature immunology* 18, 45-53, (2017).

107 Chang, J. T., Wherry, E. J. & Goldrath, A. W. Molecular regulation of effector and memory T cell differentiation. *Nature immunology* 15, 1104-1115, (2014).

108 Avgustinova, A. & Benitah, S. A. Epigenetic control of adult stem cell function. *Nature reviews. Molecular cell biology* 17, 643-658, (2016).

109 Wilson, C. B., Rowell, E. & Sekimata, M. Epigenetic control of T-helper-cell differentiation. *Nature reviews. Immunology* 9, 91-105, (2009).

110 Clements, W. K. & Traver, D. Signalling pathways that control vertebrate haematopoietic stem cell specification. *Nature reviews. Immunology* 13, 336-348, (2013).

111 Hagman, J., Ramírez, J. & Lukin, K. B Lymphocyte Lineage Specification, Commitment and Epigenetic Control of Transcription by Early B Cell Factor 1. *Current topics in microbiology and immunology* 356, 17-38, (2012).

112 Ji, H. *et al.* A comprehensive methylome map of lineage commitment from hematopoietic progenitors. *Nature* 467, 338-342, (2010).

113 Borgel, J. *et al.* Targets and dynamics of promoter DNA methylation during early mouse development. *Nature genetics* 42, 1093-1100, (2010).

114 Trowbridge, J. J., Snow, J. W., Kim, J. & Orkin, S. H. DNA Methyltransferase 1 Is Essential for and Uniquely Regulates Hematopoietic Stem and Progenitor Cells. *Cell stem cell* 5, 442-449, (2009).

115 Broske, A.-M. *et al.* DNA methylation protects hematopoietic stem cell multipotency from myeloerythroid restriction. *Nature genetics* 41, 1207-1215, (2009).

116 Challen, G. A. *et al.* Dnmt3a is essential for hematopoietic stem cell differentiation. *Nature genetics* 44, 23-31, (2012).

117 Challen, Grant A. *et al.* Dnmt3a and Dnmt3b Have Overlapping and Distinct Functions in Hematopoietic Stem Cells. *Cell stem cell* 15, 350-364.

118 Moran-Crusio, K. *et al.* Tet2 Loss Leads to Increased Hematopoietic Stem Cell Self-Renewal and Myeloid Transformation. *Cancer cell* 20, 11-24, (2011).

119 Quivoron, C. *et al.* TET2 Inactivation Results in Pleiotropic Hematopoietic Abnormalities in Mouse and Is a Recurrent Event during Human Lymphomagenesis. *Cancer cell* 20, 25-38, (2011).

120 Kaech, S. M., Wherry, E. J. & Ahmed, R. Effector and memory T-cell differentiation: implications for vaccine development. *Nature reviews. Immunology* 2, 251-262, (2002).

121 Rothenberg, E. V. & Zhang, J. T-cell identity and epigenetic memory. *Current topics in microbiology and immunology* 356, 117-143, (2012).

122 Sen, D. R. *et al.* The epigenetic landscape of T cell exhaustion. *Science*, (2016).

123 Mishra, A. *et al.* Aberrant overexpression of IL-15 initiates large granular lymphocyte leukemia through chromosomal instability and DNA hypermethylation. *Cancer cell* 22, 645-655, (2012).

124 Buenrostro, J. D., Giresi, P. G., Zaba, L. C., Chang, H. Y. & Greenleaf, W. J. Transposition of native chromatin for fast and sensitive epigenomic profiling of open chromatin, DNA-binding proteins and nucleosome position. *Nature methods* 10, 1213-1218, (2013).

125 Brand, M., Rampalli, S., Chaturvedi, C. P. & Dilworth, F. J. Analysis of epigenetic modifications of chromatin at specific gene loci by native chromatin immunoprecipitation of nucleosomes isolated using hydroxyapatite chromatography. *Nature protocols* 3, 398-409, (2008).

126 Grzybowski, A. T., Chen, Z. & Ruthenburg, A. J. Calibrating ChIP-Seq with Nucleosomal Internal Standards to Measure Histone Modification Density Genome Wide. *Molecular cell* 58, 886-899, (2015).

127 Song, C. X. *et al.* Selective chemical labeling reveals the genome-wide distribution of 5-hydroxymethylcytosine. *Nature biotechnology* 29, 68-72, (2011).

128 Kim, D. *et al.* TopHat2: accurate alignment of transcriptomes in the presence of insertions, deletions and gene fusions. *Genome biology* 14, R36, (2013).

129 Anders, S., Pyl, P. T. & Huber, W. HTSeq--a Python framework to work with high-throughput sequencing data. *Bioinformatics* 31, 166-169, (2015).

130 Bindea, G. *et al.* ClueGO: a Cytoscape plug-in to decipher functionally grouped gene ontology and pathway annotation networks. *Bioinformatics* 25, 1091-1093, (2009).

131 Dobin, A. *et al.* STAR: ultrafast universal RNA-seq aligner. *Bioinformatics* 29, 15-21, (2013).

132 Zhang, Y. *et al.* Model-based analysis of ChIP-Seq (MACS). *Genome biology* 9, R137, (2008).

133 Breese, M. R. & Liu, Y. NGSUtils: a software suite for analyzing and manipulating next-generation sequencing datasets. *Bioinformatics* 29, 494-496, (2013).

134 Ritchie, M. E. *et al.* limma powers differential expression analyses for RNA-sequencing and microarray studies. *Nucleic acids research* 43, e47, (2015).

135 Li, H. & Durbin, R. Fast and accurate short read alignment with Burrows-Wheeler transform. *Bioinformatics* 25, 1754-1760, (2009).

136 Pique-Regi, R. *et al.* Accurate inference of transcription factor binding from DNA sequence and chromatin accessibility data. *Genome research* 21, 447-455, (2011).

137 Heinz, S. *et al.* Simple combinations of lineage-determining transcription factors prime cis-regulatory elements required for macrophage and B cell identities. *Molecular cell* 38, 576-589, (2010).

138 Quinlan, A. R. & Hall, I. M. BEDTools: a flexible suite of utilities for comparing genomic features. *Bioinformatics* 26, 841-842, (2010).

139 Zhou, X. & Wang, T. Using the Wash U Epigenome Browser to examine genome-wide sequencing data. *Current protocols in bioinformatics / editorial board, Andreas D. Baxevanis ... [et al.]* Chapter 10, Unit10 10, (2012).

140 Shen, L., Shao, N., Liu, X. & Nestler, E. ngs.plot: Quick mining and visualization of next-generation sequencing data by integrating genomic databases. *BMC genomics* 15, 284, (2014).

141 Benahmed, M. *et al.* Inhibition of TGF-beta signaling by IL-15: a new role for IL-15 in the loss of immune homeostasis in celiac disease. *Gastroenterology* 132, 994-1008, (2007).

142 Sanjabi, S., Mosaheb, M. M. & Flavell, R. A. Opposing effects of TGF-beta and IL-15 cytokines control the number of short-lived effector CD8+ T cells. *Immunity* 31, 131-144, (2009).

143 Wang, S. *et al.* FoxO1-mediated autophagy is required for NK cell development and innate immunity. 7, 11023, (2016).

144 Huntington, N. D. *et al.* Interleukin 15-mediated survival of natural killer cells is determined by interactions among Bim, Noxa and Mcl-1. *Nature immunology* 8, 856-863, (2007).

145 Man, K. & Kallies, A. Synchronizing transcriptional control of T cell metabolism and function. *Nature reviews. Immunology* 15, 574-584, (2015).

146 Mao, Y. *et al.* IL-15 activates mTOR and primes stress-activated gene expression leading to prolonged antitumor capacity of NK cells. *Blood* 128, 1475-1489, (2016).

147 Marcais, A. *et al.* The metabolic checkpoint kinase mTOR is essential for IL-15 signaling during the development and activation of NK cells. *Nature immunology* 15, 749-757, (2014).

148 Durek, P. *et al.* Epigenomic Profiling of Human CD4+ T Cells Supports a Linear Differentiation Model and Highlights Molecular Regulators of Memory Development. *Immunity* 45, 1148-1161, (2016).

149 Scott-Browne, J. P. *et al.* Dynamic Changes in Chromatin Accessibility Occur in CD8+ T Cells Responding to Viral Infection. *Immunity* 45, 1327-1340, (2016).

150 Pacis, A. *et al.* Bacterial infection remodels the DNA methylation landscape of human dendritic cells. *Genome research* 25, 1801-1811, (2015).

151 Bird, A. The essentials of DNA methylation. *Cell* 70, 5-8, (1992).

152 Li, E. & Zhang, Y. DNA methylation in mammals. *Cold Spring Harbor perspectives in biology* 6, a019133, (2014).

153 Bhutani, N., Burns, D. M. & Blau, H. M. DNA demethylation dynamics. *Cell* 146, 866-872, (2011).

154 Yamaguchi, S. *et al.* Dynamics of 5-methylcytosine and 5-hydroxymethylcytosine during germ cell reprogramming. *Cell research* 23, 329-339, (2013).

155 Hill, P. W., Amouroux, R. & Hajkova, P. DNA demethylation, Tet proteins and 5-hydroxymethylcytosine in epigenetic reprogramming: an emerging complex story. *Genomics* 104, 324-333, (2014).

156 Pastor, W. A., Aravind, L. & Rao, A. TETonic shift: biological roles of TET proteins in DNA demethylation and transcription. *Nature reviews. Molecular cell biology* 14, 341-356, (2013).

157 Shen, L. & Zhang, Y. 5-Hydroxymethylcytosine: generation, fate, and genomic distribution. *Current opinion in cell biology* 25, 289-296, (2013).

158 Zhang, Q. *et al.* Tet2 is required to resolve inflammation by recruiting Hdac2 to specifically repress IL-6. *Nature* 525, 389-393, (2015).

159 Muto, H. *et al.* Reduced TET2 function leads to T-cell lymphoma with follicular helper T-cell-like features in mice. *Blood cancer journal* 4, e264, (2014).

160 Rasmussen, K. D. *et al.* Loss of TET2 in hematopoietic cells leads to DNA hypermethylation of active enhancers and induction of leukemogenesis. *Genes & development* 29, 910-922, (2015).

161 Shuai, K. & Liu, B. Regulation of JAK-STAT signalling in the immune system. *Nature reviews. Immunology* 3, 900-911, (2003).

162 Ito, S. *et al.* Role of Tet proteins in 5mC to 5hmC conversion, ES-cell self-renewal and inner cell mass specification. *Nature* 466, 1129-1133, (2010).

163 Costa, Y. *et al.* NANOG-dependent function of TET1 and TET2 in establishment of pluripotency. *Nature* 495, 370-374, (2013).

164 Doege, C. A. *et al.* Early-stage epigenetic modification during somatic cell reprogramming by Parp1 and Tet2. *Nature* 488, 652-655, (2012).

165 Hu, L. *et al.* Crystal structure of TET2-DNA complex: insight into TET-mediated 5mC oxidation. *Cell* 155, 1545-1555, (2013).

166 Mercher, T. *et al.* TET2, a tumor suppressor in hematological disorders. *Biochimica et Biophysica Acta (BBA) - Reviews on Cancer* 1825, 173-177, (2012).

167 Dai, H.-Q. *et al.* TET-mediated DNA demethylation controls gastrulation by regulating Lefty–Nodal signalling. *Nature* 538, 528-532, (2016).

168 Lio, C.-W. *et al.* Tet2 and Tet3 cooperate with B-lineage transcription factors to regulate DNA modification and chromatin accessibility. *eLife* 5, e18290, (2016).

169 Li, C. *et al.* Overlapping Requirements for Tet2 and Tet3 in Normal Development and Hematopoietic Stem Cell Emergence. *Cell reports* 12, 1133-1143, (2015).

170 Fu, L. *et al.* Tet-Mediated Formation of 5-Hydroxymethylcytosine in RNA. *Journal of the American Chemical Society* 136, 11582-11585, (2014).

171 Meresse, B., Malamut, G. & Cerf-Bensussan, N. Celiac disease: an immunological jigsaw. *Immunity*  
36, 907-919, (2012).